Title
The Detection, Prevalence and Properties of Aggregate-Based Small Molecule Inhibition

Author
Feng, Brian Yi Chuan

Publication Date
2007-06-18

Peer reviewed|Thesis/dissertation

The Detection, Prevalence and Properties of Aggregate-Based Small Molecule Inhibition

by

Brian Y. Feng

DISSERTATION

Submitted in partial satisfaction of the requirements for the degree of

DOCTOR OF PHILOSOPHY

in

Chemistry and Chemical Biology

in the

GRADUATE DIVISION

of the

UNIVERSITY OF CALIFORNIA, SAN FRANCISCO

[redacted]

I would like to dedicate this dissertation to my parents (in chronological order):
Gayle, Paul, Larry and Ming.

Acknowledgements

I would like to acknowledge many people's help and influence in the work described here. First, I would like to thank my advisor, Brian Shoichet, for his mentorship and guidance in my formative years as a scientist. I would like to thank Jennifer Weisman, whose love has enriched my life and supported me throughout the completion of this work. I would like to acknowledge the friendship and support of all members of the Shoichet Lab, past and present, and especially Susan McGovern, upon whose work so much of this dissertation is based.

Many thanks go to my committee, Bob Stroud and Jim Wells, for their valuable input and insightful discussions. Thanks also to Chris Olson, the CCB program manager, who has always been a source of support and guidance, as well as a tremendous help in preparing this dissertation. Thanks as well to my collaborators over the last few years, including Kip Guy, Anang Shelat, Tom Doman, Anton Simeonov, Ajit Jadhav, Brandon Toyama, Sean Collins, Barnaby May and Holger Wille.

This dissertation is mainly composed of my four first-author publications. The material in Chapter 1 originally appeared in *Nature Chemical Biology* in 2005. It was reproduced here with permission from Feng, B. Y.; Shelat, A.; Doman, T. N.; Guy, R. K.; Shoichet, B. K. High-Throughput Assays for Promiscuous Inhibitors. *Nature Chemical Biology* **2005,** 1, 146 – 148. © 2005 *Nature Publishing Group*. The supplementary material from this publication has been included here as Appendix A.

The material in Chapter 2 was originally published in the *Journal of Medicinal Chemistry* in 2006. It was reproduced with permission from Feng, B.; Shoichet, B. K. Synergy and Antagonism of Promiscuous Inhibition in Multiple-Compound Mixtures. *J. Med. Chem.* **2006,** 49, 2151-2154. © 2006 *American Chemical Society*. The supplementary material for this publication has been included here as Appendix C.

The material in Chapter 3 originally appeared in the *Journal of Medicinal Chemistry* in 2007. It was reproduced here with permission from Feng, B. Y.; Simeonov, A.; Jadhav, A.; Babaoglu, K.; Inglese, J.; Shoichet, B. K.; Austin, C. P. A High-Throughput Screen for Aggregation-Based Inhibition in a Large Compound Library. *J. Med. Chem.* **2007,** 50, 2385-2390. © 2007 *American Chemical Society*. The companion publication to this article was submitted for publication in the journal *Nature Biotechnology* in 2007 as Babaoglu, K., Simeonov, A., Irwin, J.J., Nelson, M.E., Feng, B.Y., Thomas, C.J., Cancian, L., Costi, M.P.,Maltby, D.A., Jadhav, A., Inglese, J., Austin, C.P., and Shoichet, B.K. "A Comprehensive Parallel Virtual and Experimental High-Throughput Screen for β-Lactamase Inhibitors." It is under review.

The material in Appendix B originally appeared in *Nature Protocols* in 2006. It was reproduced here with permission from Feng, B. Y.; Shoichet, B. K. A Detergent-Based Assay for the Detection of Promiscuous Inhibitors. *Nature Protocols* **2006,** 1, 550-553. © 2005 *Nature Publishing Group*.

Abstract

The Detection, Prevalence and Properties of Aggregate-based Small Molecule Inhibition

Brian Y. Feng

In the early phases of drug discovery, high-throughput screening (HTS) has emerged as the dominant technique used to discover potential therapeutics. A critical weakness of this technique is sensitivity to artifactual, nonspecific inhibition. One source of nonspecific inhibition is the aggregation of organic molecules into colloidal particles. These aggregates have a unique property—they nonspecifically associate with proteins and inhibit enzyme function. If uncontrolled for, this inhibition is difficult to distinguish from classical mechanisms of small-molecule inhibition. In the context of high-throughput screening, this poses a large problem, as aggregate-forming molecules inherently lack the specificity desired in therapeutics or chemical tools. Thus, they cloud screening results by obscuring potentially desirable specific inhibitors.

Much of the work contained in this dissertation concerns the development of a high-throughput methodology to detect small-molecule aggregates. This was undertaken to provide a robust method for identification of aggregates and to probe the prevalence of this phenomenon. Two technologies were evaluated. First, an enzymatic assay was developed that detects detergent-sensitive inhibition, a conspicuous characteristic of aggregate-based inhibition. Second, a light scattering approach was employed to detect

aggregate particles in solution. Subsequently, the more robust detergent-dependant inhibition assay was applied to a large library of small molecules in order to measure the prevalence of aggregate-formation. Finally, to complement the methods developed to detect aggregates, the ability of aggregates to inhibit a non-enzymatic reaction, amyloid fibrillization, was studied using an *in vitro* fluorescence assay and electron microscopy.

Several conclusions emerge from this dissertation. First, screening for detergent-sensitive inhibition is a robust and efficient method for identifying aggregate-based enzyme inhibition. Second, aggregate formation is common; nearly 2% of a 70,563 molecule library formed aggregates below 30 μM. Third, whereas there are many mechanisms of nonspecific inhibition, aggregate formation may be the most common. Fourth, aggregate formation can be accentuated or reduced in mixtures of molecules, suggesting caution in mixture-based HTS. Finally, beyond enzymes, aggregates also inhibit the formation of amyloid fibrils, and should be considered as a source of artifact in screens for small molecule inhibitors amyloid formation.

Table of contents

List of Tables

List of Figures

Introduction

"The origin of penicillin was the contamination of a culture plate of *staphylococci* by a mould. It was noticed that for some distance around the mould colony the staphylococcal colonies had become translucent and evidently lysis was going on. This was an extraordinary appearance and seemed to demand investigation, so the mould was isolated in pure culture and some of its properties were determined."

--Alexander Flemming, Nobel Lecture, December 11, 1945

In the early days of drug discovery, empirical observation was the only method available to scientists for identifying novel therapeutic substances. Alexander Flemming noticed a peculiar green mold growing in his petri dish, which led to the discovery of penicillin.[1] Likewise, the age-old reputation of willow bark's analgesic properties was painstakingly traced by Peroux and Piria to a single crystalline substance—salicylic acid, which later lead to the drug aspirin.[2] Although the mechanism by which these substances worked was then unknown, they were among the first pure molecules seen to be useful in treating disease. By providing humanity with the ability to acutely combat disease, chemical therapeutics have greatly increased our success as a species.

Though chemistry has long been studied on a molecular level, it was not until the advent of molecular biology in the twentieth century that we could, with the same facility, study individual proteins—the molecular machines that comprise the vast majority of pharmaceutical targets. This technology has allowed scientists to understand the three-dimensional atomic structures of these machines. And recently, with the sequencing of the human genome, scientists have in hand a parts list of all the proteins made in the human body. This serves as a blueprint for how these molecular machines

are constructed and networked together to govern our existence. Now, instead of relying on empirical observations to deliver new drugs, we make our own opportunities by identifying the individual proteins that are important in a disease, and search for small molecules that will inhibit their function. This is the era of Rational Drug Design.

Ironically, despite its name, this strategy is still handcuffed to serendipity. The typical drug discovery campaign begins with an approach called High-Throughput Screening (HTS). Large, curated collections of pure chemicals ("libraries") are tested ("screened") for the ability to bind to and interfere with the function of a purified protein target. This approach has become increasingly dominant in the industry as technological innovations have enabled the automation of most steps in this process. Promising candidate molecules ("hits") are then chemically optimized ("leads") and screened in more complicated biological models for the disease, such as in animals. However, the eventual success of this enterprise is dependant on the quality of the initial hits from the HTS.

A complex interplay of physical interactions governs the binding of a small molecule to a protein (Figure 1). For those small molecules we use as drugs, specific binding—that is, the propensity for a small molecule to inhibit only one protein (or in some cases, a few)—is required to avoid toxicity and side-effects. Thus, early drug discovery resembles a needle-in-the-haystack problem, where scientists must screen a mind-boggling number of small molecules for those few that specifically recognize and inhibit the protein target. From among hundreds of thousands of molecules screened, perhaps only one or two leads will emerge that are promising enough for human clinical trials (Figure 2). Here, further attrition occurs, as perhaps only 10% of molecules which

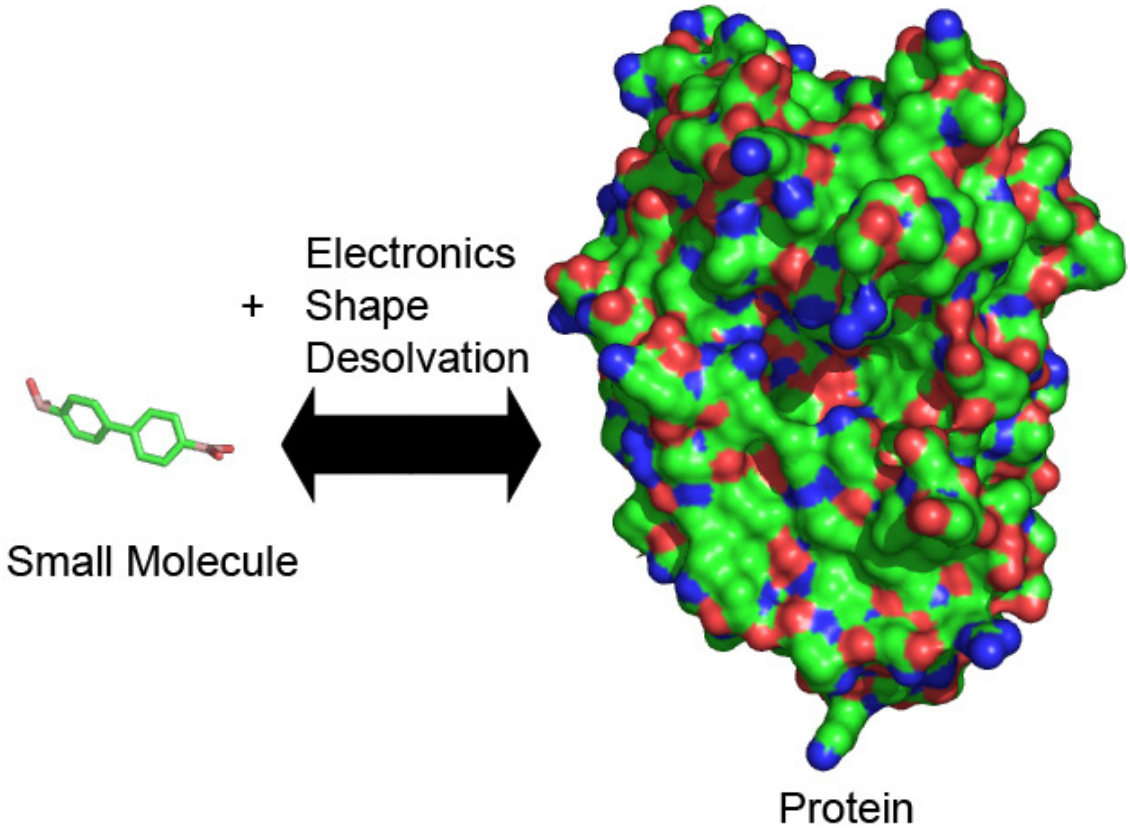

Figure 1. The association of small molecules and protein depends on many factors, including favorable electronic, shape and desolvation interactions.

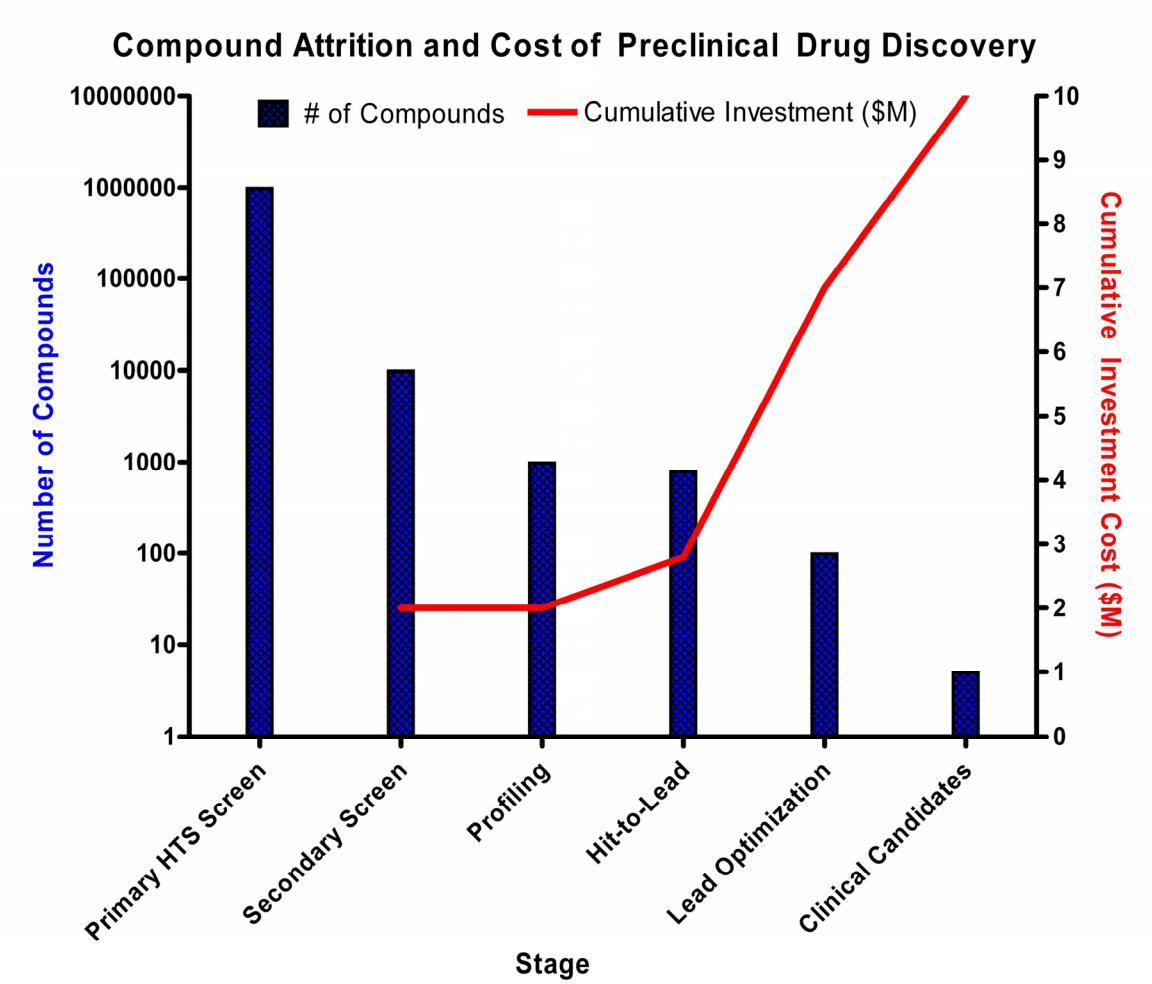

Figure 2. The stages of preclinical drug discovery and their estimated costs. Adapted from Walmsley et al.[3]

begin clinical trials possess the correct balance of properties (stability in the body, specificity, efficacy and safety) to be approved as drugs.[4] In the end, the cost of this process averages out to approximately 800 million dollars per drug.[5]

Recently, acadaemia has also adopted HTS techniques in an effort to contribute to early drug discovery. Because of the high costs involved in developing a new drug, the pharmaceutical industry has become conservative in choosing diseases to target. Many diseases, especially those endemic in developing countries, are neglected by the pharmaceutical industry simply because those afflicted are too poor to pay for new therapies. Acadaemia thus hopes to spur the discovery of therapeutics for the treatment of these neglected diseases by discovering promising candidates by HTS. Another area of interest for the academic screening community are small molecules capable of inhibiting the pathological aggregation of proteins, a process that underlies many diseases such as Alzheimer's, Parkinson's, diabetes and prion diseases (see below).

HTS tackles the needle-in-a-haystack problem through brute force. Every small molecule in the library is screened, and those that inhibit are considered for optimization. However, what wasn't understood before the advent of HTS is that whereas only a few small molecules are capable of specifically inhibiting a given protein, many more are capable of *nonspecifically* inhibiting *any* protein. That is to say, the haystack contains thousands of fake needles.

There are many mechanisms of nonspecific inhibition, and the Achilles' heel of HTS is how common such inhibition is. One source of nonspecific inhibition is the topic of this dissertation: the peculiar propensity for some molecules to aggregate into large, micron-sized particles, which nonspecifically associate with proteins and inhibit

enzymes. The process of distinguishing such artifacts from the minority of truly interesting hits is laborious, and is a significant part of why drug discovery costs so much. Aggregate-forming molecules are particulary devious in that they often structually resemble drugs and drug-like molecules; these molecules often appear to be promising drug candidates, but are eventually revealed to be worthless artifacts.

Early work by McGovern and colleagues described the basic properties of this phenomenon,[6-9] and the work collected here builds upon that foundation to assesss questions of the prevalence of promiscuous aggregates and their wider implications.

In Chapter 1, I describe the development of an efficient screen that allows for promiscuous aggregate-forming molecules to be distinguished from specific inhibition. This technique was tested on a set of 1,000 molecules to investigate the prevalence of aggregate-formation. This group of molecules was also used as a test set to evaluate the performance of predictive computational models for aggregation. A surprisingly large percentage of this set of molecules displayed the tendency to aggregate.

Development of this assay allowed us to evaluate the propensity for aggregation under different experimental conditions. One approach to HTS is to screen mixtures of molecules simultaneously, to increase the efficiency of the experiment. Given that aggregation appears to be a common behavior, we hypothesized that such mixtures might contain aggregates. Studying aggregation in the context of small molecule mixtures comprises Chapter 2 of this dissertation.

The preliminary studies described in Chapter 1 made some indication as to the prevalence of small-molecule aggregation. Chapter 3 discusses the further study of this issue using a larger test set of molecules. In collaboration with the NIH Chemical

Genomics Center (NCGC), our aggregate-detection assay was implemented in a more efficient format that allows for the simultaneous screening of 1,536 molecules per experiment. Using this assay, we screened 70,563 molecules for aggregation.

As the list of known aggregating molecules has grown, we noticed that some aggregators were also cited in the literature as inhibiting pathological protein aggregation—the abnormal assembly of proteins into long, toxic fibrils called amyloid. Therapeutic intervention in these diseases has been difficult, and most approved drugs treat the symptoms of each disease or ancillary biological processes rather than the central common process of fibrillization. In spite of this, many molecules have been published as inhibiting fibril formation under lab conditions. We developed the hypothesis that chemical aggregates, on account of their nonspecific affinity for protein could interfere with the *in vitro* assembly of amyloid fibrils. After examining several of these molecules, it appears that this hypothesis is correct, and aggregating small molecules may act as general inhibitors of amyloid formation. This dissertation concludes with Chapter 4, which describes recent work testing this hypothesis.

Gloss to Chapter 1.

Most drug discovery efforts, in both the pharmaceutical and academic setting, depend upon HTS to deliver promising small molecules that can specifically inhibit a given biological target. As HTS technology continues to be adopted, a suprising trend has been observed: many HTS campaigns, regardless of target, tend to generate a large percentage of hits. The reason for this is the many nonspecific mechanisms by which molecules can inhibit or appear to inhibit a given protein target, when generally only one mechanism—specific binding—is desirable. These mechanisms include chemical modification of the target, oxidation, assay interference and the formation of promiscuous aggregates. Our experience with the last led us to wonder if a simple assay could be developed to detect promiscuous aggregates, and whether we could then use such an assay to probe the prevalence of aggregation-based artifacts in HTS.

Two salient features of aggregates seemed likely to provide a reliable detection method. First, the aggregate particles themselves are large enough to observe through physical techniques such as dynamic light scattering (DLS). Second, aggregate-based inhibition can be abolished by application of small amounts of nonionic detergents such as Triton X-100. We developed 96-well format assays based on each of these two methods and tested them on a set of 1,030 small molecules. Three hundred of these molecules were chosen randomly, to provide an estimate of the prevalence of small molecule aggregation. We were shocked to discover that in the detergent assay, nearly 20% of these random molecules formed aggregates. The percentage was higher still in the DLS assay.

Simultaneously, our collaborators developed computational models to predict the identity of the aggregators in our test set, based on the physical and chemical properties of the small molecules. The results of these predictions were compared to the results of the detergent-based detection assay; they were moderately successful.

This paper was published in 2005 in the journal *Nature Chemical Biology*. It has contributed to the general awareness of this phenomenon as a source of misleading results in HTS, and has been cited 25 times as of this writing. It was also the first evidence that aggregation may be a common behavior among small molecules, a recurring theme in this dissertation. The computational methods used to develop the DLS classifier and the predictive models are included as Appendix A. The detergent-based assay was also solicited for publication in the online journal *Nature Protocols*; this experimental procedure is included as Appendix B.

Chapter 1.

High-Throughput Assays for Promiscuous Inhibitors

Brian Y. Feng[1], Anang Shelat[1], Thompson N. Doman[2], R. Kip Guy[1]

and Brian K. Shoichet[1]

[1]Department of Pharmaceutical Chemistry & Graduate Group in Chemistry and Chemical Biology, University of California-San Francisco, 1700 4th St., CA 94143-2550, [2]Eli-Lily & Company Corporate Center, Drop Code 1523, Indianapolis, IN 46285

Email: rguy@cgl.ucsf.edu, shoichet@cgl.ucsf.edu

High-throughput screening (HTS) is the dominant technique in early-stage drug discovery. A key problem in HTS is the prevalence of non-specific inhibitors, which can dominate hit-lists[10]. Several explanations have been proposed to account for these non-specific inhibitors, including chemical reactivity[10, 11], interference in assay read-out[11], high molecular flexibility[12] and hydrophobicity[11, 13]. The diversity of these models reflects the diversity of the molecules whose actions they seek to explain. Recently, we proposed a single mechanism for non-specific inhibition that explains the effects of many promiscuous inhibitors: some organic molecules form large colloid-like aggregates that sequester and thereby inhibit enzymes[7]. A diverse group of molecules, including hits from HTS, leads for drug discovery, and even several drugs act through this mechanism at micromolar concentrations[6-9, 14]. Here we report two rapid assays for detecting promiscuous aggregates that were tested using 1,030 Lipinski-compliant molecules. The empirical results were used to test two preliminary computational models of this phenomenon.

To investigate the severity of the problem posed by promiscuous aggregation, and to allow others to examine their own libraries, we developed two rapid, 96-well plate-based assays to detect this behavior. The first assay screens for the detergent-sensitive nature of aggregate-based inhibition[7, 15]. Inhibition of β-lactamase[6] was measured in the presence and absence of 0.1% Triton X-100; molecules that inhibit only in the absence of detergent are considered likely promiscuous aggregators. The second uses a Dynamic Light Scattering (DLS) plate reader to measure particle formation. Control experiments

suggested that both assays behaved comparably to their low throughput counterparts[6, 7, 9] and could distinguish known aggregators from known non-aggregators and known promiscuous inhibitors from specific inhibitors (**Appendix A-Supplementary Figs. 1** and **2**).

We selected 1,030 molecules to test these assays, purchased from Chemical Diversity, Inc., a major supplier for HTS libraries. The molecules were chosen by several criteria, including full Lipinski-compliance[16] and chemical diversity; overall, the molecules covered the same physical property space as did the CMC database of drugs (**Appendix A-Supplementary Table 1**). They made up three subsets: 298 were chosen at random, 493 were predicted aggregators and 239 were predicted non-aggregators. The latter two classes were selected using two preliminary computation models for aggregation (see below and **Appendix A-Supplementary Methods**). All molecules were screened at 30μM in the DLS assay and at both 30μM and 5μM in the detergent-dependent enzyme assay.

In the detergent-dependent inhibition assay, a surprising 19% of the randomly-selected molecules were detergent-sensitive inhibitors at 30μM. Of the predicted aggregators, 39% displayed detergent-sensitive inhibition whereas only 6% of predicted non-aggregators did so (**Fig. 3a**). Some of these molecules were visibly insoluble; upon removing them from consideration, 21% of the random set, 40% of the predicted aggregators and 7% of the predicted non-aggregators showed detergent-sensitive inhibition. For all molecules, any inhibition displayed in the absence of detergent was largely or completely attenuated in the presence of 0.1% Triton X-100, a property characteristic of aggregate-based inhibition[15].

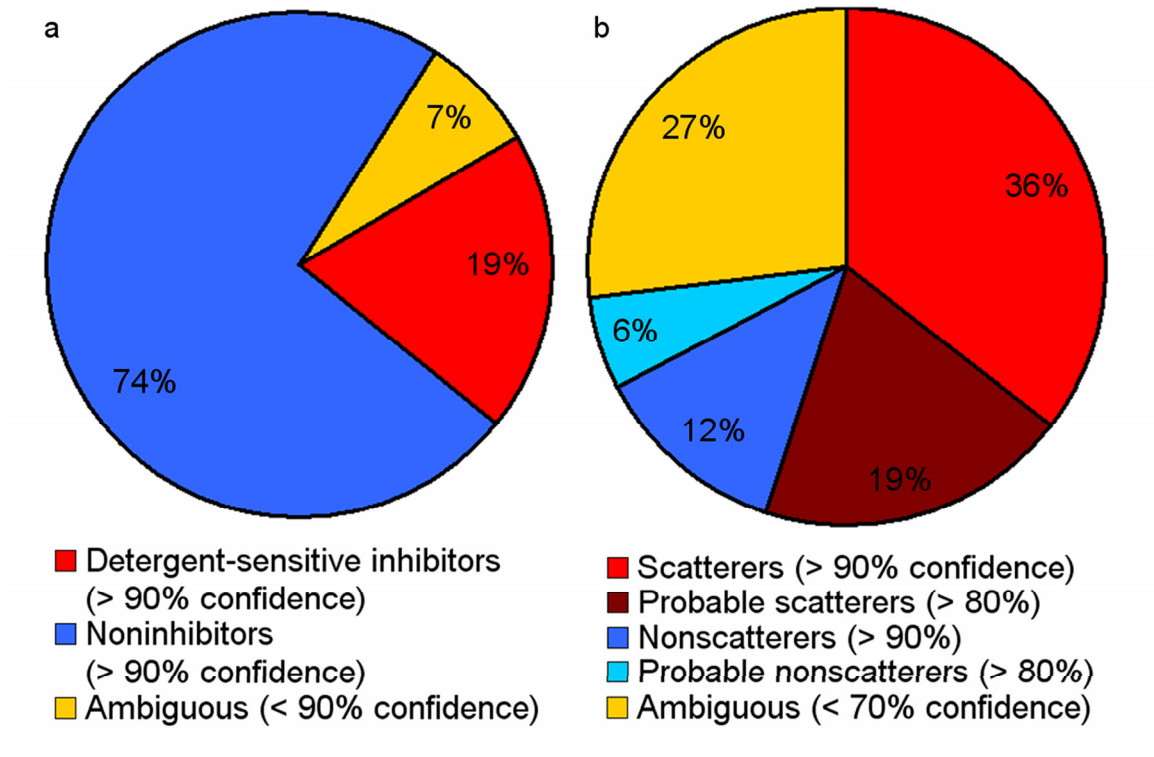

Figure 3. Results of the high-throughput assays applied to random drug-like molecules. Behavior of 298 randomly-selected molecules in (**a**) the detergent-dependent inhibition screen and (**b**) the DLS screen. The statistical percent confidence of the assignments is given in parentheses. Both assays were conducted at 30μM.

To examine the reliability of these results, molecules from the putative inhibitor and non-inhibitor populations were tested in a more sensitive, low-throughput version of the assay. Nine molecules from each population were tested one-at-a-time; their behavior in the two assays was well correlated. All putative inhibitors also inhibited chymotrypsin at 100μM, consistent with the observation that detergent sensitivity is a good proxy for aggregate-based promiscuity (**Appendix A-Supplementary Table 2**).

In the DLS assay, 36% of the 298 randomly-selected molecules scattered light at intensities high enough to indicate particle formation. 52% of the predicted aggregators and 15% of the predicted non-aggregators did so as well (**Fig. 3b**). As in the enzyme assay, 13 molecules from the putative scattering population and 12 from the non-scattering were tested in a more rigorous, low-throughput version of the assay (**Appendix A-Supplementary Table 3**). All behaved similarly in this more sensitive assay. Thus, the identification of particle formation by the DLS plate reader seems reliable, with three caveats. First, other aggregative phenomena, such as precipitation, can also lead to light scattering. Second, due to the size heterogeneity of aggregates in solution, many acquisitions were required to obtain sufficient data for DLS analysis; DLS assays sometimes required up to 3 hours of acquisition per plate. Third, many molecules scattered light with intermediate intensity, with over a quarter not clearly a member of either population. The presence of particles could not be determined for these cases.

There are interesting discrepancies in the results of the two screens. Whereas 39% of tested molecules scatter light, only 26% promiscuously inhibit (**Fig. 4**). Insoluble, light-scattering precipitates that lack inhibitory activity contribute to this discrepancy. Indeed, among visibly insoluble molecules only 14% inhibited, suggesting that

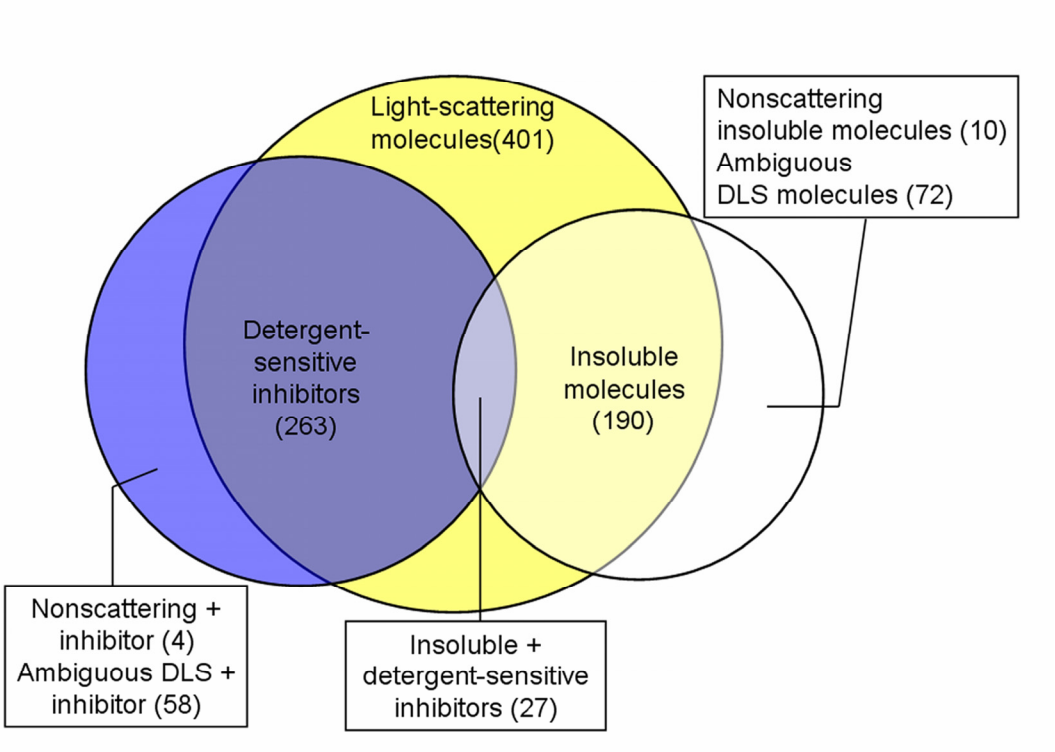

Figure 4. Comparison of the two high-throughput assays.

Overlap of positive results from the DLS and the detergent-dependent enzyme assays at 30μM.

precipitation and aggregation are distinct phenomena. Conversely, four detergent-sensitive inhibitors did not scatter light by DLS. These molecules may have optical properties which interfere with observation in DLS; this is the case for many known aggregators such as Congo red, which can only be studied by DLS at concentrations 100 times its IC_{50} versus β-lactamase[6]. Overall, our view is that the detergent-dependent enzyme assay gives the fastest and most reliable single indication of aggregate-based inhibition.

To investigate the concentration-dependence of aggregate-based inhibition, all 1,030 molecules were re-screened in the enzyme assay at 5 μM. Detergent-dependent inhibition among the random molecules dropped to 1.4% (from 19%). 8.6% of predicted aggregators and none of the predicted non-aggregators inhibited (**Fig. 5**).

Until now, we have referred to the computational predictions of promiscuous aggregating and non-aggregating molecules as coherent sets. In fact, two models were use to select these molecules: a Naïve Bayesian (NB) method, and a previously described Recursive Partitioning (RP) method[9] (**Appendix A-Supplementary Methods**). Whereas both models successfully enriched for promiscuous inhibitors among their predicted aggregators and non-inhibitors among predicted non-aggregators, both also predicted many false positives and false negatives (**Fig. 5**). Overall, the NB model seemed better at predicting aggregate-based inhibition, though both scored comparably at predicting light scattering.

To improve model accuracy, the experimental results from the predicted molecule sets was used to retrain the two models; the 298 molecules from the random subset were withheld as a test set. Originally, both the NB and RP models had a misclassification

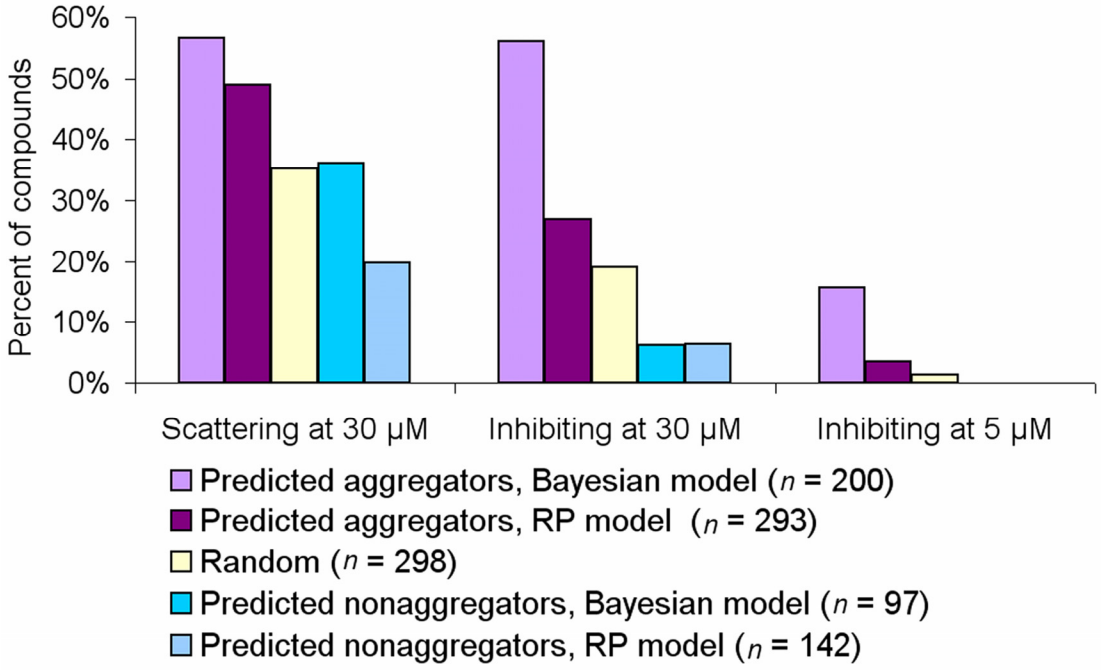

Figure 5. Accuracy of preliminary predictive models.

Percentage of positive results among the subsets of test molecules predicted by of the Bayesian and RP models in the DLS and detergent-dependent inhibition screens.

rate (MR) of 26% on the random set. Upon retraining, the MR of the refined NB model improved to 20%. A Random Forest model[17] replaced the RP model; upon training with the larger set, the MR for this model was 11% (**Appendix A-Supplementary Table 4**). Intriguingly, both computational models were more accurate at predicting inhibitors than predictions based on DLS (MR = 46%). These results may suggest that aggregation-based inhibition involves more than simple particle formation alone. It should also be mentioned that descriptor-based computational models remain too crude to capture the concentration dependence of aggregate formation.

Four noteworthy results emerge from these studies. First, remarkably high percentage, 19%, of randomly-selected, drug-like molecules form promiscuous aggregates at screening-relevant concentrations (here, at 30 μM) in simple biochemical buffers. This percentage is so high as to dominate any high-throughput screen not controlling for this effect. Even at 5 μM, 1.4% of randomly selected molecules acted as promiscuous aggregates, a number large enough to complicate many screens. Second and more optimistically, promiscuous aggregates may be detected rapidly and robustly. The detergent-dependent enzyme assay, in particular, should be deployable on libraries much larger than that described here. Third, this phenomenon has steep concentration dependence, possibly reflecting an underlying critical point phenomenon such as micelle formation. Fourth, predictive models show some potential for predicting aggregation-based promiscuity in large libraries. To allow for further development, we have made available our experimental results for all 1,030 molecules (http://shoichetlab.compbio.ucsf.edu). In summary, promiscuous inhibition induced by

aggregation is common among "drug-like" molecules at micromolar concentrations, and simple assays may be deployed to rapidly and reliably detect such inhibitors.

Methods:

DLS-Plate Reader and low-throughput assays:

Plate-reader assays were conducted on a Proterion DynaPro Plate Reader. The Dynamics Software package V6.0 was used to analyze the data. All compound solutions were made up in filtered 50mM KPi, pH 7.0. Samples were diluted from 10mM stocks (neat DMSO) and analyzed in 10 second acquisitions at 30% laser power. Samples were analyzed in Corning 96-well UV-transparent plates (model #3679). Low-throughput DLS assays were conducted on a DynaPro MS/X light scattering instrument as previously described[9].

β-lactamase assays:

AmpC β-lactamase was purified and assayed as described[6, 18]. β-lactamase inhibition assays were carried out as follows: Reactions contained 1 nM AmpC β-lactamase, 100 μM Nitrocefin in 50 mM KPi, pH 7.0 at room temperature. These reactions also contained 0.00002% Triton X-100 in order to stabilize the enzyme. Compound and enzyme were incubated together for 5 minutes before the reaction was initiated by the addition of substrate. Nitrocefin hydrolysis was monitored at 482 nm on a SpectraMax 340 UV-vis plate reader for high-throughput assays and a HP8453 UV-vis spectrophotometer for the low-throughput assays. To test for detergent effects on

putative aggregators, reactions were conducted as above with the exception that buffer containing 0.1% Triton X-100 was added prior to the introduction of compound.

Chymotrypsin assays:

All Chymotrypsin assays were conducted as previously described[6].

Calibration of High-Throughput Assays:

The high-throughput enzyme assay was calibrated on a set of 19 known aggregators and 27 known non-aggregators. The high-throughput DLS assay was calibrated on a set of 16 known aggregators and 33 known non-aggregators. In both assays, the behavior of these control compounds was used to develop statistical cutoffs for classifying unknown molecules (**Appendix A-Supplementary Methods**).

Test Set Selection:

The 1,030 test set molecules were purchased from Chemical Diversity, Inc. Prediction set molecules were classified as either promiscuous aggregators or non-aggregators by one of two models: a previously described recursive partitioning model[9] (RP) or a naïve Bayesian model (NB, **Appendix A-Supplementary Methods**). The predicted set contained 493 predicted aggregators (200 Bayesian/298 RP) and 239 predicted non-aggregators (97 Bayesian/ 142 RP). The random set contained 298 molecules. All compounds were prepared as 10 mM stocks in neat DMSO.

All selected compounds satisfied the following Lipinski criteria: (Nitrogen_Count + Oxygen_Count) <= 10, Molecular_Weight <= 500, Num_H-Bond_Donors <= 5, and AlogP <= 5.6[16]. An upper bound of 5.6 is more appropriate for the AlogP-based estimation of logP[19]. To further ensure that our test sets were reasonable representations of drug-like molecules, we compared common physical property distributions in our Prediction set, the Random set, and the Comprehensive Medicinal Chemistry (CMC) database (MDL, 2004). The CMC was filtered to remove compounds that were unlikely to be orally bioavailable, such as contrast agents, solvents, and pharmaceutical aids (denoted CMC*)[19]. The interquartile ranges of chemical properties for both the Prediction and Random sets are similar to those of the CMC* (**Appendix A-Supplementary Methods**).

Statistical Analyses:

Population normality and confidence intervals for the enzyme inhibition data were calculated using GraphpadPro by Prism. The Bayesian DLS classifier and the Bayesian predictive model for aggregate-based inhibitors were developed using the naïve Bayesian classifier algorithm in Pipeline Pilot 4.5.0 (Scitegic, Inc). The algorithm calculates the sum of conditional probabilities for the occurrence of a given feature in a set of molecules representing two classes. The Random Forest model was developed using the Arbor software package (**Appendix A-Supplementary Methods**).

Supplementary Information: Assay development procedures, the predictive models, example DLS data, screening results and a complete list of the 1,030 molecules

(**Supplementary Table 5**) are available free of charge on the Nature Chemical Biology website and at http://shoichetlab.ucsf.edu.

Correspondence and requests for materials should be sent to Brian K. Shoichet.

ACKNOWLEDGMENTS. Supported by GM71630, the QB3 fund and the Burroughs-Wellcome Fund (AS). We thank J. Weisman and Shoichet lab members for reading this manuscript. BYF and AS contributed equally to this work.

Competing interests statement: The authors declare that they have no competing financial interests.

Gloss to Chapter 2

Based on the experiments described in the previous chapter, it seemed to us that small molecule aggregation might be more common than previously thought. And through conversations with Mike Snider and colleagues at Berlex Pharmaceuticals, we were introduced to an approach towards HTS that may be especially sensitive to aggregate-based artifact: screening in mixtures of small molecules.

Screening in mixtures is common practice in the pharmaceutical industry which involves simultaneously screening a mixture of multiple molecules against a single enzyme target. Active mixtures are identified and retrospectively deconvoluted, and the active ingredient of the mixture is identified. Mixture-based screening is a practice that has seen it's share of controversy; adherents of this technique tout its efficiency over single-molecule screening, whereas it's critics cite anecdotes in which active mixtures do not deconvolute into any single active components. Our hypothesis was that for screens run in this fashion, small-molecule aggregation may be a significant source of false-positive hits.

This manuscript was published in the Journal of Medicinal Chemistry in 2006. It describes how we assembled random mixtures of ten molecules each from the same set of 1,030 used in the previous study. We compared inhibition of these mixtures to expected levels of inhibition, given the activity of the individual compounds. We observed not only examples where in the context of a mixture, aggregate-based inhibition was clearly favored (synergy), but also examples where it was disfavored (antagonism). As expected, both effects were attenuated upon application of detergent, though not entirely.

The surprising presence of both synergy and antagonism indicated that somehow, the behavior of each mixture was dependent on the identity of the molecules comprising the mixture. Additionally, these results suggest that promiscuous aggregates can obscure the results of mixture-based screening, and even mask the presence of a true specific inhibitor. A detergent-based counter screen is also more difficult to apply in this situation, because residual inhibition in the presence of detergent could either indicate the presence of a specific inhibitor in the mixture, or the contributions of stubborn aggregators.

Chapter 2.

Synergy and Antagonism of Promiscuous Inhibition in Multiple-Compound Mixtures

Brian Y. Feng[§] and Brian K. Shoichet[§*]

[§]*Department of Pharmaceutical Chemistry & Graduate Group in Chemistry and Chemical Biology, University of California-San Francisco, 1700 4th St., San Francisco, CA 94143-2550,.*

Received January 10, 2006

Abstract

Screening in mixtures is a common approach for increasing the efficiency of high-throughput screening. Here we investigate how the "compound load" of mixtures influences promiscuous aggregate-based inhibition. We screened 764 molecules individually and in mixtures of 10 at 5 μM each, comparing the observed inhibition of the mixtures to that predicted from single-compound results. Synergistic effects on aggregation predominated, although antagonism was also observed. These results suggest that screening mixtures can increase aggregation-based inhibition in a non-additive manner.

High-throughput screening (HTS) is widely used to interrogate large libraries of small molecules for biological reagents or new leads for drug discovery. A common approach in HTS is the screening of mixtures of small molecules.[20-25] This approach is efficient from the standpoint of reagent consumption, increases throughput, and is often required when screening natural products[26] or combinatorial libraries. Typically, the screening of mixtures is followed by a deconvolution step where active agents in promising mixtures are identified. Several deconvolution methods are used, including iterative,[27, 28] positional scanning,[29] and self-deconvoluting matrices.[21, 30]

A problem in HTS is the occurrence of false-positive hits–molecules that appear to inhibit the target but on investigation do so for what turn out to be uninteresting mechanisms. These include chemical modification of the target, interference in the assay readout and promiscuous aggregate-based inhibition. Such phenomena have inspired a considerable literature.[10, 13, 31-34] Our own interest has focused on the formation of

promiscuous aggregates. These are large particles, 100-1000 nm in diameter, formed by the self-association of small molecules at micromolar concentrations in aqueous media.[6-9] They nonspecifically interact with enzymes, sequestering them from substrate. Intruigingly, this inhibition is reversed in the presence of low concentrations of non-ionic detergents. Recently we exploited this effect to develop a high-throughput assay for detecting aggregates *via* detergent-sensitive inhibition. When we used this assay to screen a diverse set of drug-like organic molecules, we found that 19% of them formed promiscuous aggregates at 30 μM.[35]

Anecdotal evidence suggests that screening molecules in mixtures, as opposed to individually, may lead to its own set of artifacts: synergistic or antagonistic effects on inhibition that can obscure the presence of true actives. This issue has been the source of some controversy.[25, 36, 37] Our interest in this debate stems from the effects of "compound load," which may be considered the total concentration of organic material in a mixture, on the formation of promiscuous aggregates. Whereas most molecules might be well-behaved at low concentrations in isolation, upon mixing they might affect each other non-additively, specifically through aggregation. Here, we investigate how the behavior of mixtures of known promiscuous aggregators and non-aggregators deviates from a simple summation model for combinations of mutually exclusive inhibitors.

A set of 764 soluble, diverse, drug-like molecules were purchased from Chemical Diversity, Inc. and randomly combined into 80 mixtures of, on average, 10 molecules. Each molecule was present at a concentration of 5 μM for a total chemical load of 50 μM. The mixtures were assayed for inhibition against the model enzyme β-lactamase as previously described.[6-9, 35] Each of the molecules were also screened individually at 5

μM, both in the presence and absence of non-ionic detergent.[35] These experiments indicated that the 764 molecules consisted of 128 aggregators, 564 non-aggregators, and 72 molecules with intermediate inhibition. An aggregator was defined as a molecule that showed detergent-reversible inhibition greater than 24%, and a non-aggregator inhibited less than 11%.[35] There were no molecules whose inhibition was not reversible by detergent in this set.

These individual screening results were fed into a model of the null hypothesis– that inhibitors in a mixture would act exclusively and reversibly, and exist in equilibrium with free enzyme (Figure 6). According to this model, the total percent of enzyme inhibited by a mixture of *n* mutually exclusive inhibitors is given by the following equation, adapted from refs. [38-40]:

$$\text{Total \% Inhibition} = 100 * \frac{\sum_{i=1}^{n}\left(\frac{[I_i \cdot E]}{[E]}\right)}{\sum_{i=1}^{n}\left(\frac{[I_i \cdot E]}{[E]}\right)+1} \qquad \text{(Eq.1)}$$

One consequence of this classical summation model is that a combination of inhibitors very quickly yields diminishing returns. For example, a mixture of 3 well-behaved competing inhibitors that individually have percent inhibitions of 75%, 25% and 50% (i.e., $([I_i \cdot E]/[E]) = 3$, 1/3 and 1 respectively) will only have an overall inhibition of 81% as a mixture. To be conservative, we included what would normally be considered insignificant levels of inhibition (<11%)[35] when calculating predicted inhibition by Equation 1. This resulted in increased levels of predicted inhibition in the mixtures and thus reduction of the apparent synergistic effects.

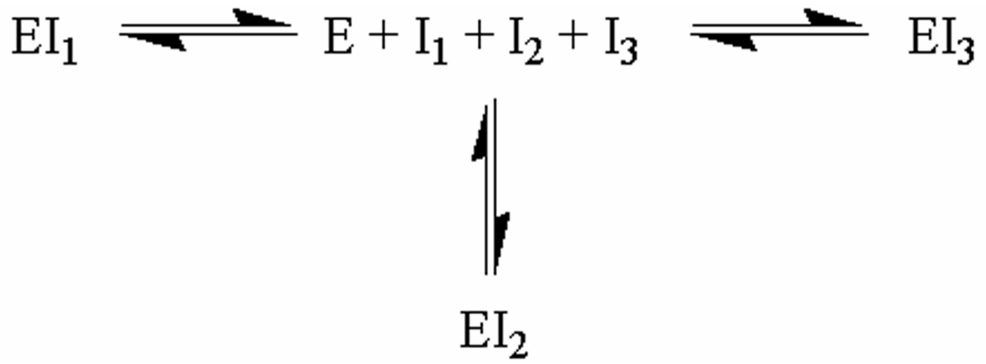

Figure 6. Equilibrium diagram for a mixture of mutually exclusive inhibitors. Total inhibition can be determined from Eq. 1.

The apparent IC_{50} of any single, non-cooperative and well-behaved inhibitor is given by the concentration of that inhibitor divided by the ratio of its percent inhibition to its percent activity, i.e., $([I_i]/([I_i \cdot E]/[E]))$. It is appropriate to use this ratio-based apparent IC_{50} when comparing the predicted and observed behavior of mixtures since, unlike raw percent inhibition, this term is linear with potency (e.g., at a fixed concentration, a molecule exhibiting 80% inhibition is actually sixteen-fold more potent than an inhibitor exhibiting 20% inhibition). We define antagonism and synergy as the measured inhibition of mixtures that is less than and more than predicted by Equation 1, respectively.

The 80 mixtures were screened in quadruplicate against β-lactamase (Figure 7a). Predicted potencies, calculated from single-molecule assays, are compared to observed potencies in Figure 7b. In the ideal case that a mixture behaved as a collection of simple, mutually exclusive inhibitors, the ratio between the predicted potency and the observed potency would be one, and the Log of the ratio would equal zero. In reality, large deviations between predicted and experimental results were observed for most mixtures; 45% of the mixtures were at least two-fold more potent than predicted and 16% of mixtures showed at least a two-fold diminution. Large deviations were seen for 24% of the mixtures, which were greater than ten-fold more potent than predicted, and 10% of the mixtures, which were at least ten-fold less potent than expected. Overall, the deviation ranged from 200-fold less potent to 447-fold more potent than predicted. In an effort to keep extreme levels of inhibition from skewing these results, maximum inhibition was arbitrarily set to 95%. Had we not done this, the bias towards extreme synergism and antagonism would have been higher still. Modeling mixtures as being

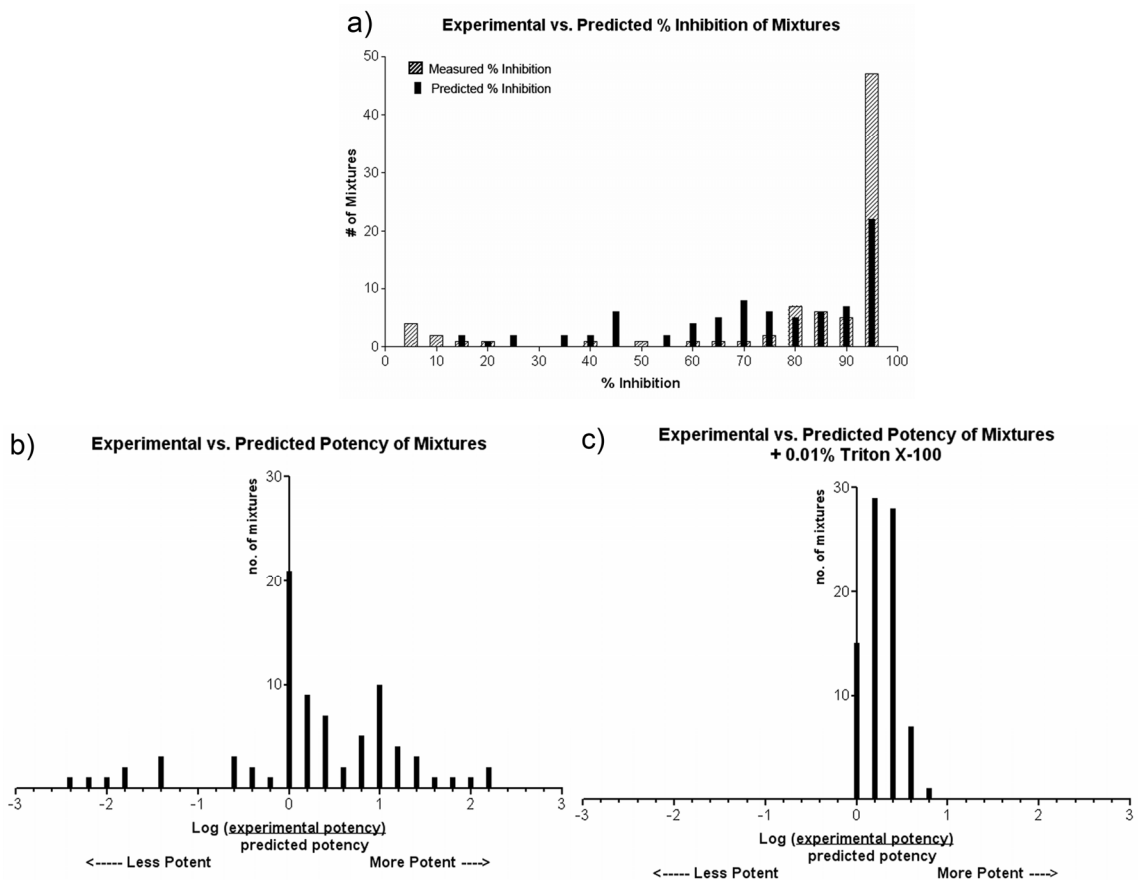

Figure 7. a) 80 mixtures binned according to their observed and predicted percent inhibition. b) 80 mixtures of molecules binned according to the deviation between the observed and predicted results. The deviation is a comparison of the predicted and observed potency (see text). c) Identical analysis as in *b*) for 80 mixtures of molecules screened in the presence of 0.01% Triton X-100.

comprised of mutually non-exclusive[38] or cooperative inhibitors[40] did not explain these non-additive effects; synergistic effects are larger than even a non-exclusive model predicts, and neither of these alternate treatments of the data explain the observed antagonism (analyses not shown).

Deviations from prediction were largely eliminated when the multi-compound assays were repeated in the presence of 0.01% Triton X-100, a non-ionic detergent that disrupts aggregates (Figure 7c).[7, 9, 35] As expected, some mixtures retained low levels of inhibition at this concentration of detergent. As before, the minimum predicted inhibition of each mixture was set to 5% to minimize the effect of dividing small numbers. In the presence of Triton X-100, effects ranged from 0 (no effect) to six-fold more potent than expected (Figure 7c), indicating almost total reversal of inhibition, synergy, and antagonism for most mixtures.

To investigate the reliability of these results, six mixtures were re-screened alongside their individual components in the high-throughput, plate-based assay as well as in a low-throughput version of the assay(each in duplicate).[35] This format allowed for the most precise individual compound data to be used in predicting the inhibition of the mixtures. The low-throughput assay was conducted in 1 mL cuvettes, on a HP 8453 spectrophotometer. Of the six mixtures, three were chosen from among the most synergistic, two were chosen from among the most antagonistic and one mixture was chosen that lacked non-additive effects. These mixtures behaved identically when rescreened with the high-throughput assay: the three mixtures displaying synergistic effects continued to inhibit significantly more than predicted, based on single compound

assays that were conducted at the same time, on the same plate. Correspondingly, the antagonistic mixtures continued to inhibit less than expected (Appendix C).

The low-throughput results were qualitatively the same, though the actual magnitude of inhibition both in the one-at-a-time and mixture assays was somewhat diminished, reflecting a general tendency of low-volume, plate-based assays to be more sensitive to promiscuous aggregation than high-volume cuvette-based assays. Nevertheless, the low-throughput assay essentially reproduced the high-throughput results.

Taken together, these results suggest a role for "compound load" in aggregation-based inhibition, typically potentiating, though occasionally antagonizing it. Unexpectedly, the magnitude of these effects were uncorrelated with the number of "active" (known aggregator or ambiguous) molecules in the well (data not shown). Extreme examples of synergy included Mixtures **1** and **2**, which were composed entirely of molecules inactive at 5 μM individually that when combined potently inhibited β-lactamase (98% and 97% inhibition, respectively). The simplest interpretation of these effects is that the chemical load in the mixtures is greater than the concentration at which aggregation occurs. Thus, though none of the components in Mixtures **1** and **2** were promiscuous aggregators at 5 μM, four molecules from Mixture **1** and three from Mixture **2** did form aggregates at a concentration of 30 μM, as determined in our previous study of these molecules.[35] This supports the notion that chemical load is the dominant factor in the appearance of these non-additive effects, though it does not suggest an obvious distinction between synergistic or antagonistic mixtures. As expected, the inhibition

displayed by these mixtures was largely eliminated by 0.01% Triton X-100, consistent with an aggregation-based mechanism.

To confirm that aggregates were present in these cases, we used dynamic light scattering (DLS) to measure particle formation in two of these mixtures as well as in solutions of the individual molecules. Consistent with their lack of inhibition, no particles were observed in the individual solutions (Figure 8). However, mixtures of these molecules exhibited intense light scattering, and particles were observed with radii in the 100 nm size range. Admittedly, a caveat to these observations is that light scattering was also observed in a mixture that did not significantly inhibit β-lactamase (data not shown). This result is, however, consistent with earlier observations that light scattering is a necessary-but-not-sufficient condition for the presence of promiscuous aggregates.[35]

These results raise the question of what effect aggregators may have on classical, well-behaved enzyme inhibitors in a mixture. We turned to the transition-state analog benzo[*b*]thiophene-2-boronic acid (BZB), a pure competitive inhibitor of β-lactamase that has been extensively characterized.[18] The potency of two aggregate-containing mixtures increased when they were doped with BZB; when these same mixtures were assayed in the presence of Triton X-100, inhibition fell to the level expected BZB alone (data not shown). These results suggest that synergistic or antagonistic effects, caused by aggregates, may obscure the presence of well-behaved inhibitors in mixtures. Artifactual synergy or antagonism is largely eliminated by addition of non-ionic detergent, leaving the effects of the classical inhibitor intact. It

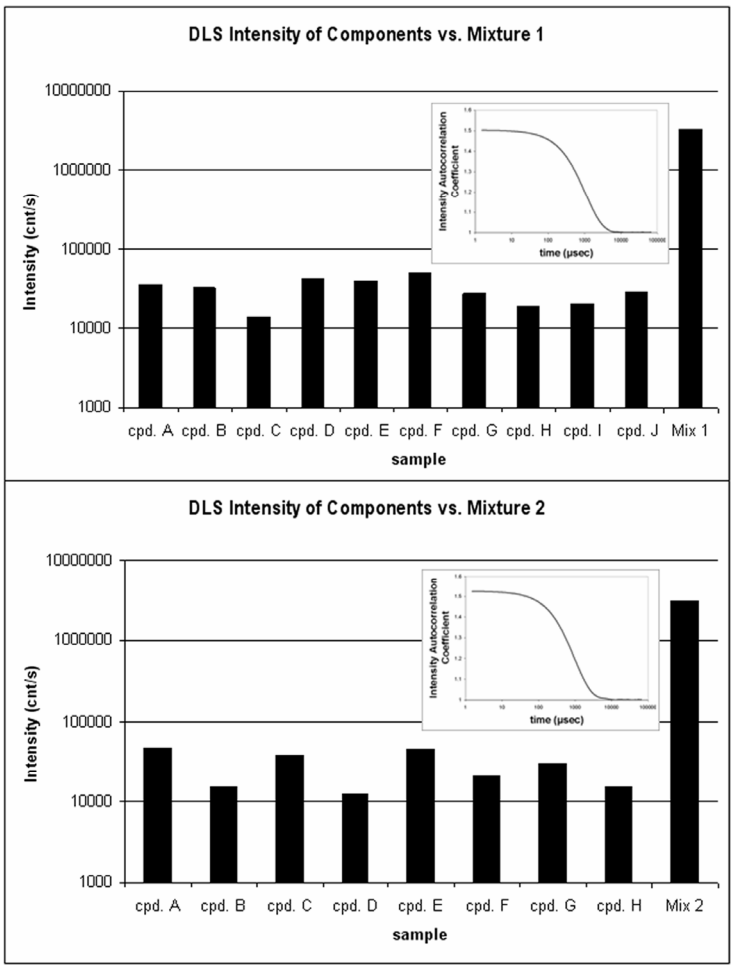

Figure 8. Light scattering study for two mixtures comprised of inactive molecules. Both mixtures scattered > 10-fold more intensely than any individual components. Inset: Autocorrelation functions for each mixture, consistent with the presence of large particles.

should also be noted however, that sensitivity to detergent varies from aggregate to aggregate, and residual inhibition detected in the presence of detergent (e.g. Fig. 7c) may be caused by a stubborn aggregator rather than a *bona fide* inhibitor.

Multi-compound mixtures are widely used in HTS, considerably improving throughput and conserving sometimes scarce assay resources. Three key observations emerge from this study with implications for this common strategy. First, "compound load" is a critical consideration in mixtures. Even at low concentrations of the individual components, here 5 μM, mixtures can display non-ideal, non-additive behaviors resulting from formation of large aggregates that inhibit enzymes. Second, and less expected, sometimes mixtures of compounds can act antagonistically, leading to less-than-expected inhibition. We do not fully understand this phenomenon, but believe it to be real– addition of detergent eliminates both synergistic *and* antagonistic effects of mixtures. We note that the majority of effects that we observed were synergistic. Finally, since the addition of detergent largely eliminates aggregate based-inhibition while leaving classical inhibition intact, it can be used to identify a classical competitive inhibitor from among a mixture of aggregates. However, since the reversal of inhibition is dependent on detergent concentration, and varies by compound, the persistence of reduced inhibition must be interpreted carefully. Overall, these results suggest heightened caution when interpreting the results of mixture-based high-throughput screening. This is merited by the widespread occurrence of aggregators among drug-like molecules and their non-classical, non-additive behavior in aqueous media.

Supporting Information Available: High-throughput and low-throughput data is available for the follow-up experiments. This material is available free of charge via the internet at http://pubs.acs.org.

Acknowledgement. This work was supported by GM71630. We thank Kristin Coan, Sarah Boyce and Michael Keiser for reading this manuscript.

Gloss to Chapter 3

Our initial experiments examining the prevalence of small-molecule aggregation seemed to indicate that aggregation may be a fairly common behavior. However, to confirm this observation, we needed to examine a larger test set than the 1,000 molecules described in Chapters 1 and 2.

Though the assay we developed was efficient and reliable on the scale of a thousand molecules, a rigorous sampling would require as many as ten or one hundred times as many molecules. Such an experiment was beyond our reach, so we struck up a collaboration with the NIH Chemical Genomics Center, a facility with industrial expertise in HTS. To increase the efficiency of the detergent-dependant assay, it was miniturized from a 96-well format to a 1,536 well format. This process was not straightforward, as it involved nearly a one-hundred fold reduction in reaction volume. However, after optimizing the conditions of the assay and some of the machinery involved, our collaborators were able to develop a reliable assay.

With this assay in hand, the NCGC screened 70,563 molecules from the Molecular Libraries Small Molecule Repository (MLSMR). This small molecule library was assembled by the NIH to provide a common library for the 10 national screening centers established by the NIH roadmap intiative. Essentially, this library is a common resource that the scientific community at-large may mine for useful small molecules. Experimental data concerning these molecules are collected and made publicly available on the internet via a central database called PubChem. Thus, in addition to making a

larger sampling of how common aggregation is among small molecules, this screen served to annotate potential problem compounds in the PubChem database. Additionally, we also hoped the screen would yield novel inhibitors of β-lactamase, a *bona fide* antibiotic target that is an area of focus in the lab.

This article, which was published in 2007 in the *Journal of Medicinal Chemistry* describes the results of the screen. Most notably, we established that the detergent-dependent-detection assay is robust in extremely high-throughput formats. We identified 1,204 aggregate-based inhibitors, which comprised nearly 2% of the MLSMR library. This number, while not as high as the 20% indicated previously, is easily still high enough warrant serious concern in the screening community. Indeed, the number of aggregators identified dwarfed the number of inhibitors acting by other mechanisms of inhibition, including specific inhibition. Only 70 molecules exhibited non-aggregate-based inhibition. Subsequent studies have shown that none of these were actually promising novel inhibitors—most were simply another form of artifact. This suggests that the dominant source of artifactual inhibition, indeed, any inhibition at all, in HTS screens is not due to more conventional mechanisms such as assay interference or covalent modification of the protein, but small-molecule aggregation.

Chapter 3.

A High-Throughput Screen for Aggregation-Based Inhibition in a Large Compound Library

Brian Y. Feng[1,†], Anton Simeonov[2,†], Ajit Jadhav[2], Kerim Babaoglu[1], James Inglese[2], Brian K. Shoichet[1,*] and Christopher P. Austin[2,*]

[1]Department of Pharmaceutical Chemistry & Graduate Group in Chemistry and Chemical Biology, 1700 4th St., University of California San Francisco, San Francisco, CA 94158-2330, USA

[2]NIH Chemical Genomics Center, National Human Genome Research Institute, National Institutes of Health, Bethesda, MD 20892-3370, USA

[†]These authors contributed equally to this work.

[*]To whom correspondence should addressed:

E-mail: shoichet@cgl.ucsf.edu, Phone: 415-514-4126, Fax: 415-514-4260.

E-mail: austinc@mail.nih.gov, Phone: 301-217-5725, Fax: 301-217-5736

Abstract

High-throughput screening (HTS) is the primary technique for new lead identification in drug discovery and chemical biology. Unfortunately, it is susceptible to false-positive hits. One common mechanism for such false-positives is the congregation of organic molecules into colloidal aggregates, which nonspecifically inhibit enzymes. To both evaluate the feasibility of large-scale identification of aggregate-based inhibition, and quantify its prevalence among screening hits, we tested 70,563 molecules from the National Institutes of Health Chemical Genomics Center (NCGC) library for detergent-sensitive inhibition. Each molecule was screened in at least seven concentrations, such that dose-response curves were obtained for all molecules in the library. There were 1,274 inhibitors identified in total, of which 1,204 were unambiguously detergent-sensitive. We identified these as aggregate-based inhibitors. Thirty-one library molecules were independently purchased and retested in secondary low-throughput experiments; 29 of these were confirmed as either aggregators or non-aggregators, as appropriate. Finally, with the dose-response information collected for every compound, we could examine the correlation between aggregate-based inhibition and steep dose-response curves. Three key results emerge from this study: first, detergent-dependent identification of aggregate-based inhibition is feasible on the large scale. Second, 95% of the actives obtained in this screen are aggregate-based inhibitors. Third, aggregate-based inhibition is correlated with steep dose-response curves, though not absolutely. The results of this screen are being released publicly via the PubChem database.

Introduction

High-throughput screening (HTS) is the most widespread technique used to identify new candidate leads for drug and chemical probe discovery. Although screening has had notable successes[41, 42], it can also generate a crippling number of false-positive "hits." Lipinski's well-known rules[16] were a first step to avoiding such misleading "hits"; subsequently, computational filters have been widely deployed to flag problematic compounds[13, 32, 43, 44]. These filters attempt to capture artifactual causes of nonspecific inhibition such as molecules that interfere with assay read-out[31], oxidize or chemically modify the target[10, 31, 34], or form colloidal aggregates[6-9, 14, 15, 35, 45-48]. In this latter mechanism, small molecules self-aggregate into a suspension of large particles that indiscriminately associate with proteins and sequester enzymes from substrate. Recent work has suggested that aggregate-based inhibition may explain a large number of promiscuous inhibitors, though exactly how common they are remains unclear.

Aggregate-based inhibition has several characteristic features. Perhaps the most exploitable of these is the sensitivity of this inhibition to non-ionic detergents[7, 15]. Moderate concentrations (0.01-0.1%) of such detergents not only disrupt aggregate formation, but can dissociate the protein-aggregate interaction and reverse inhibition. In earlier work, we exploited this characteristic to design a detergent-based counter-screen for aggregation, where detergent-sensitive, aggregate-based inhibition is isolated from detergent-resistant inhibition[35]. We found that this counter-screen was sufficiently reliable to evaluate aggregation in a small, 1,000-compound library. Here, we test this method in a 1,536-well format screen of 70,563 molecules from the NCGC small-

molecule library. For each molecule, a dose-response curve encompassing seven to fifteen points from 3 nM to 30 μM was calculated according to the recently described qHTS technique[49]. As explained in Inglese et al[49], curves were classified 1 to 4 according to quality, with Class 1 curves being the highest quality fits and displaying a top and a bottom asymptote. Class 2 curves contain a single asymptote and Class 3 curves show significant inhibition only at the highest concentration point. Class 4 curves are assigned to inactive molecules. These dose-response curves also allowed us to investigate the frequent coincidence of aggregate-based inhibition and steep dose-response curves. Curves with such high Hill slopes are frequently a harbinger of pathological behavior[33], and we wished to understand if they were an indicator of aggregate-based inhibition.

Here we address the following questions: Is the detergent-dependent assay for detecting aggregators robust in a low-volume, high-throughput format? How prevalent are aggregates in a well-curated screening library, and how common are they compared to other types of inhibitors? Is aggregate-based inhibition correlated with steep dose-response? Because we have tested every compound at no less than seven concentrations across a large range, we anticipate that these studies will offer useful guides to what may be expected in screening campaigns, at least against enzyme targets.

Results

Library Composition. The NCGC library that was screened consisted of 70,563 molecules, most of which were part of the NIH Molecular Libraries Small Molecule Repository (MLSMR, http://mlsmr.discoverypartners.com/MLSMR_HomePage/,

~59,000 molecules). Compounds from this library generally display lead-like[50] or drug-like[16] properties. The MLSMR was additionally supplemented by small collections from various commercial vendors (see methods).

Screening Results. After optimizing enzyme, detergent and substrate concentrations (see Methods), we screened 70,563 compounds from the NCGC small-molecule library against β-lactamase under both detergent(-) and detergent(+) conditions (Figure 9a, b). The detergent(-) screen was run continuously in 65 hours while the detergent(+) screen was finished in 51 hours. Acceptable signal-to-noise levels were achieved in both cases, as measured by the Z' score, a standard metric of HTS quality[51]. The detergent(-) screen had an average Z' of 0.77, whereas the detergent(+) screen had an average Z' of 0.82. For both assays, the Z' is well above 0.5, the standard cutoff score for assay reliability. Kinetic data for each reaction were collected, though for this analysis only the first and last point were used to calculate percent inhibition (we are making the full time courses of each reaction publicly available, as these may be a useful source of data for further study). We considered any molecule that displayed dose-dependent inhibition to be an active in the detergent(-) screen. Two criteria were used to describe detergent-sensitivity: first, each dose-response curve was qualitatively classified (the curve class[49]) based on the completeness of the curve and the quality of the fit (r^2). We required the curve class of putative aggregators be more defined (lower in curve class value) in the absence of detergent than in its presence. For example, a molecule that has a dose-response curve of Class 1 in the detergent(-) screen, but of Class 4 in the detergent(+) screen would satisfy this criterion (Figure 9c, d). Second, the maximum inhibition observed across the

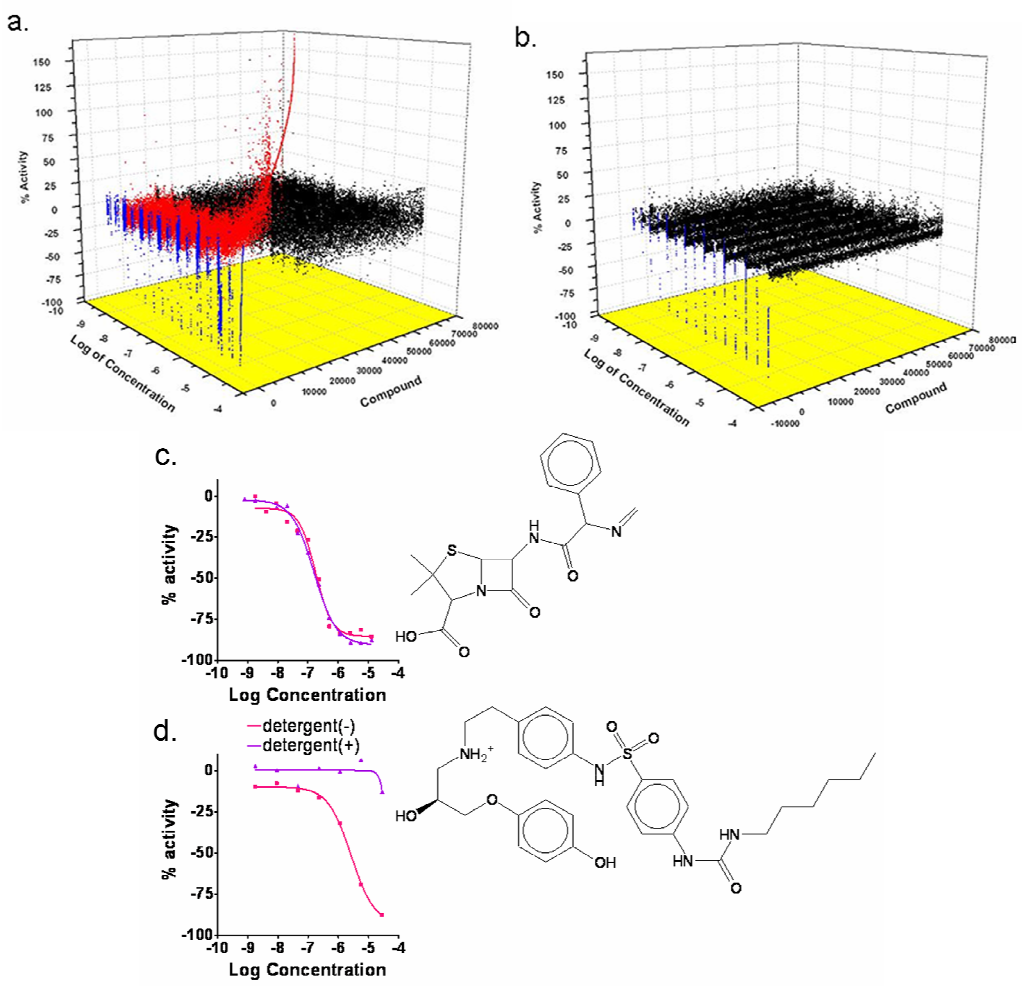

Figure 9. A 3D scatter plot of qHTS data. Concentration-response relationships for all 70,563 molecules are shown, colored as: no relationship (black), inhibition (blue) or activation (red). Comparison between detergent(-) (a) and detergent(+) (b) screening reveals the presence of aggregation-based activity in the detergent(-) assay. Example dose-response curves obtained from qHTS data for detergent-resistant (c) and detergent-sensitive (d) inhibitors.

titration series had to decrease in the detergent(+) screen relative to the detergent(-) screen. We took a significant decrease to be 3 standard-deviation units from the mean difference in activity upon addition of detergent for the whole library. By these criteria, the assay results fell into four categories: detergent-sensitive inhibition, detergent-insensitive inhibition, inconclusive results, where only one of the criteria for detergent-sensitive inhibition was satisfied, and compounds for which no inhibition was observed in either assay.

Overall, 1204 molecules (1.7%) met both the inhibition and curve criteria and were identified as aggregation-based inhibitors, whereas only 70 (0.1%) were identified as detergent-insensitive. These 70 included 25 known β-lactam inhibitors or substrates of β-lactamase. Of the remaining molecules, 562 were unable to be categorized, exhibiting only one of the criteria for detergent-sensitive inhibition (Figure 10). These consisted mostly of molecules that exhibited marginal levels of inhibition—and while most did show some response to detergent, they fell outside the range of statistical confidence. Aggregators varied in their ability to inhibit β-lactamase, but the most potent had IC_{50} values near 1 μM. The concentration-dependence of these molecules was consistent with a colloidal mechanism of inhibition; few aggregators were detected below 1 μM, but by 5 μM 60% of the aggregate-based inhibitors were apparent.

Secondary Assays. To test the reliability of these measurements, 31 molecules were independently purchased (i.e., re-sourced from the vendors) and retested in secondary assays. These molecules, identified in the primary screen as 17 aggregators and 14 inactives, were examined in the same β-lactamase assay, conducted in a one-at-a-time

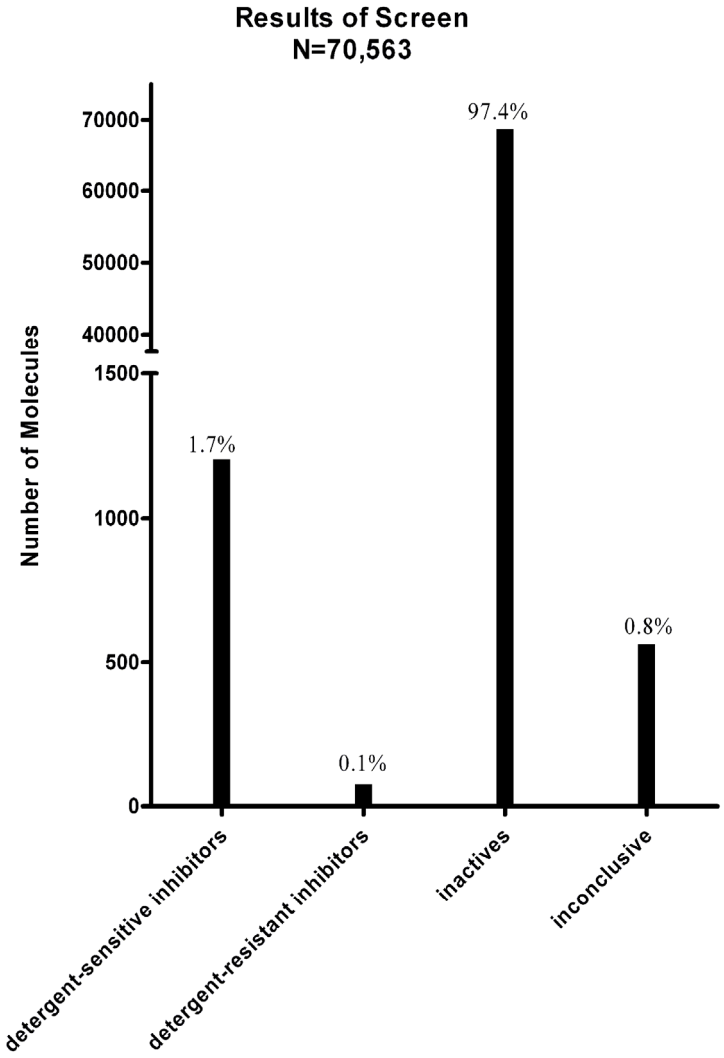

Figure 10. Classification and quantification of inhibitors found in the screen. 1,204 molecules were identified as detergent-sensitive inhibitors, based on two difference criteria between the detergent(-) and detergent(+) conditions: deterioration in the curve class of the molecule, and a decrease in the maximum observed inhibition across the dilution series. Seventy molecules were detergent-insensitive inhibitors, 68,727 showed no activity, and 562 were ambiguous, only fulfilling one of the two criteria necessary to be identified as an aggregation-based inhibitor.

cuvette-format. Though the conditions of these experiments were similar to the primary screen, these experiments varied the concentration of DMSO, enzyme, and detergent, as well as the reaction volume (1 mL vs. 8 μL) and path length. Of the 17 molecules identified as aggregators in the primary screen, 15 exhibited aggregate-based inhibition upon re-testing in the secondary assay. Likewise, of the 14 inactive molecules retested, none inhibited under screening conditions. However, 10 of these exhibited aggregate-based inhibition at higher concentrations or under relaxed assay conditions, i.e. using decreased enzyme concentration and less detergent in the detergent(-) condition of the primary high-throughput assay (Table 1).

A curious feature of the primary screening data was that some molecules appeared to activate β-lactamase in the detergent-free screen; this activation was eliminated on detergent-addition. Six of these putative activators were independently purchased and re-tested under several conditions in low-throughput, cuvette-based assays. In a contrast to the aggregators and nonaggregators identified in the primary screen, activation was not reproducible in these secondary assays. Subsequently, another one hundred of these apparent activators were re-sourced from the vendors and stocks were re-made directly from solid powder. These compounds were then tested under medium throughput conditions, such as 96- or 384-well formats. Owing to the larger volume of these assays, compared to the 1536 well formats, it was often possible to observe the compound immediately after addition to the assay. In these cases, we often observed what appeared to be precipitants, typically at the bottom of the wells at the solvent-polymer interface. Also, when the compounds were tested at these higher volumes, much of the former activation was attenuated, though many of these compounds did still lead to activation.

Type of Molecule	Number Tested	Number of Aggregators- Stringent Screening Conditions[a]	Number of Aggregators- Relaxed Screening Conditions[b]
Primary Screen	17	15	15
Aggregator-Primary Screen Nonaggregator-	14	0	10

Table 1. Results of low-throughput secondary assays. [a] Primary screening conditions. [b]Less-stringent conditions (4-fold less enzyme, 5-fold less stabilizing detergent).

Taken together, these results suggest that activation is a phenomenon peculiar to the very low volume, high-throughput formats used in the primary screen. We will not consider it further here.

Hill Slope Analysis. The dose-response information obtained in this screen allowed us to investigate the correlation between aggregate-based inhibition and steep dose-response curves, which are common among high-throughput screening hits[8, 33]. We analyzed the Hill slopes of the highest-quality dose-response curves, consisting of 174 aggregate-based inhibitors, 24 β-lactam-based irreversible inhibitors, and 17 reversible inhibitors of β-lactamase (Figure 11a). The reversible inhibitors displayed standard, single-site dose response curves with slopes near one, whereas the β-lactam inhibitors were biased towards somewhat steeper curves, as expected for very potent inhibitors.[52,53] However, the aggregators displayed a mixed tendency—many had Hill coefficients close to one, but many others showed steep curves, even steeper than the covalent β-lactam inhibitors, and similar to those seen for other aggregating inhibitors[6]. Of the 174 aggregators in this set, 70 had Hill slopes steeper than 1.5.

Data Sets. The full results of these screens are publicly available through PubChem (http://pubchem.ncbi.nlm.nih.gov/) and the Shoichet Lab website (http://shoichetlab.compbio.ucsf.edu/).

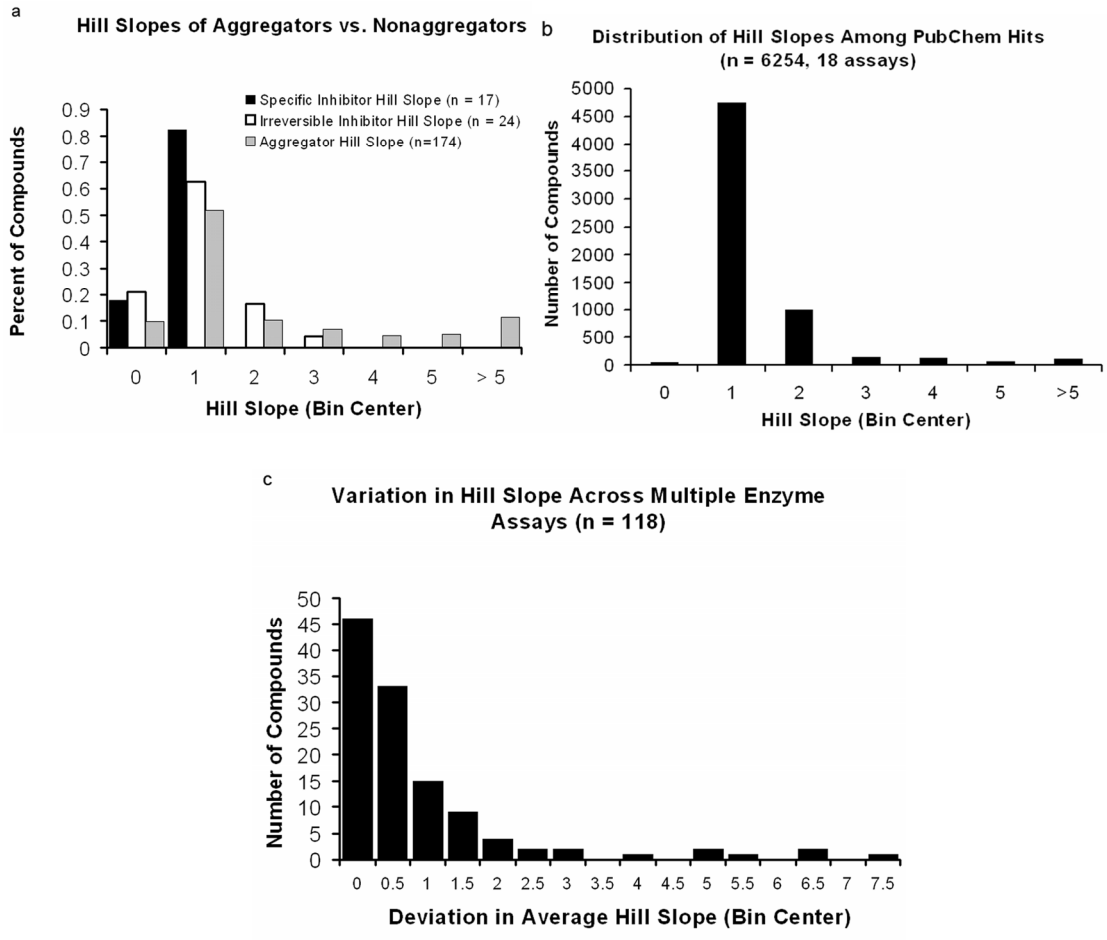

Figure 11. (a) Correlation between aggregation-based inhibitors and those with high Hill slopes. Compared to a set of specific, reversible β-lactamase inhibitors and a set of irreversible inhibitors, aggregators are more likely to have steep dose-response curves. (b) Distribution of Hill slopes among the active molecules discovered from 18 enzyme screens currently annotated in PubChem. (c) Variation in the slopes of high-Hill slope molecules that were tested in at least two enzyme assays. Hill slopes appear consistent for most of these molecules.

Discussion

Perhaps the most practical conclusion to be drawn from this screen is that the detergent-sensitive assay can reliably identify aggregate-based enzyme inhibitors in a genuinely high-throughput format. A counter-screen consisting of 0.01% Triton X-100 effectively separated 1,274 assay actives into 1,204 aggregators and 70 molecules that act by other mechanisms (Figure 10). This assay may be used to characterize other libraries, or adapted to other enzymes for direct use as a counter-screen.

Many mechanisms have been proposed to explain promiscuous inhibition, including interference in assay read-out[31], compound oxidation[34], chemical modification of the target[10, 31, 34]. A striking result of this screen is that 95% of the actives can be attributed to a single one of these: aggregate-based inhibition. How the remaining five percent of actives are distributed among other mechanisms—including true specific, reversible inhibition—is currently under investigation in our laboratory; few of these mechanisms are as rapidly and decisively identified as promiscuous aggregation. What we can say at this point is that 25 of these 70 actives are β-lactam-based inhibitors of β-lactamase, which act by covalently modifying the catalytic nucleophile, Ser64[54, 55]. Also, 5-10 of these appear to be aggregates that are resistant to 0.01% Triton X-100, but are sensitive at 0.1%, the concentration used in the original screen[35]. This leaves only about 35 molecules that act by all other mechanisms.

Though the vast majority of hits in this screen inhibited through aggregate formation, the overall percentage of aggregators identified in the library is smaller than what we found in an initial, smaller-scale screen. This previous study suggested that as many as 19% of 298 randomly-selected drug-like molecules behave as aggregators at 30

μM[35]. Two factors contribute to this discrepancy. The first relates to the sensitivity of aggregate-based inhibition to assay conditions. For reasons of enzyme stability in the 1,536-well format, a low level of detergent (0.0001%) was present in the detergent(-) screen; this concentration of detergent is five-fold greater than the amount required in the original 96-well assay[35]. Additionally, the concentration of enzyme was increased four-fold relative to the original assay, while the concentration of detergent used in the detergent(+) screen was reduced ten-fold to 0.01%. These changes reduced the number of aggregators found under detergent(-) conditions, resulting in a more stringent screen. Among the 31 compounds retested in low-throughput secondary assays, the original conditions were more sensitive to aggregate-based inhibition than the new high-throughput conditions. At least a two-fold difference in potency was observed for most aggregators tested under both conditions (Table 2). Finally, we can't discount the possibility of compound bias in our original set of 298 rule-of-5-compliant molecules. The much larger NCGC library not only allows for more robust statistics, but its careful curation may have also contributed to the lower rate of aggregate-based inhibition.

Steep dose-response curves are often harbingers of pathology in HTS results[33]. Since many aggregators also have such curves, it is tempting to correlate the two phenomena. The qHTS titrations allowed us to investigate this possibility. We selected the highest quality dose-response curves, consisting of 174 aggregators, 17 previously-

Structure	IC_{50} (μM)		Detergent Sensitive?	Aggregator?	PubChem SID
	Stringent conditions	Relaxed conditions			
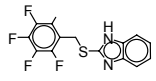	> 300 [b]	130	Yes	Yes	7973586
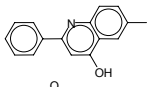	> 100 [b]	> 100 [b]	Yes	Yes	7975152
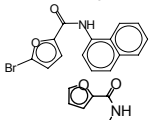	> 200 [b]	120	Yes	Yes	7973072
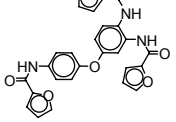	40	20	Yes	Yes	4259752
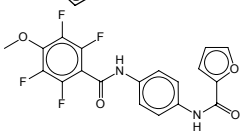	> 66[b]	20	Yes	Yes	4265457
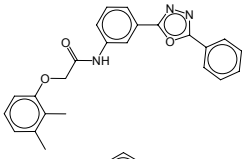	> 66[b]	13[a]	Yes	Yes	4255506
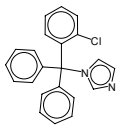	150 [a]	35	Yes	Yes	11110962
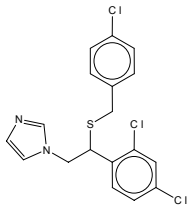	100 [a]	20	Yes	Yes	11112813
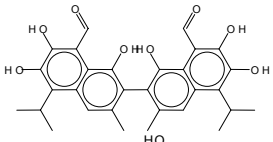	82[a]	46 [a]	Yes	Yes	11112318
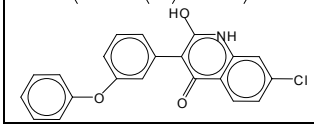	126[a]	22[a]	Yes	Yes	11113780

Table 2. Sensitivity to assay conditions among "nonaggregators". [a]Extrapolated IC_{50} values. [b]Highest soluble concentration.

known specific, reversible inhibitors of β-lactamase (from our previous work with this enzyme) and 24 known specific, covalent inhibitors (Figure 11a). The classical, competitive inhibitors all had dose-response curves consistent with single-site inhibition, with Hill coefficients near one. In contrast, the aggregators were biased toward steeper curves, with an average slope of 2.2 versus an average slope of 0.7 for the reversible inhibitors. The aggregator curves were also on average steeper than a set of irreversible β-lactam inhibitors, which had an average Hill slope of 1.2. The steep dose-response curves for the β-lactams is expected, given their generally low K_d values[52, 53]. Overall, 40% (70/174) of the aggregators had Hill coefficients greater than 1.5. Also, every compound with a high Hill slope was either an aggregator (93% of the time) or a covalent modifier (7% of the time). Thus, increased Hill coefficients may be reliable predictors of aggregation-based or, less frequently, potent covalent inhibition, though these predictions will also miss some aggregators. The high Hill slopes of both potent covalent and aggregation-based inhibitors, and indeed those of potent reversible inhibitors, have the same mechanistic origin: all are stoichiometric inhibitors with very low K_d values. For such molecules, inhibition is only observed when the inhibitor concentration approaches that of the enzyme. Since the latter is well-above the true K_d of the inhibitor, inhibition rises very quickly in this concentration range, leading to steep curves. Thus, for both aggregators and certain covalent inhibitors, high Hill slopes have nothing to do with cooperative binding and everything to do with high enzyme-to- K_d ratios[53].

A question that naturally arises is how often the aggregators found in this screen are active other enzyme screens of the MLSMR. More generally, do aggregates turn up with the same frequency in the other screens? It is difficult to probe the promiscuity of

the aggregators identified in this screen: few of the enzyme screens reported in PubChem test all, or even most of the MLSMR molecules; also the conditions of the screen and the definition of "actives" differ from screen to screen (many use detergent, for instance). However, one criterion that may be directly compared across enzyme screens is the Hill slope of active molecules. As of this writing, eighteen enzyme screens with annotated Hill slopes for each active are available in PubChem. This collection of screens has 6,254 actives associated. Of these, 1,452 (23%) have Hill slopes greater than 1.5 (Figure 11b). For those high-Hill slope molecules that were tested in two or more assays, the Hill coefficient was fairly stable, suggesting that these measurements are reliable and transferable (Figure 11c). In the β-lactamase screen, all molecules that had steep dose-response curves were either aggregators (93%) or covalent modifiers (7%). And while sensitivity to various mechanisms of false-positives may change from enzyme to enzyme, if this pattern extends to the other enzyme screens, it suggests that, despite the use of detergents and other adjuvants, at least 20% of the other enzyme actives are also aggregators. Since only about 45% of the aggregators identified in this study had high Hill slopes, the percentage of aggregation-based artifacts among the enzyme screens is likely to be higher still.

Our interest in undertaking this study was to test an assay that could quantify the presence of aggregate-based inhibitors in a high-throughput setting. Several caveats deserve mention. A surprising conclusion from this study is that so many of the actives were aggregators, and so few can be attributed to other mechanisms of inhibition. Whereas we suspect that similar patterns might occur in other enzyme assays, this inference is tentative, as enzymes with greater liabilities to chemical reactivity, or indeed

libraries with different compounds, may show different patterns. Also, we note that identification of an aggregating molecule does not disqualify that molecule from future activity. Whereas aggregators should be flagged for future screens, aggregation is concentration and condition dependent, and a molecule that aggregates under one condition and concentration may behave well under different conditions or lower concentrations. More importantly, counter-screens for aggregation should always be considered—one lesson of this study is that such assays may be straight-forward.

Perhaps the greatest liability of HTS is the occurrence of false-positive hits, and many mechanisms have been proposed to explain these. A key result of this study is that, at least for robust enzymes like β-lactamase, 95% of the artifactual hits owe to a single mechanism: colloidal aggregation followed by enzyme sequestration. Only five percent can be attributed to all other mechanisms of inhibition *put together*, including covalent modification, oxidation and assay interference. For well-behaved enzymes, the chemical reactivity mechanisms about which the field most worries may be rare in well-curated libraries. Instead, it may be the physical behavior of organic molecules that most contributes to false-positive hits in screening. Certainly, assays that ignore this effect risk drowning in a sea of artifacts. By the same coin, an encouraging aspect of aggregation is that it is a physical phenomenon that we can hope to understand and for which we can control. Pragmatically, we can deploy a simple high-throughput assay to detect it; this assay can be applied to most screening collections, in the highest-format assays, and can do much to prioritize molecules for follow-up experiments.

Materials and Methods:

Compound Library. The 70,563-member library was collected from several sources: 1,280 pharmacologically active compounds from LOPAC (Sigma-Aldrich), 1,120 compounds from Prestwick Chemical (Illkirch, France), 280 purified natural products from TimTec (Newark, DE), three 1,000-member combinatorial libraries from Pharmacopeia (Princeton, NJ), 1,106 compounds from Tocris (Bristol,U.K.), 59,684 compounds from the National Institutes of Health Molecular Libraries Small Molecule Repository (MLSMR, http://mlsmr.discoverypartners.com/MLSMR_HomePage/), 1,981 compounds from the National Cancer Institute (the NCI Diversity Set, http://dtp.nci.nih.gov/branches/dscb/diversity_explanation.html), 148 NCGC internally generated compounds, 20 control compounds from the Shoichet laboratory (UCSF), 96 beta-peptides from the Gellman laboratory (University of Wisconsin, Madison), 726 compounds from University of Pittsburg Center for Chemical Methodology and Library Development, and 1,121 compounds from Boston University Center for Chemical Methodology and Library Development. The library was deployed as DMSO solutions (7 μL each in 1536-well Greiner polypropylene compound plate) at initial concentrations ranging between 2 and 10 mM. Plates were serially diluted and compounds were assayed at final concentrations ranging from 4 nM to 30 μM. Plate-to-plate (vertical) dilutions and 384-to-1536 compressions were performed on an Evolution P3 dispense system equipped with a 384-tip pipetting head and two RapidStak units (Perkin-Elmer, Wellesley, MA). Additional details on the preparation of the compound library are provided elsewhere.[49]

Assay Implementation. The detergent-dependent screen was adapted from a previously described, 96-well format assay for the identification of promiscuous inhibitors.[47] Moving to a 1536-well format demanded changes to ensure a high signal-to-noise ratio; both a four-fold increase in enzyme and a two-fold increase in substrate concentration were required to maintain a high signal-to-noise ratio. Also, a five-fold increase in the concentration of Triton X-100, to 0.0001%, in the detergent(-) screen was needed to stabilize the enzyme. Meanwhile, the Triton X-100 concentration in the detergent(+) screen was lowered from 0.1% to 0.01% to avoid excess bubble formation. Technical adjustments to the liquid handling systems were also necessary to deal with this problem. Finally, serial dilutions were carried out in 5-fold intervals, resulting in DMSO percentages of 0.3%.

β-lactamase assays. AmpC β-lactamase was purified and assayed as described[6, 18], unless otherwise noted. The enzyme was present at 4 nM in a final reaction volume of 8 μL. Reactions were conducted in 1536-well Greiner black clear bottom plates, and liquids were handled using a solenoid-based dispenser. Compounds and controls (23 nL) were transferred via a Kalypsys PinTool equipped with a 1536-pin array and inline washing stations. The plates were incubated for 15 min at room temperature (22-23 °C) and reactions were initiated by the addition of substrate (dissolved in buffer, final concentration 400 μM). The plates were immediately transferred to a ViewLux (Perkin-Elmer) high-throughput CCD imager and read every 20 seconds for 4 min at 480 nm. During liquid handling, reagent bottles (AmpC, buffer, and nitrocefin solution) were kept

submerged in a 4 °C water bath. All screening operations were performed on a Kalypsys robotic system (Kalypsys Inc., San Diego CA) containing one RX-130 and two RX-90 anthropomorphic robotic arms. The absorbance difference between the last and first time points was used to compute the reaction progress.

Cuvette-based assays (1 mL reaction volume) either replicated the above conditions (stringent conditions) or contained 1 nM AmpC β-lactamase, 200 μM nitrocefin and 0.00002% Triton X-100 (relaxed conditions). Cuvette-based assays contained between 1-2% DMSO. Compound and enzyme were incubated for 5 minutes before the reaction was initiated by addition of substrate. Nitrocefin hydrolysis was monitored at 482 nm on a HP8453 UV-visible spectrophotometer.

Data Analysis. Initial curve-fitting and data analysis were conducted as previously described[49]. Briefly, concentration-effect relationships were derived using the GeneData Screener software package. Curves were categorized according to fit quality, response magnitude and degree of measured activity. Manual curve re-fitting was performed using Graphpad 5.0. The results of these screens are available through PubChem (http://pubchem.ncbi.nlm.nih.gov/) and the Shoichet Lab website (http://shoichetlab.compbio.ucsf.edu/).

Gloss to Chapter 4

The pathological aggregation of protein molecules into long fibrils is a process that occurs in many diseases, such as Alzheimer's, Parkinson's, prion diseases, diabetes and many more. The precise process by which these protein aggregates, called amyloid fibers, are involved in the progression of these diseases is unknown. Nonetheless, inhibition of this process is an important therapeutic target. Many small molecules have been observed to inhibit amyloid formation *in vitro*, some of which have even shown beneficial properties in cell or animal models of disease. However, none have been approved as drugs. One principal reason for this is that the mechanism by which these molecules inhibit fibril formation is poorly understood.

Many of these inhibitors resemble known aggregate-forming inhibitors. Since promiscuous aggregate particles nonspecifically associate with proteins, it is tempting to hypothesize that if these particles are able to sequester enzymes from substrate, they should be equally capable of sequestering proteins from other proteins. This chapter summarizes the progress made so far in testing this hypothesis. If true, many inhibitors of amyloid formation may be acting via the formation of promiscuous aggregates, rather than a more specific mechanism. It could be that aggregate-forming molecules are up to their old tricks, conveying, as Brian Shoichet says, "a cruel imitation of fidelity" on molecules seen to inhibit fibril formation *in vitro*. These molecules could be red herrings in the search for useful inhibitors of amyloid formation.

To approach this problem, a panel of known aggregators was assembled, and tested for the ability to inhibit amyloid formation in two well-studied models for amyloid

formation: the yeast protein Sup35 and Human Prion Protein (PrP). All 7 known aggregators did so. This panel was supplemented by three known inhibitors of amyloid formation culled from the literature. These molecules were shown to form promiscuous aggregates, and also inhibited amyloid formation of Sup35 and PrP. Aggregate-based inhibition of amyloid fibril formation was also directly observed by electron microscopy, further supporting our hypothesis.

The impact of this work will hopefully be to illustrate a novel mechanism for the inhibition of amyloid formation. It also seems likely that many—perhaps most—previously-identified inhibitors of amyloid fibril formation operate by this mechanism. I hope that this work will be instructive to those who are searching for novel inhibitors of fibril formation.

It is rare that a conceptually pretty hypothesis such as this—that chemical aggregates can inhibit pathological protein aggregation—turns out to be correct. Usually, these ideas are the first to be discarded when the data comes in. However, it has been exciting to discover that this idea may, in fact, have some merit. It seems fitting to close this dissertation with the project that has been the most enjoyable of my time in graduate school.

Chapter 4.

Inhibition of Amyloid formation by Promiscuous Small-molecule Aggregates

Brian Y. Feng[1], Brandon H. Toyama[2], Holger Wille[3], Dave Colby[3], Sean R. Collins[2], Barnaby May[3], Stan Prusiner[3], Jonathan Weissman[2] and Brian K. Shoichet[1,*]

[1]Department of Pharmaceutical Chemistry & Graduate Group in Chemistry and Chemical Biology, 1700 4th Street, University of California San Francisco, San Francisco, CA 94158-2330

[2]Howard Hughes Medical Institute, Department of Cellular and Molecular Pharmacology, University of California–San Francisco and California Institute for Quantitative Biomedical Research, San Francisco, CA 94143, USA.

[3]Institute for Neurodegenerative Diseases, University of California, San Francisco, CA 94143-0518, USA

[*]To whom correspondence should addressed:

E-mail: shoichet@cgl.ucsf.edu, Phone: 415-514-4126, Fax: 415-514-4260.

Abstract:

The formation of amyloid fibers by protein is implicated in many diseases. And though therapeutic interventions have been developed for some of these, no approved small-molecule therapeutics target the common step of amyloid formation. However, *in vitro* experiments, and increasingly, high-throughput screens (HTS) have detected many small molecules capable of inhibiting the formation of amyloid fibrils. One prominent source of false-positive results in HTS campaigns targeting enzymes is the tendancy of some small molecules to aggregate, and form colloidal particles which nonspecifically associate with proteins and sequester enzymes from substrate. Here, we examine the hypothesis that these aggregate-forming molecules can also inhibit the polymerization of amyloid fibrils. Fibril formation was monitored by thioflavin-T fluorescence, dynamic light scattering (DLS) and electron microscopy. A panel of ten known aggregators and two nonaggregators was assembled, and all ten inhibited fibrillization to varying degrees, while neither of the nonaggregators did. Consistent with an aggregate-based mechanism of inhibition, inhibition was sensitive to the presence of BSA, and aggregators also inhibited polymerization of the human prion protein PrP^{sc}. Thus, it appears that small molecule aggregates can nonspecifically inhibit amyloid formation in addition to enzyme function, and may act as false-positives in screens for novel small-molecule inhibitors of these processes.

Introduction

The aggregation of some proteins into amyloid fibrils is coincident with a growing list of diseases, including prion diseases, diabetes, Alzheimer's, Parkinsons, Huntingtons and more. In all of these cases, proteins of diverse sequence and structure are observed to adopt a prion-like cross-β conformation[56, 57] which aggregates into unbranched fibrils. Therapies for these disorders typically target disease symptoms or ancillary biological processes; so far, little therapeutic success has been had in trying to inhibit the formation of amyloid. In contrast to this, many small molecules have been shown to inhibit fibril formation *in vitro*[58-67]—some even have effects *in vivo* in animal models or man.[68, 69] High-throughput screens (HTS) for inhibition are being conducted increasingly often. The principle assay used in such campaigns monitors the fluorescence of thioflavin dyes, which have a characteristic absorbance/emission spectrum when associated with amyloid fibrils.

Though they allow efficient sampling of large numbers of molecules for inhibition, HTS traditionally exhibits high rates of false-positive inhibition. Many mechanisms have been proposed to explain artifactual inhibition, including assay interference[31], chemical reactivity[10] and oxidation[34]. In some screens, nearly all false-positive inhibition can be attributed to one additional mechanism: the aggregation of small molecules into large colloidal aggregates, which nonspecifically interact with proteins and inhibit enzymes.[70]

As with amyloid fibrillization, small molecule aggregation has been observed across a diverse range of chemical structures, and appears to be a common behavior among organic molecules. The peculiar inhibitory properties of these aggregating small

molecules have been well-studied in screens of enzyme targets[6-9, 46]. Here, we describe how this common class of small molecules also act as nonspecific inhibitors of amyloid fibril formation. We have observed this inhibition by multiple methods, including thioflavin-T fluorescence, dynamic light scattering (DLS) and transmission electron microscopy (TEM). This inhibition has been observed in two amyloid-forming protein systems: the yeast prion model system Sup35[71], and the human scrapie associated prion protein, Prp^{sc}.[72]

Results

Inhibition of Sup35 polymerization

A panel of molecules was assembled that had been previously studied for aggregate-based inhibition, consisting of seven aggregators and two nonaggregators. This group was supplemented by three promiscuous aggregate-forming molecules cited in the literature for inhibition of amyloid formation: the flavonoid baicalein, the chelator clioquinol, and DAPH. These three molecules had IC_{50}'s against β-lactamase of 30, 25, and 23 μM respectively (data not shown). All together, ten aggregators and two nonaggregators were screened for Sup35 inhibition. All ten inhibited seeded Sup35 fibrillization (Table 1). Among the most potent was tetraiodophenolpthalein (TIPT), which had an IC_{50} against Sup35 fibrillization of 2.5 μM (Figure 12a,b). Percent inhibition was calculated based on the initial rate of seeded fibrillization. Inhibition was also observed against unseeded Sup35 fibrillization (Figure 12c).

Table 3. Inhibition of 10 aggregators and 2 nonaggregator +/- BSA

Compound	Structure	% inhibition– Sup35	% inhibition– Sup35 + BSA
30 μM TIPT	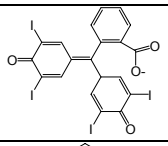	99.3	6.8
50 μM Clotrimazole	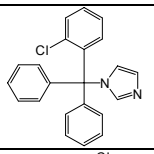	62.7	5.6
50 μM Sulconazole	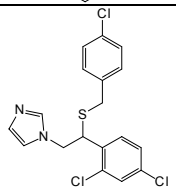	75.5	10.1
50 μM Nicardipine	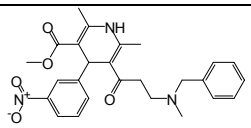	61.5	0.0
30 μM Rottlerin	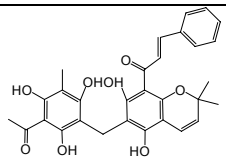	99.4	40.5
50 μM Baicalein	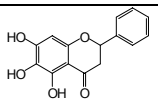	95.4	17.6
50 μM S3218	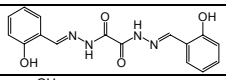	33.7	0
50 μM Clioquinol	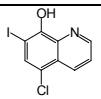	54.7	0
10 μM 4BPAP	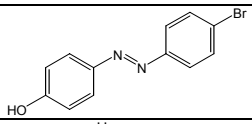	36.4	2.1
50 μM DAPH	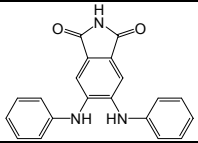	87.1	44.7
50 μM Lidocaine	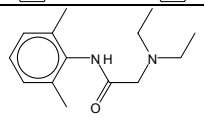	1.1	0
50 μM Fluconazole	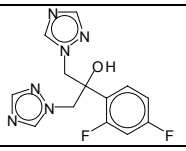	0	9

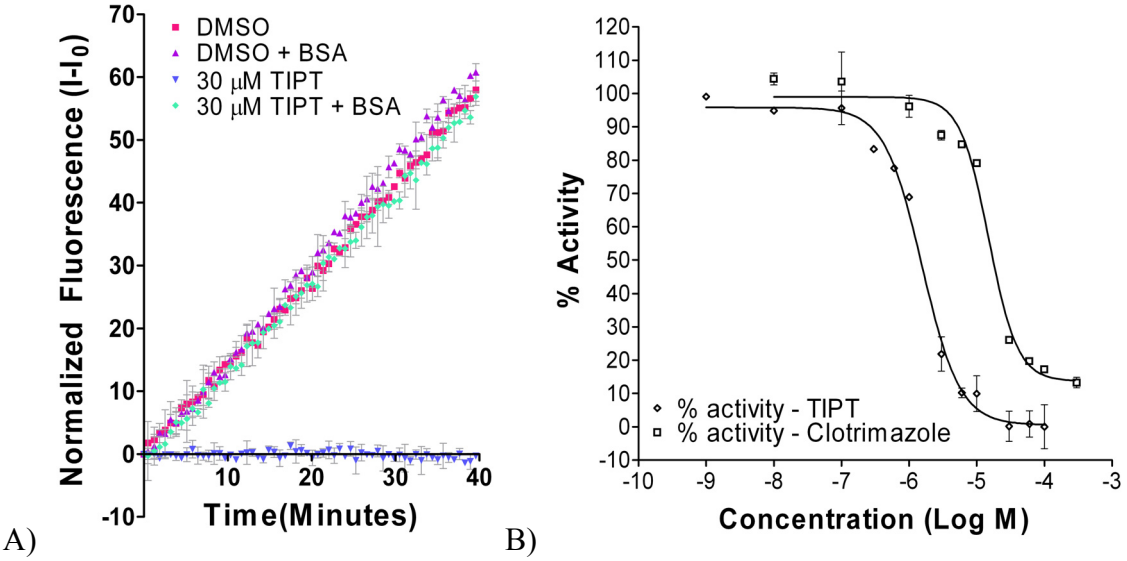

A) B)

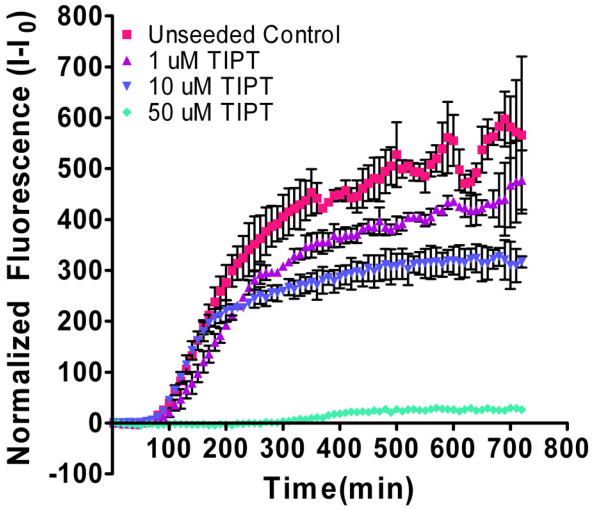

C)

Figure 12. Inhibition of Sup35 polymerization as measured by thioflavin-T fluorescence. A) Seeded polymerization fluorescence plotted vs. time. Inhibition by 30 µM TIPT (blue) is reversed in the presence of 5 mg/ml BSA (pink). B) Inhibition by aggregate-formers TIPT and clotrimazole is dose-dependant. C) Dose-dependant inhibition of unseeded Sup35 polymerization by TIPT. Unless otherwise mentioned, percent inhibition is calculated as a measure of initial polymerization relative to control.

Inhibition is due to the presence of small molecule aggregates

Many observations link this inhibition to the aggregate-based inhibition of enzymes. First, inhibition is time-dependant, and increases after preincubation of aggregate and seed for five minutes (data not shown), as seen for aggregate-based inhibition of enzymes. Additonally, the amount of inhibition observed is dependent on amount of seed fibril used in the fibrillization reaction (Figure 13)—likewise, the potency of aggregate-based inhibitors against enzymes is dependant on the enzyme concentration. A key characteristic of aggregate-based inhibition is sensitivity to detergent. However, in the case of Sup35 and other amyloid-forming proteins, nonionic detergents themselves disrupt polymerization. An alternative to detergent is preincubation with BSA, which, instead of disrupting aggregates, saturates the available binding area on the surface of the aggregate.[73] For all ten of the aggregators, inhibition was at least partially reversed in the presence of 5 mg/ml BSA (Figure 12a, Table 3). No inhibition was detected by the nonaggregators.

Aggregate-based inhibition can be observed using physical methods

Though the thioflavin assay is the most common method of reporting amyloid inhibition, it unfortunately relies on a reporter dye whose specific binding mechanism is still not fully understood.[74] Indeed, it has even been recently reported that thioflavin-T forms particles which associate with amyloid fibrils.[75] However, thioflavin-T appears distinct from the aggregators tested here in that it does not inhibit unrelated

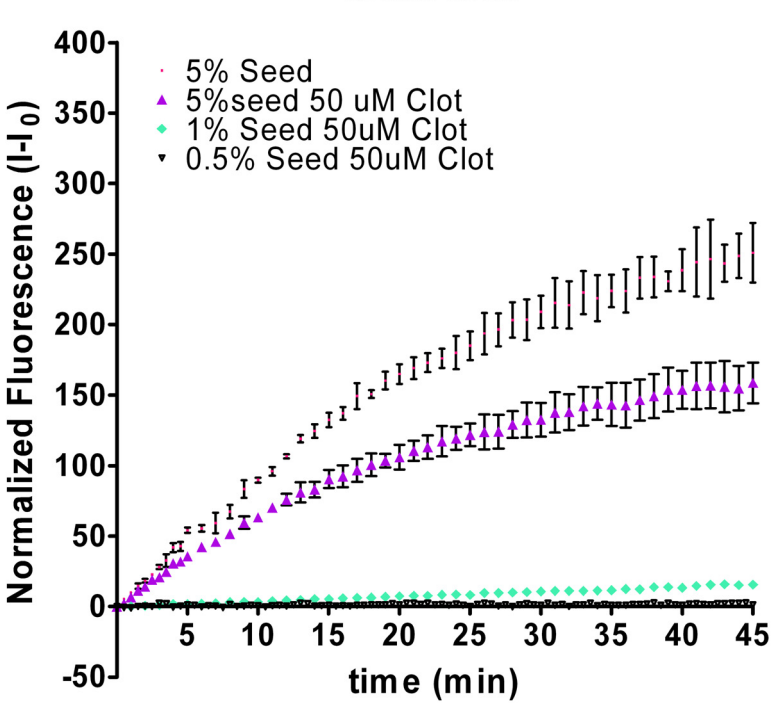

Figure 13. Percent inhibition is inversely dependant on the concentration of seed in the reaction.

enzymes such as β-lactamase (data not shown). We turned to a physical method of monitoring fibrillization, DLS. We tested two molecules by DLS: TIPT and clotrimazole, and both displayed inhibition of Sup35 (Figure 14).

Fibrils of both Sup35 and PrP^{sc} were examined by electron microscopy to qualitatively verify the results of the fibrillization assays. Previously, aggregators such as TIPT were imaged by negative stain; they appeared the same in these studies (data not shown). For both fibril-forming proteins, control fibrils grown in the presence of DMSO were easily visualized (Figure 15a, d) and were distributed densely on the grid. However, for grids prepared with fibrils grown in the presence of 50-100 μM TIPT, drastically fewer fibrils could be observed (Figure 15c,f); indeed, hardly anything was present on the grid at all. Instead, in the case of Sup35, small irregularly-shapped particles were observed, which appeared to be unpolymerized monomer (Figure 15c). Rarely, a small cluster of fibrils was observed associated with TIPT aggregates under these conditions. As a control, preformed fibrils of both proteins were mixed with a solution of 100 μM TIPT, and fibrils densely coated with aggregtes were observed (Figure 15b,c). As a variation on this experiment, we also prepared grids first by depositing Sup35 fibrils, and then subsequently depositing 100 μM TIPT. For these grids, aggregates were only visualized associated with amyloid fibril; no aggregates were visualized elsewhere on the grid.

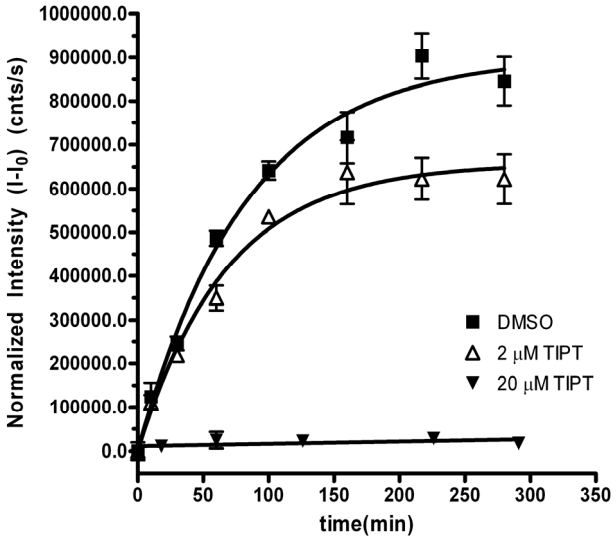

A)

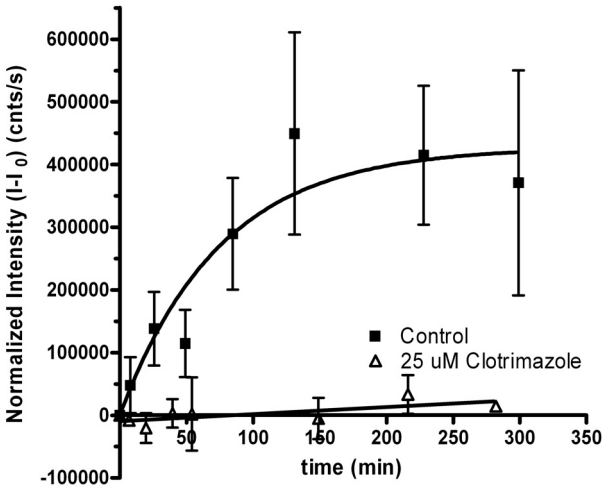

B)

Figure 14. Sup35 polymerization inhibited by A) 2 μM and 20 μM TIPT and B) 25 μM clotrimazole as monitored by dynamic light scattering.

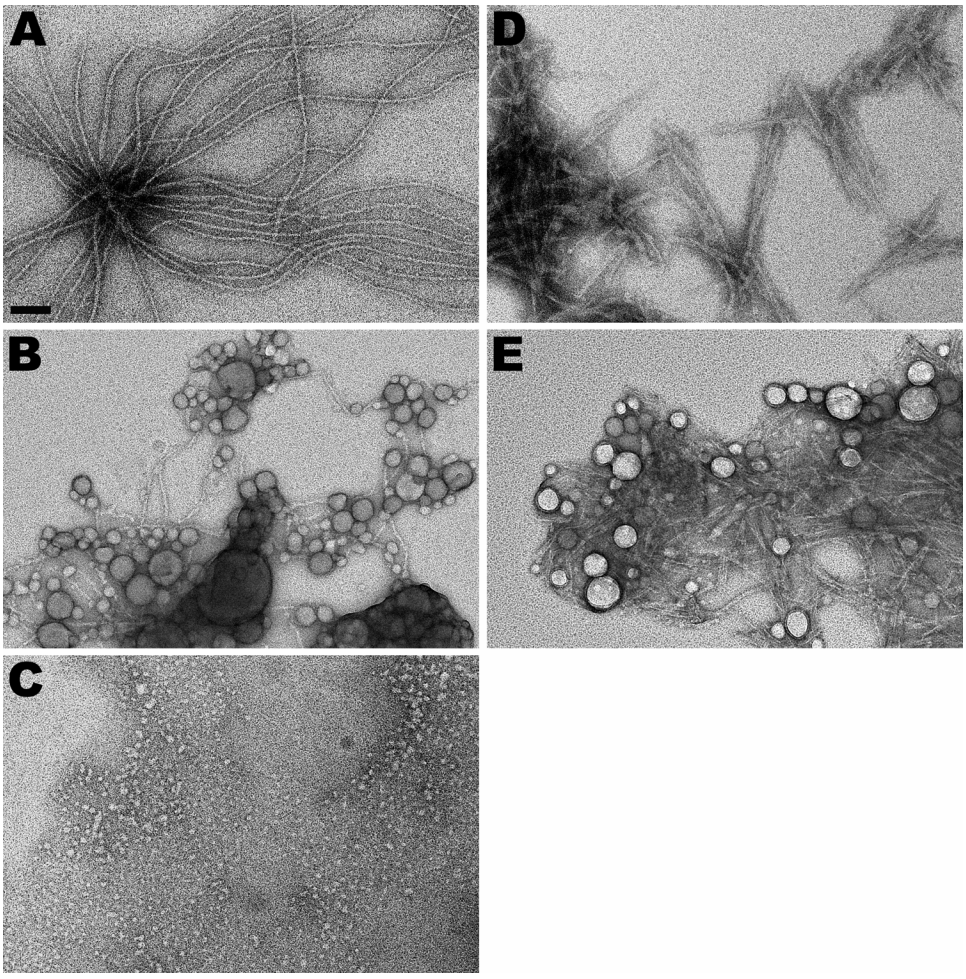

Figure 15. Electron microscopy studies of Sup35 and PrP^{sc}. A) Sup35 fibrils alone. B) 100 μM TIPT + pre-formed Sup35 fibrils. C) 50 μM TIPT + Sup35 fibrillization reaction. D) PrP^{sc} fibrils alone. E) 100 μM TIPT + pre-formed PrP^{sc} fibrils.

Aggregate-based inhibitors are nonspecific for Sup35 fibrillization

Based on the nonspecificity of aggregate-protein interactions, it seems reasonable to think that aggregate-based inhibition is capable of affecting the *in vitro* fibrillization of all amyloid-forming proteins. To test this hypothesis, four aggregate-based inhibitors and one nonaggregator were tested for inhibition of human prion protein (PrP^{sc}) fibrillization. All aggregators inhibited (Figure 16) PrP^{sc} polymerization with similar potencies as against Sup35.

Multiple mechanisms of inhibition observed in unseeded fibrillization

Aggregate-based inhibition of unseeded fibrillization yielded an additional observation. One aggregator, TIPT, exhibited a significant effect on the total extent of fibrillization, and a somewhat less-pronounced effect on the duration of the lag phase of fibrillization. In contrast, clotrimazole exhibited almost no effect on the extent of fibrillization, but significantly extended the duration of the lag phase (Figure 17a). To control for the possbility this difference may be due to interference in the assay readout rather than any real difference in the extent of fibrillization, the results of unseeded fibrillization were examined on a gel, the total amount of monomer was quantified via western blot. The concentration of the monomer in the TIPT-containing reaction was significantly higher than that of the control and clotrimazole-containing reactions (Figure 17b,c).

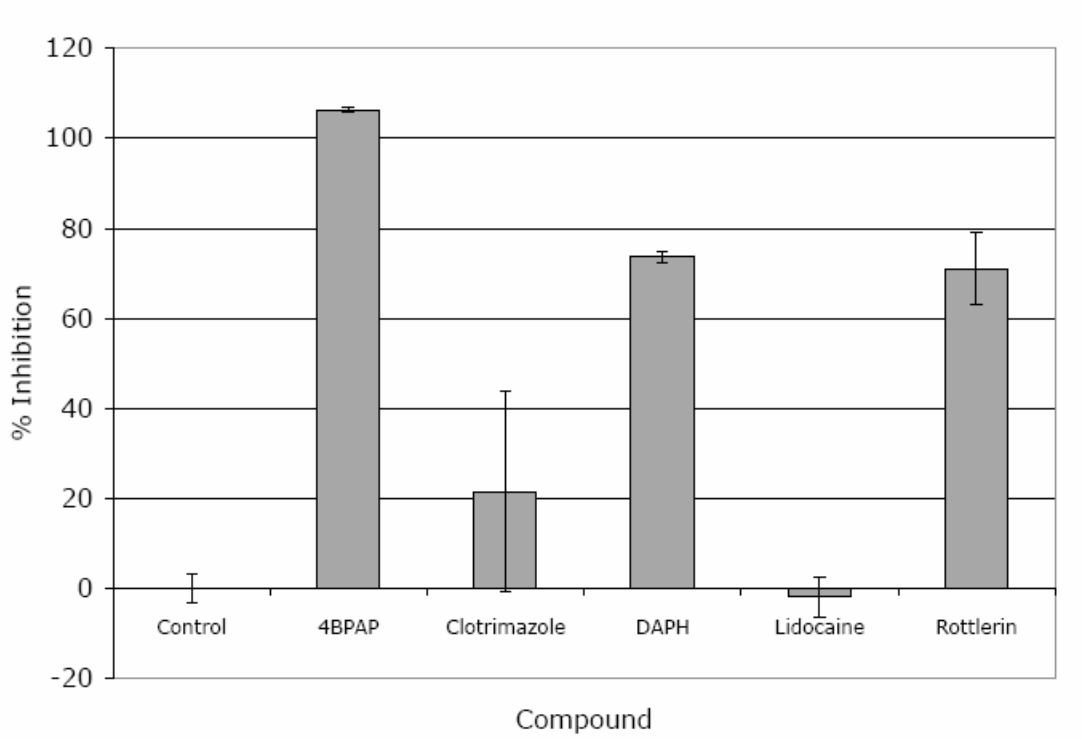

Figure 16. Inhibition of human prion protein by 4 aggregators and 1 nonaggregator.

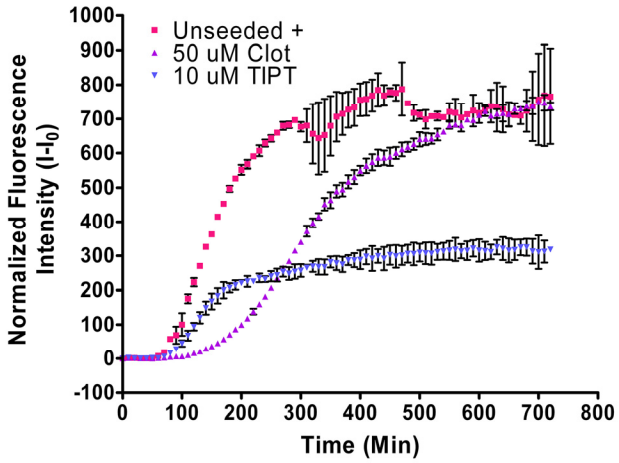

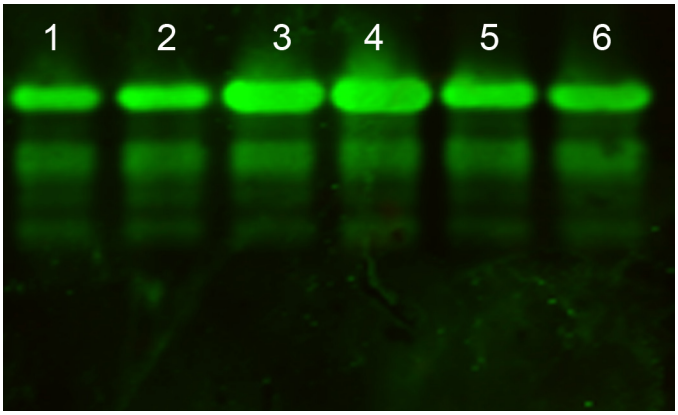

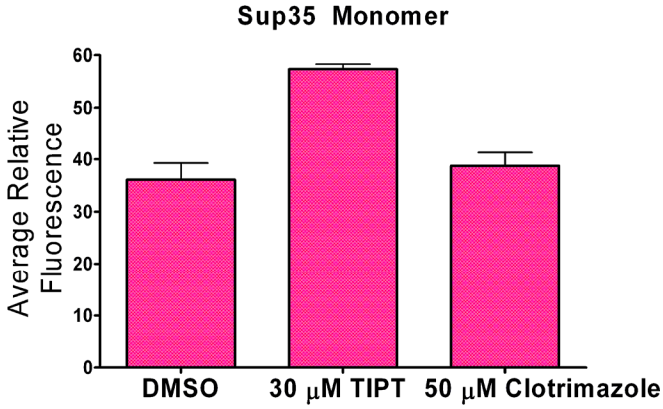

Figure 17. Differing patterns of unseeded inhibition by TIPT and clotrimazole. A) Thioflavin-T fluorescence of unseeded inhibition. B) Western blot of the results of an unseeded polymerization reaction. Lanes 1,2-DMSO control, 3,4-TIPT inhibited reaction, 5,6-clotrimazole inhibited reaction. C) Quantification of western blot results.

Discussion

Perhaps the most important conclusion to be drawn from this study is that small molecule aggregation presents a novel mechanism for inhibition of amyloid fibrillization. Ten-of-ten tested aggregators inhibited seeded fibrillization to varying extent, while two known nonaggregator was inactive (Table 1). This inhibition displayed all of the hallmarks of aggregate-based inhibition: time-dependance, concentration dependance and reversal in the presence of BSA, here used as a proxy for detergent. Fibrillization is inhibited in a dose-dependant manner, and dose-response curves were calculated for two compounds, TIPT and clotrimazole. These curves are noteworthy in that they both exhibit steeper-than-normal Hill slopes—1.6 and 2 respectively (Figure 12b). Such steepness is also a feature of aggregate-based inhibition.

Mechanistically, it is difficult to attribute inhibition due to a direct association of aggregate and protein on the basis of the above observations alone. One alternative hypothesis may be that in fact the aggregates are simply competing with thioflavin-T for binding to fibrils. However, physical measurements of fibrillization by DLS and TEM suggest that the promiscuous aggregates are directly associating with the fibrils and inhibiting polymerization. The observation that inhibition can be competed away with increasing seed fibrils also supports this. Thus, we propose that aggregates are nonspecifically inhibiting amyloid formation much in the way that they associate with enzyme molecules. However, in this case, instead of sequestering enzyme from

substrate, aggregates are binding both nucleating particles of amyloid and soluble monomers, preventing their interaction and the formation of mature fibrils.

Historically, electron microscopy has been a valuable technique for studying both chemical aggregates and amyloid-forming proteins. Such studies have been used as a physical means of observing both inhibition of fibril growth and aggregate-based inhibition. Here, we use it to support the hypothesis that chemical aggregates are capable of inhibiting fibrillization. This is not without precedent, as similar images have previously been shown in the literature.[58] Compared to control images of TEM fibrillization reactions, aggregate-treated reactions showed a dramatic decrease in observed fibrils—essentially an empty grid in most cases. There seem to be two explanations; either aggregates thoroughly inhibited fibrillization, or the aggregates were interfering with the deposition of amyloid onto the grid. To control for this latter possibility, preformed fibrils were mixed with a solution of aggregate and imaged. Under this condition, mature amyloid fibrils were observed thoroughly coated with chemical aggregates (Figure 15b,e). However, when fibers alone were first deposited on the grid, and a solution of aggregates was applied on top of this, we again observed dense labeling of the fibrils by aggregates, whereas unassociated aggregates were not observed. High concentrations of compound had to be used in these experiments, as TIPT aggregates were easily washed from the grid surface.

Because of the nonspecific nature of protein-aggregate interactions, it seems likely that aggregate-based inhibition of amyloid should extend to multiple amyloidogenic proteins. To test this hypothesis, we also screened 5 molecules for inhibition of PrP fibrillization in a thioflavin-T assay (Figure 16). Notably, the buffer

conditions, protein and mechanics of the assay were different from the Sup35 experiments.[76] The nonspecificity of small molecules that inhibit amyloid is not a new observation; for example, baicalein has been shown to inhibit fibrillization of α-synuclein and lactalbumin, as well as inhibiting Aβ-induced cytotoxicity.[63, 77, 78]

The detergent-sensitivity of aggregate-based inhibition has traditionally been a feature with which to distinguish specific inhibition. Unfortunately, it seems quite common for detergents themselves to possess inhibitory properties against fibrillization. The second-line test for reversability in such cases is the use of BSA to saturate the surface of the aggregate.[73] As a counter-screen for aggregate-based inhibition of amyloid formation, this has two problems. First, BSA can sequester monomeric small molecules in addition to saturating the binding sites of aggregates. Secondly, BSA can also inhibit fibrillization of some amyloid proteins, such as PrP^{sc}. Thus, for proteins where BSA has no effect on fibrillization, this approach is an efficient method for distinguishing aggregate-based inhibition from specific inhibition. However, for systems where BSA interferes with fibrillization, other features of aggregate-based inhibition can be used to separate it from specific inhibition; for example, inhibition of an unrelated enzyme, such as β-lactamase, the time-dependance of inhibition or a the dependance of potency on protein concentration.

Aggregate-based inhibition was also observed in unseeded polymerization reactions. Strikingly, we observed two different patterns of inhibition among the two of the aggregators tested. This raises the possibility of multiple mechanisms of aggregate-based inhibition. The thioflavin-T data suggests that TIPT exhibits it's most pronounced effect on the extent of fibrillization, while clotrimazole mainly affects the duration of the

lag phase was striking (Figure 17). To see if these experiments actually correlated with a difference in the extent of fibrillization, we quantified the amount of monomer present at the end of unseeded fibrillization reactions containing the two molecules. This experiment showed significantly more monomer present in the TIPT-inhibited reaction than in the clotrimazole-inhibited reaction, though the extent of the difference between TIPT-inhibited and clotrimazole-inhibition were not consistent between these two experimental methods. However, consistent with the thioflavin results, the concentration of monomer in the clotrimazole-inhibited reaction was equivalent to that of the control reaction in the western blot. It may be that the different conditions of the two experiments make direct numerical comparison of these results difficult. Together, these results suggest that inhibition of unseeded polymerization due to clotrimazole aggregates is perhaps not quite as complete as TIPT-mediated inhibition, and is eventually surmountable. No such recovery was observed in seeded reactions. This is consistent with the observation that aggregates of different small molecules have different properties, such as size, affinity for protein and sensitivity to detergent or BSA.

The advent of high-throughput screening introduced many mechanisms of artifactual inhibition to the screening community. One such mechanism, perhaps the most common of all, is the tendancy for some small molecules to aggregate and nonspecifically associate with protein and inhibit enzymes. Here, we describe how this same class of small molecules, as a result of a similar nonspecific association, can inhibit amyloidogenesis. We hypothesize that this may constitute a source of false-positive inhibition that could interfere with the search for small-molecule inhibitors of amyloid formation. It seems likely that aggregate-based inhibitors are not good candidates for

chemically interfering with amyloid formation. First, based on these experiments, it appears aggregates have affinity for both the monomeric conformations of proteins as well as the amyloid form (not to mention any other proteins present in the reaction). Secondly, they are unlikely to be active in more complicated biological contexts—five aggregators were tested in a cell-based assay for human prion formation and showed no effect (data not shown). One exception to this may be amyloid-mediated cytotoxicity; conceivably aggregates could sequester amyloid particles and prevent their interaction with cells. Notably, many of the molecules described here are known to have effects *in vivo*. We expect that these effects are distinct from their behavior in *in vitro* assays for fibril formation, and may be due to more conventional types of interactions with proteins. As the search for chemical inhibitors of amyloid formation continues, it will be necessary to distinguish nonspecific fibril inhibition from more specific inhibition. Thus, we hope that the above experiments offer a framework for how this can be done, and to assist in the discovery of more usefull small molecules.

Materials and Methods

Compounds

Thioflvain-T, Tetraiodophenolpthalein, Sulconazole, Rottlerin, Baicalein, S3218, Clioquinol, and 4BPAP were purchased from Sigma (St. Louis, MO). Clotrimazole, Fluconazole, Lidocaine

and Nicardipine were purchased from MP Biomedicals (Solon, OH). DAPH was purchased from Wako Chemical USA, Inc. (Richmond, VA). Compounds were prepared as 10 mM stocks in neat DMSO. Thioflavin-T was dissolved in 50 mM Glycine, pH 8.5. BSA was also purchased from Sigma and dissolved in fibrillization buffer (see below).

Purification of Sup35

Sup35-NM was expressed and purified as previously described.[79-81] Briefly, a polyhistadine-tagged Sup35-NM construct was expressed in *E. coli* BL21(DE3) cells and purified over a nickel column.

Sup35 Thioflavin-T assays

Unless otherwise specified, Sup35 polymerization was assayed as follows. The fibrillization buffer consisted of 150 mM NaCl, 5mM KPO_3, pH 7.4. Reactions were monitored at $\lambda_{ex/em}$ 442/483 nm, in the presence of 12.5 μM thioflavin-T, at room temperature on a SpectraMax M2. Seed fibrils were grown at room temperature overnight, and sonicated briefly. Seeded reactions contained 1% seed. Inhibition reactions were prepared as follows: small molecule was incubated for 5 minutes with seed, followed by addition of thioflavin-T. Reactions were initiated by the addition of monomer. BSA containing fibrillization reactions contained 5 mg/ml BSA. These reactions were carried out as above, except for an additional preincubation step of BSA and small molecule for five minutes prior to the addition of seed fibrils. Unseeded reactions were carried out as above, simply without the addition of seed.

Purification of PrP

PrP was purified as previously described.[82, 83]

PrP Thioflavin-T assays

Thioflavin-T association with amyloid was measured as previously described.[84]

DLS experiments

DLS experiments were conducted on a Protein Solutions (now Wyatt) Dynapro MS/X. Fibrillization reactions were prepared as above, without thioflavin-T. Triplicate samples were analyzed for time point and the average intensity of scattered light was plotted over time.

Negative Staining and Electron Microscopy

Negative staining was carried out as described previously.[85] Briefly, formvar / carbon coated 200 mesh copper grids (Ted Pella, Inc.; Redding, CA) were glow discharged prior to staining. Five-μL samples were adsorbed for ~30 seconds, then the grids were washed with 1 drop (50 μL) of each 0.1 M and 0.01 M ammonium acetate (pH 7.4), afterwards the grids were stained with 2 drops (50 μL) of freshly filtered stain (2% uranyl acetate or 2% ammonium molybdate). After drying, the samples were viewed in a FEI Tecnai F20 electron microscope (Eindhoven, The Netherlands) at 80 kV and a standard magnification of 25,000. Electron micrographs were recorded with a Gatan Ultrascan CCD camera. The magnification was calibrated using negatively stained catalase crystals and ferritin.

Future Directions

Small molecules have been known to aggregate for many years. Many aggregation phenomena have been studied extensively, which has resulted in important technological innovations in the areas of detergents, drug delivery, dyes and optics. The key observation that some small molecule aggregates nonspecifically associate with protein and inhibit enzymes is a striking one, and this dissertation has described the prevalence of this phenomenon and some of its properties. However, many basic aspects remain shrouded in mystery.

What are promiscuous aggregates?

The behavior of other aggregative phenomena, such as micelle formation or liquid crystals are understood at the thermodynamic level. However, the thermodynamic forces that drive aggregate formation, and the energetics of the aggregate-protein association have not been studied. Calorimetry could be used to study both of these questions. Preliminary studies indicate that aggregation does resemble a phase transition, and so differential scanning calorimetry could be used to measure the energetics of aggregate formation. This experiment would indicate if this process is driven by the hydrophobic effect or favorable enthalpic interactions. Likewise, isothermal titration calorimetry could be used to measure the binding affinity of aggregate and protein, provided the concentration of aggregate particles be known. Insights into the thermodynamic

properties of these particles may provide clues as to why this behavior is so common, and what its applications might be.

It is possible that aggregate formation is a relative of better-studied phenomena. Some preliminary data supports the notion that promiscuous aggregates may share some properties with liquid crystals, a group of molecules that have very useful optical properties. A small number of known liquid crystal-forming molecules were examined, all of which exhibited detergent-sensitive inhibition of β-lactamase and detectable particles by DLS. Further studies using known liquid crystal forming molecules should be pursued to develop this relationship.

From a structural perspective, little is understood about how aggregates and proteins interact. Why are aggregate-associated enzymes inhibited? Are protein molecules sequestered inside hollow aggregate particles as well as on their surface? Microscopy and possibly tomography offer the potential to view aggregates and proteins associated in three dimensions, which may help to address questions as to the nature of their interaction. One experiment that was pursued briefly was to decorate the surface of an aggregate with colloidal-gold linked antibodies. The colloidal gold particles would then serve as points of contrast allowing for more sophisticated microscopic techniques. Pilot experiments worked well, but there were complications with glycerol in the antibody solution that obscured imaging.

The biological relevance of promiscuous aggregates

Given how common aggregate formation is among small molecules, is it possible that aggregates have a wider biological relevance? For instance, how do aggregates

interact with cells? Although many known aggregate-formers, such as the flavonoids quercetin and baicalein, have been historically seen to have *in vivo* effects, it has been difficult to relate these effects to aggregate-formation. On the other hand, recent work has suggested that aggregates are stable in high protein environments, so perhaps there is more to the story.[73] One possibility is that aggregates may be able to interact with receptors and proteins at the cell surface. Circumstantially, the literature is full of molecules that resemble aggregators inhibiting cell-surface proteins. Some preliminary data suggested that aggregators were capable of inhibiting the P2X ion channel, though these results were hard to produce reliably. Other experiments, conducted in conjunction with the now-closed company Berlex indicated that aggregators had no effect in many cell-based receptor assays. The question remains open, and awaits only someone with the time and expertise to run these complicated assays.

Nonspecific protein aggregation and precipitation is a common problem in molecular biology as well as in the design of therapeutic peptides. Additionally, small protein aggregates have also been observed to possess cytotoxic properties. Perhaps a possible application of aggregating small molecules is as a chemical chaperone that can prevent the unwanted aggregation of proteins in *in vitro* systems and shield cells from unwanted cytotoxic effects. Simple cytotoxicity assays are easily obtainable, and could be used to probe this hypothesis.

Promiscuous aggregates represent a novel association between small molecules and proteins. Much remains unknown about this association, but what has been observed has already had a significant effect on the HTS community—perhaps the clearest lesson

they have provided is that we should be attentive and skeptical of small molecules. There is much we don't know, and much more to learn.

References

(1) Flemming, A. On the Antibacterial Action of Cultures of a Penicillium, with Special Reference to Their Use in the Isolation of *B. Influenzæ*. *Br J Exp Pathol* **1929,** 10, 226–236.

(2) Jones, R. Nonsteroidal Anti-Inflammatory Drug Prescribing: Past, Present, and Future. *Am. J. Med.* **2001,** 110, S4-S7.

(3) Walmsley, R.; Tweats, D. Reducing Late Stage Attrition with Early High-Throughput Genotoxicity Screening. *Drug Plus International* **2006**.

(4) Brown, D.; Superti-Furga, G. Rediscovering the Sweet Spot in Drug Discovery. *DDT* **2003,** 8, 1067-1077.

(5) DiMasi, J. A.; Hansen, R. W.; Grabowski, H. G. The Price of Innovation: New Estimates of Drug Development Costs. *J Health Econ* **2003,** 22, 151-185.

(6) McGovern, S. L.; Caselli, E.; Grigorieff, N.; Shoichet, B. K. A Common Mechanism Underlying Promiscuous Inhibitors from Virtual and High-Throughput Screening. *J. Med. Chem.* **2002,** 45, 1712-1722.

(7) McGovern, S. L.; Helfand, B. T.; Feng, B. Y.; Shoichet, B. K. A Specific Mechanism of Nonspecific Inhibition. *J. Med. Chem.* **2003,** 46, 4265-4272.

(8) McGovern, S. L.; Shoichet, B. K. Kinase Inhibitors: Not Just for Kinases Anymore. *J. Med. Chem.* **2003,** 46, 1478-1483.

(9) Seidler, J.; McGovern, S. L.; Doman, T.; Shoichet, B. K. Identification and Prediction of Promiscuous Aggregating Inhibitors among Known Drugs. *J. Med. Chem.* **2003,** 46, 4477-4486.

(10) Rishton, G. M. Reactive Compounds and *in Vitro* False Positives in Hts. *DDT* **1997,** 2, 382-384.

(11) Walters, W. P.; Ajay; Murcko, M. A. Recognizing Molecules with Drug-Like Properties. *Curr. Opin. Chem. Biol.* **1999,** 3, 384-387.

(12) Veber, D. F.; Johnson, S. R.; Cheng, H. Y.; Smith, B. R.; Ward, K. W.; Kopple, K. D. Molecular Properties That Influence the Oral Bioavailability of Drug Candidates. *J. Med. Chem.* **2002,** 45, 2615-2623.

(13) Roche, O.; Schneider, P.; Zuegge, J.; Guba, W.; Kansy, M.; Alanine, A.; Bleicher, K.; Danel, F.; Gutknecht, E. M.; Rogers-evans, M.; Neidhart, W.; Stalder, H.; Dillon, M.; Sjogren, E.; Fotouhi, N.; Gillespie, P.; Goodnow, R.; Harris, W.; Jones, P.; Taniguchi, M.; Tsujii, S.; Vvon Der Saal, W.; Zimmermann, G.; Schneider, G. Development of a Virtual Screening Method for Identification of "Frequent Hitters" in Compound Libraries. *J. Med. Chem.* **2002,** 45, 137-142.

(14) Frenkel, Y. V.; Clark, A. D., Jr.; Das, K.; Y.-H., W.; Lewi, P. J.; Janssen, P. A. J.; Arnold, E. Concentration and Ph Dependent Aggregation of Hydrophobic Drug Molecules and Relevance to Oral Bioavailability. *J. Med. Chem.* **2005,** in press.

(15) Ryan, A. J.; Gray, N. M.; Lowe, P. N.; Chung, C.-w. Effect of Detergent on "Promiscuous" Inhibitors. *J. Med. Chem.* **2003**, 3448-3451.

(16) Lipinski, C. A.; Lombardo, F.; Dominy, B. W.; Feeney, P. J. Experimental and Computational Approaches to Estimate Solubility and Permeability in Drug Discovery and Development Settings. *Adv Drug Deliv Rev* **1997,** 23, 3-25.

(17) Breiman, L. Random Forests. *Machine Learning* **2001,** 45, 5-32.
(18) Weston, G. S.; Blazquez, J.; Baquero, F.; Shoichet, B. K. Structure-Based Enhancement of Boronic Acid-Based Inhibitors of Ampc Beta-Lactamase. *J. Med. Chem.* **1998,** 41, 4577-4586.
(19) Ghose, A. K.; Viswanadham, V. M.; Wendoloski, J. J. A Knowledge-Based Approach in Designing Combinatorial or Medicinal Chemistry Libraries for Drug Discovery. 1. A Qualitative and Quantitative Characterization of Known Drug Databases. *Journal of Combinatorial Chemistry* **1999,** 1, 55-68.
(20) Houghten, R.; Pinilla, C.; Appel, J.; Blondelle, S.; Dooley, C.; Eichler, J.; Nefzi, A.; Ostresh, J. Mixture-Based Synthetic Combinatorial Libraries. *J. Med. Chem.* **1999,** 42, 3743-3777.
(21) Devlin, J.; Lian, A.; Trinh, L.; Polokoff, M.; Senator, D.; Zheng, W.; Kondracki, J.; Kretschmer, P.; Morser, J.; Lipson, S.; Spann, R.; Loughlin, J.; Dunn, K.; Morrissey, M. High Capacity Screening of Pooled Compounds: Identification of the Active Compound without Re-Assay of Pool Members. *Drug Dev. Res.* **1996,** 37, 80-85.
(22) Pinilla, C.; Appel, J.; Borras, E.; Houghten, R. Advances in the Use of Synthetic Combinatorial Chemistry: Mixture-Based Libraries. *Nature Medicine* **2003,** 9.
(23) Taylor, E.; Gibbons, J.; Braeckman, R. Intestinal Absorption Screening of Mixtures from Combinatorial Libraries Ni the Caco-2 Model. *Pharm. Res.* **1997,** 14, 572-577.
(24) Wu, X.; Glickman, J.; Bowen, B.; Sills, M. Comparison of Assay Technologies for a Nuclear Receptor Assay Screen Reveals Differences in the Sets of Identified Functional Antagonists. *J. Biomol. Screening* **2003,** 8, 381-392.
(25) Snider, M. Screening of Compound Libraries...Consomme or Gumbo? *J. Biomol. Screening* **1998,** 3, 169-170.
(26) Hamers, T.; Molin, K.; Koeman, J.; Murk, A. A Small-Volume Bioassay for Quantification of the Esterase Inhibiting Potency of Mixtures of Organophosphate and Carbamate Insecticides in Rainwater: Development and Optimization. *Toxicol. Sci.* **2000,** 58, 60-67.
(27) Geysen, H.; Rodda, S.; Mason, T. A Priori Delineation of a Peptide Which Mimics a Discontinuous Antigenic Determinant. *Mol. Immunol.* **1986,** 23, 709-715.
(28) Houghten, R.; Pinilla, C.; Blondelle, S.; Appel, J.; Dooley, C.; Cuervo, J. Generation and Use of Synthetic Peptide Combinatorial Libraries for Basic Research and Drug Discovery. *Nature* **1991,** 354, 84-86.
(29) Pinilla, C.; Appel, J.; Blanc, P.; Houghten, R. Rapid Identification of High Affinity Peptide Ligands Using Positional Scanning Synthetic Peptide Combinatorial Libraries. *Biotechniques* **1992,** 13, 901-905.
(30) Ferrand, S.; Schmid, A.; Engeloch, C.; Glickman, J. Statistical Evaluation of a Self-Deconvoluting Matrix Strategy for High-Throughput Screening of the Cxcr3 Receptor. *Assay and Drug Development Technologies* **2005,** 3, 413.
(31) Walters, W. P.; Ajay, A.; Murcko, M. A. Recognizing Molecules with Drug-Like Properties. *Curr. Opin. Chem. Biol.* **1999,** 3, 384-387.
(32) Rishton, G. M. Nonleadlikeness and Leadlikeness in Biochemical Screening. *DDT* **2003,** 8, 86-96.

(33) Walters, W. P.; Namchuk, M. Designing Screens: How to Make Your Hits a Hit. *Nat Rev Drug Discov.* **2003,** 2, 259-266.
(34) Huth, J.; Mendoza, R.; Olejniczak, E.; Johnson, R.; Cothron, D.; Liu, Y.; Lerner, C.; Chen, J.; Hajduk, P. Alarm Nmr: A Rapid and Robust Experimental Method to Detect Reactive False Positives in Biochemical Screens. *J. Am. Chem. Soc.* **2005,** 127, 217-224.
(35) Feng, B. Y.; Shelat, A.; Doman, T. N.; Guy, R. K.; Shoichet, B. K. High-Throughput Assays for Promiscuous Inhibitors. *Nature Chemical Biology* **2005,** 1, 146 - 148.
(36) Chung, T. Screen Compounds Singly: Why Muck It Up? *J. Biomol. Screening* **1998,** 3, 171.
(37) Wilson-Lingardo, L.; Davis, P. W.; Ecker, D. J.; Hebert, N.; Acevedo, O.; Sprankle, K.; Brennan, T.; Schwarcz, L.; Freier, S. M.; Wyatt, J. R. Deconvolution of Combinatorial Libraries for Drug Discovery: Experimental Comparison of Pooling Strategies. *J. Med. Chem.* **1996,** 39, 2720 -2726.
(38) Chou, T.; Talalay, P. A Simple Generalized Equation for the Analysis of Multiple Inhibitions of Michaelis-Menten Kinetic Systems. *J Biol Chem* **1977,** 252, 6438-6442.
(39) Chou, T.; Talalay, P., Quantitative Analysis of Dose-Effect Relationships: The Combined Effects of Multiple Drugs or Enzyme Inhibitors. In *Advances in Enzyme Regulation*, ed.; 'Ed.'^'Eds.' 1984; 'Vol.' 22, p^pp 27-55.
(40) Chou, T.; Talalay, P. Generalized Equations for the Analysis of Inhibitions of Michaelis-Menten and Higher-Order Kinetic Systems with Two or More Mutually Exclusive and Nonexclusive Inhibitors. *Eur. J. Biochem.* **1987,** 115, 207-216.
(41) Proudfoot, J. R. Drugs, Leads, and Drug-Likeness: An Analysis of Some Recently Launched Drugs. *Bioorganic Med. Chem. Lett.* **2002,** 12, 1647-1650.
(42) Druker, B. J.; Lydon, N. B. Lessons Learned from the Development of an Abl Tyrosine Kinase Inhibitor for Chronic Myelogenous Leukemia. *J. Clin. Invest.* **2000,** 105, 3-7.
(43) Oldenburg, K. High Throughput Sonication: Evaluation for Compound Solubilization. *Comb Chem High Throughput Screen* **2005,** 8, 499-512.
(44) Martin, Y. C. A Bioavailability Score. *J. Med. Chem.* **2005,** 48, 3164-3170.
(45) Liu, H.; Wang, Z.; Regni, C.; Zou, X.; Tipton, P. A. Detailed Kinetic Studies of an Aggregating Inhibitor; Inhibition of Phosphomannomutase/Phosphoglucomutase by Disperse Blue 56. *Biochemistry* **2004,** 27, 8662-8669.
(46) Feng, B.; Shoichet, B. K. Synergy and Antagonism of Promiscuous Inhibition in Multiple-Compound Mixtures. *J. Med. Chem.* **2006,** 49, 2151-2154.
(47) Feng, B. Y.; Shoichet, B. K. A Detergent-Based Assay for the Detection of Promiscuous Inhibitors. *Nature Protocols* **2006,** 1, 550-553.
(48) Reddie, K. G.; Roberts, D. R.; Dore, T. M. Inhibition of Kinesin Motor Proteins by Adociasulfate-2. *J. Med. Chem.* **2006,** 49, 4857-4860.
(49) Inglese, J.; Auld, D.; Jadhav, A.; Johnson, R.; Simeonov, A.; Yasgar, A.; W, Z.; CP, A. Quantitative High-Throughput Screening: A Titration-Based Approach

That Efficiently Identifies Biological Activities in Large Chemical Libraries. *PNAS* **2006,** 103, 11473-11478.

(50) Hann, M. M.; Oprea, T. I. Pursuing the Leadlikeness Concept in Pharmaceutical Research. *Curr Opin Chem Biol.* **2004,** 8, 255-263.

(51) Zhang, J.; Chung, T.; Oldenburg, K. A Simple Statistical Parameter for Use in Evaluation and Validation of High Throughput Screening Assays. *Journal of Biomolecular Screening* **1999,** 4, 67-73.

(52) Straus, O. H.; Goldstein, A. Zone Behavior of Enzymes: Illustrated by the Effect of Dissociation Constant and Dilution on the System Cholinesteratse-Physostigmine. *J. Gen. Physiol.* **1943,** 26, 559-585.

(53) Shoichet, B. K. Interpreting Steep Dose-Response Curves in Early Inhibitor Discovery. *J. Med. Chem.* **2006,** In Press.

(54) Usher, K. C.; Blaszczak, L. C.; Weston, G. S.; Shoichet, B. K.; Remington, S. J. Three-Dimensional Structure of Ampc Beta-Lactamase from Escherichia Coli Bound to a Transition-State Analogue: Possible Implications for the Oxyanion Hypothesis and for Inhibitor Design. *Biochemistry* **1998,** 37, 16082-16090.

(55) Chen, Y.; Minasov, G.; Roth, T. A.; Prati, F.; Shoichet, B. K. The Deacylation Mechanism of Ampc Beta-Lactamase at Ultrahigh Resolution. *J. Am. Chem. Soc.* **2006,** 128, 2970-2976.

(56) Nelson, R.; Sawaya, M. R.; Balbirnie, M.; Madesen, A. Ø.; Riekel, C.; Grothe, R.; Eisenberg, D. Structure of the Cross-Beta Spine of Amyloid-Like Fibrils. *Nature* **2005,** 435, 773-778.

(57) Blake, C.; Serpell, L. Synchrotron X-Ray Studies Suggest That the Core of the Transthyretin Amyloid Fibril Is a Continuous Beta-Sheet Helix. *Structure* **1996,** 4, 989-998.

(58) Yang, F.; Lim, G. P.; Begum, A. N.; Ubeda, O. J.; Simmons, M. R.; Ambegaokar, S. S.; Chen, P.; Kayed, R.; Glabe, C. G.; Frautschy, S. A.; Cole, G. M. Curcumin Inhibits Formation of Amyloid B Oligomers and Fibrils, Binsd Plaques, and Reduces Amyloid *in Vivo*. *The Journal of Biological Chemistry* **2005,** 280, 5892-5901.

(59) Riviere, C.; Richard, T.; Quentin, L.; Krisa, S.; Merillon, J.; Monti, J. Inhibitory Activity of Stilbenes on Alzheimer's Beta-Amyloid Fibrils in Vitro. *Bioorg. Med. Chem.* **2007,** 15, 1160-1167.

(60) Lashuel, H. A.; Hartley, D. M.; Balakhaneh, D.; Aggarwal, A.; Teichberg, S.; Callaway, D. J. E. New Class of Inhibitors of Amyloid-Beta Fibril Formation. *J Biol Chem* **2002,** 45, 42881-42890.

(61) Julius, R. L.; Farha, O. K.; Chiang, J.; Perry, J.; Hawthorne, M. F. Synthesis and Evaluation of Transthyretin Amyloidosis Inhibitors Containing Carborane Pharmacophores. *PNAS* **2007,** 104, 4808-4813.

(62) Johnson, S. M.; Petrassi, H. M.; Palaninathan, S. K.; Mohamedmohaideen, N. N.; Purkey, H. E.; Nichols, C.; Chiang, K. P.; Walkup, T.; Sacchettini, J. C.; Sharpless, K. B.; Kelly, J. W. Bisaryloxime Ethers as Potent Inhibitors of Transthyretin Amyloid Fibril Formation. *J. Med. Chem.* **2005,** 48, 1576-1587.

(63) Zhu, M.; Rajamani, S.; Kaylor, J.; Han, S.; Zhou, F.; Fink, A. L. The Flavonoid Baicalein Inhibits Fibrillation of Alpha-Synuclein and Disaggregates Existing Fibrils. *J Biol Chem* **2004,** 279, 26846-26857.

(64) Pickhardt, M.; Gazova, Z.; von Bergen, M.; Khlistunova, I.; Wang, Y.; Hascher, A.; Mandelkow, E. M.; Biernat, J.; Mandelkow, E. Anthraquinones Inhibit Tau Aggregation and Dissolve Alzheimer's Paired Helical Filaments *in Vitro* and in Cells. *J Biol Chem* **2005,** 280, 3628-3635.

(65) Heiser, V.; Scherzinger, E.; Boeddrich, A.; Nordhoff, E.; Lurz, R.; Schugardt, N.; Lehrach, H.; Wanker, E. E. Inhibition of Huntingtin Fibrillogenesis by Specific Antibodies and Small Molecules: Implications for Huntington's Disease Therapy. *PNAS* **2000,** 97, 6739-6744.

(66) Blanchard, B. J.; Chen, A.; Rozeboom, L. M.; Stafford, K. A.; Weigele, P.; Ingram, V. M. Efficient Reversal of Alzheimer's Disease Fibril Formation and Eliminationof Neurotoxicity by a Small Molecule. *PNAS* **2004,** 101, 14326-14332.

(67) Shoval, H.; Lichtenberg, D.; Gazit, E. The Molecular Mechanisms of the Anti-Amyloid Effects of Phenols. *Amyloid* **2007,** 14, 73-87.

(68) Lim, G. P.; Chu, T.; Yang, F.; Bech, W.; Frautschy, S. A.; Cole, G. M. The Curry Spice Curcumin Reduces Oxidative Damage and Amyloid Pathology in an Alzheimer Transgenic Mouse. *J. Neurosci.* **2001,** 21, 8370-8377.

(69) Nguyen, T.; Hamby, A.; Massa, S. M. Clioquinol Down-Regulates Mutant Huntingtin Expression in Vitro and Mitigates Pathology in a Huntington's Disease Mouse Model. *PNAS* **2005,** 102, 11840-11845.

(70) Feng, B. Y.; Simeonov, A.; Jadhav, A.; Babaoglu, K.; Inglese, J.; Shoichet, B. K.; Austin, C. P. A High-Throughput Screen for Aggregation-Based Inhibition in a Large Compound Library. *J. Med. Chem.* **2007,** In Press.

(71) True, H. L.; Lindquist, S. L. A Yeast Prion Provides a Mechanism for Genetic Variation and Phenotypic Diversity. *Nature* **2000,** 407, 477-483.

(72) Abid, K.; Soto, C. The Intriguing Prion Disorders. *Cell Mol Life Sci.* **2006,** 63, 2342-2351.

(73) Coan, K. E. D.; Shoichet, B. K. Stability and Equilibria of Promiscuous Aggregates in High Protein Milieus. *Mol Biosyst* **2007,** 3, 208-213.

(74) Groenning, M.; Olsen, L.; van de Weert, M.; Flink, J. M.; Frokjaer, S.; Jorgensen, F. S. Study on the Binding of Thioflavin T to a Beta-Sheet-Rich and Non-Beta-Sheet Cavities. *J. Struct. Biol.* **2007,** 158, 358-369.

(75) Khurana, R.; Coleman, C.; Ionescu-Zanetti, C.; Carter, S. A.; Krishna, V.; Grover, R. K.; Roy, R.; Singh, S. Mechanism of Thioflavin T Bniding to Amyloid Fibrils. *Journal of Structural Biology* **2005,** 151, 229-238.

(76) Legname, G.; Baskakov, I. V.; Nguyen, H. O.; Riesner, D. C., F.E.; DeArmond, S. J.; Prusiner, S. B. Synthetic Mammalian Prions. *Science* **2004,** 305, 673-676.

(77) Bomhoff, G.; Sloan, K.; McLain, C.; Gogol, E. P.; Fisher, M. T. The Effects of the Flavonoid Baicalein and Osmolytes on the Mg 2+ Accelerated Aggregation/Fibrillation of Carboxymethylated Bovine 1ss-Alpha-Lactalbumin. *Arch Biochem Biophys.* **2006,** 453, 75-86.

(78) Heo, H. J.; Kim, D.; Choi, S. J.; Shin, D. H.; Lee, C. Y. Potent Inhibitory Effect of Flavonoids in Scutellaria Baicalensis on Amyloid Â Protein-Induced Neurotoxicity. *J. Agric. Food Chem.* **2004,** 52, 4128-4132.

(79) Santoso, A.; Chien, P.; Osherovich, L. Z.; Weissman, J. S. Molecular Basis of a Yeast Prion Species Barrier. *Cell* **2000,** 100.

(80) Glover, J. R.; Kowal, A. S.; Schirmer, E. C.; Patino, M. M.; Liu, J. J.; Lindquist, S. Self-Seeded Fibers Formed by Sup35, the Protein Determinant of [Psi$^+$], a Heritable Prion-Like Factor of S. Cerevisiae. *Cell* **1997,** 89, 811-819.
(81) Tanaka, M.; Weissman, J. S. An Efficient Protein Transformation Protocol for Introducing Prions into Yeast. *Methods Enzymol.* **2006,** 412, 185-200.
(82) Baskakov, I. V.; Legname, G.; Baldwin, M. A.; Prusiner, S. B.; Cohen, F. E. Pathway Complexity of Prion Protein Assembly into Amyloid. *J Biol Chem* **2002,** 277, 21140-21148.
(83) Mehlhorn, I.; Groth, D.; Stöckel, J.; Moffat, B.; Reilly, D.; Yansura, D.; Willett, W. S.; Baldwin, M. A.; Fletterick, R.; Cohen, F. E.; Vandlen, R.; Henner, D.; Prusiner, S. B. High-Level Expression and Characterization of a Purified 142-Residue Polypeptide of the Prion Protein. *Biochemistry* **1996,** 35, 5528-5537.
(84) Levine-IIII., H. Thioflavine T Interaction with Synthetic Alzheimer's Disease {Beta}-Amyloid Peptides: Detection of Amyloid Aggregation in Solution. *Protein Sci.* **1993,** 2, 404-410.
(85) Wille, H.; Zhang, G.; Baldwin, M. A.; Cohen, F. E.; Prusiner, S. B. Separation of Scrapie Prion Infectivity from Prp Amyloid Polymers. *J. Mol. Bio.* **1996,** 259.
(86) Svetnik, V.; Liaw, A.; Tong, C.; Culberson, J. C.; Sheridan, R. P.; Feuston, B. P. Random Forest: A Classification and Regression Tool for Compound Classification and Qsar Modeling. *J. Chem. Inf. Comput. Sci.* **2003,** 43, 1947-1958.
(87) Hajduk, P. J.; Huth, J. R.; Fesik, S. W. Druggability Indices for Protein Targets Derived from Nmr-Based Screening Data. *J. Med. Chem.* **2005,** 48, 2518-2525.

Appendix A

Supplementary Methods For:

High-Throughput Assays for Promiscuous Inhibitors

Brian Y. Feng, Anang A. Shelat, Thompson N. Doman, R. Kip Guy and Brian K. Shoichet

Materials:

DLS Known Aggregators:

The following known aggregators[1-3] were used to calibrate the DLS plate-based assay: 3-[(4-phenoxyanilino)methylene]-2-benzofuran-1(3H)-one was purchased from Bionet (Camelford, North Cornwall, UK). Indirubin was purchased from Apin Chemicals Ltd. (Abingdon, Oxon, UK). 3-(4-isopropylbenzylidene)indolin-2-one (MFCD118155) was purchased from Maybridge (Trevillett, Tintagel, UK). Vat Red 1 was purchased from Technology Catalysts International (Falls Church, VA). Clotrimazole and Miconazole were purchased from ICN (Pittsburgh, PA). 4-(4-methylbenzylideneamino) Salicylic Acid, Econazole, Estradiol, Hexachloro-4-(2,4-Dinotri-Phen) (MFCD225114), Indigo, Palatine Chrome-Black, Quercetin, S03218, Sulconazole and tetraiodophenolpthalein were purchased from Sigma-Aldritch (St. Louis, MO). All compounds were prepared as 10 mM stocks in neat DMSO.

DLS Known Non-aggregators:

The following known non-aggregators[1-3] were used to calibrate the DLS plate-based assay: 5-aminosalicylic acid and 4-aminophenyl sulfone were ordered from Acros (Pittsburgh, PA). Azelaic acid was ordered from Alfa Aesar (Ward Hill, MA). Ketoconazole was ordered from Biomol (Plymouth Meeting, PA). Carbamezepine,

Carisoprodol, Difluinsal, diphenydramine HCl, Fluconazole, Lidocaine HCl, Primidone and Propatheline bromide were purchased from ICN(Aurora, OH). Lamotrigine was purchased from Kemprotec (Middlebrough, UK). Flutamide was purchased from LKT Laboratories (St. Paul, MN). 2-amino-6-(trifluoromethoxy) benzothiazole was purchased from Matrix Scientific (Columbia, SC). Ondansetron HCl and Torasemide were purchased from Sequoia (Oxford, UK). Cinoxacim, Furosemide, guaiacol glyceryl ether, Phenolpthalein, Prazocin, Prednisone, Protriptyline, Sulfadiazine, (+/-) thalidomide, and Tripelenamine were purchased from Sigma-Aldritch (St. Louis, MO). Gemfibrozil was purchased from Spectrum Pharmaceuticals, Inc. All compounds were prepared as 10 mM stocks in neat DMSO.

Enzyme Assay Known Aggregators:

The following molecules were used to calibrate the detergent-dependant enzyme assay: Bisindolylmaleimide IX was purchased from Alexis Biochemicals (San Diego, CA). 3-[(4-phenoxyanilino)methylene]-2-benzofuran-1(3H)-one was purchased from Bionet Camelford, North Cornwall, UK). Clotrimazole and Miconazole were purchased from ICN pharmaceuticals (Pittsburgh, PA). 3-(4-isopropylbenzylidene)indolin-2-one (MFCD118155) was purchased from Maybridge (Trevillett, Tintagel, UK). 4-(4-((2,4-difluorophenyl)amino)-3,5-thiazolyl)benzene-1,2-diol was purchased from Menai Organics LTD. 4-4-bromophenoazophenol (4BPAP), Cibachrome Blue, Congo Red, Direct Yellow 20, Econazole, Eriochrome Blue Black, Quercetin, Rose Bengal Lactone Rottlerin, S3218, Sulconazole, and Tetraiodophenolpthalein were purchased from Sigma-Aldritch (St. Louis, MO). All compounds were prepared as 10 mM stocks in neat DMSO.

Known Non-aggregators:

The same known non-aggregators used to calibrate the DLS assay were used to calibrate the enzyme assay. All compounds were prepared as 10 mM stocks in neat DMSO.

Methods:

High-Throughput β-lactamase assay development:

A plate of known aggregate formers was screened in order to establish cutoffs for the ranking of unknowns (**Supplementary Table 3**). Each known aggregator had an IC_{50} of 30 μM or less, and was apparently soluble. The same plate was then screened in the presence of 0.1% Triton X-100. All known inhibitors exhibited detergent-sensitive inhibition (**Supplementary Figure 3**). This was not the case for a well-behaved, competitive inhibitor of β-lactamase, benzo-*b*-thiophene 2-boronic acid (BZB), which was unaffected by the addition of Triton X-100. Known aggregators and non-aggregators were binned by percent activity vs. β-lactamase, and cutoffs were placed at the 95% confidence interval for each distribution..

High-Throughput β-lactamase assay application:

The set 1030 unknowns was screened in the high-throughput assay. Inhibition among all of these molecules was observed to be reversed in the presence of 0.1% Triton X-100. Each molecule was categorized as an aggregator, non-aggregator or ambiguous based on its potency as an inhibitor of β-lactamase

Low-throughput verification of high-throughput enzyme assay:

Twenty-seven molecules were tested in the more rigorous low-throughput assay. Each was tested at 30 μM and 100 μM. Putative inhibitors and ambiguous inhibitors were also tested against chymotrypsin at 100 μM (**Supplementary Table 4**). Results were well

correlated to performance in the high-throughput assay.

Development of the DLS-Based Classifier

We developed a probabilistic classifier for aggregators using the high-throughput DLS intensity data to test the hypothesis that particle formation, as measured by highthroughput

DLS, is a good predictor of promiscuous aggregation. To derive a reliable classifier of particle-formation, it was necessary to use the 16 known aggregators and 33 known non-aggregators from previous studies, and 58 molecules retested by lowthroughput

DLS as a training set (**Supplementary Table 1**). This training set incorporated regions of instrument inaccuracy into the model, and as a result, the results obtained by high-throughput DLS are highly correlated to the results obtained by lowthroughput DLS. The probability of being an aggregator, $p_{AGG,}$ for an unknown compound with scattering intensity **x** was estimated using Bayes' Theorem:

$$\rho_{AGG} = \rho(\mathbf{x}|AGG) * \rho'(AGG) / (\rho(\mathbf{x}|AGG)*\rho'(AGG) + \rho(\mathbf{x}|NAGG)*\rho'(NAGG))$$

Under the assumption of a flat distribution, the prior probabilities for aggregators and non-aggregators, ρ'(AGG) and ρ'(NAGG), were set equal to 0.5. The values for ρ(**x**|AGG) and ρ(**x**|NAGG) are derived from the probability distributions of the known aggregators and non-aggregators as a function of high-throughput DLS. Examination of the raw and log-transformed scattering intensity histograms for both populations revealed significant departure from normality; thus, modeling the two probability distributions as

normal was not appropriate. Instead, the distributions were estimated for the range of the log-transformed intensity values using the *density* function in the R statistics package (version 2.0.1) with a guassian kernel and bandwidth="nrd0". For smoothing purposes, the 'adjust' parameter was set to 1 for the aggregator density and 2 for the non-aggregator density. The probability for a given distribution was set to zero far from the mean of that distribution to avoid edge effects. The distributions for ρ_{AGG} and ρ_{NAGG} ($1 - \rho_{AGG}$) as a function of log-transformed light intensity based on the initial training set of 49 molecules are shown in Supplementary Figure 2. Molecules with $\rho_{AGG} >= 0.9$ were classified as forming particles; molecules with $\rho_{AGG} <= 0.1$ were classified as non-particle forming. Molecules with $0.1 <= \rho_{AGG} <= 0.9$ were assigned as ambiguous. Using these criteria, molecules with light scattering intensity < 10991 (cnts/s) were classified as not forming particles, and molecules with light scattering intensity > 310934 (cnts/s) were classified as forming particles. It should be noted that the probabilities calculated from DLS data can *only* predict particle formation, and not selectively predict the formation of promiscuous aggregates.

Development of the Initial Naïve Bayesian (NB) Model:

The initial Bayesian model employed the naïve Bayesian classifier algorithm in Pipeline Pilot 4.5.0 (Scitegic, Inc). The algorithm calculates the sum of conditional probabilities for the occurrence of a given feature in a set of molecules representing two classes ("aggregator" and "non-aggregator" in this case). Features can be particular chemical structures (the structures represented by bits from a fingerprint), or are defined as a range for a continuous variable (e.g., molecular weight between 100 and 200 Daltons, AlogP between 2.2 and 2.4). Features that are found with greater frequency in the aggregator set

have positive probabilities; likewise, features enriched in the non-aggregator set decrease the overall model score. All conditional probabilities are modified by the Laplacian correction to avoid the occurrence of zero conditional probabilities and to reduce the influence of features with low occurrence. The set of features used in the initial model included bits from Scitegic's ECFP_6 molecular fingerprint and the first five principal components (PCs) calculated from a principal component analysis (PCA) of all 1D and 2D descriptors from MOE (Chemical Computing Group, version 2002.3). These five PCs accounted for 92.5% of the variance in the MOE descriptor space.

The initial data set contained known aggregators and non-aggregators[6, 8, 9]. Ten percent of the data set was withheld from the model building process (the "validation" set). Using the remaining 90% of the data, models were trained on 80%, and the other 20% was scored using the Receiver-Operator Characteristic (ROC, calculated in Pipeline Pilot). One hundred models were generated using different partitions of the data, and the top ten performing models were selected. The consensus model score, or CSCORE, was the mean of the 10 models. The probability of an unknown compound promiscuously aggregating was calculated using a method similar to that of the probabilistic DLS classifier (see above). A flat prior distribution was assumed. The probability mass function was modeled as two normal distributions estimated using the CSCORE distributions from known aggregators and non-aggregators in the validation set. Molecules with a posterior probability for aggregation >= 0.6 were classified as aggregators; molecules with a probability <= 0.4 were classified as non-aggregators, and no classification was made for molecules in the probability range 0.4 – 0.6.

To assess the utility of the initial Bayesian model, a test set of predicted aggregators and

predicted non-aggregators was selected from Chemical Diversity, Inc's compound library. In order to minimize uncertainty in the predictions, only aggregators with posterior probabilities > 0.99 were selected; likewise, the selected non-aggregators had aggregator probability < 0.01. These constraints yielded 968 predicted aggregators and 80,778 predicted non-aggregators. Within each set, a maximum dissimilarity metric (implemented in the *Diverse Molecules* component in Pipeline Pilot) was employed to select the most diverse set of 300 aggregators and 300 non-aggregators. From these two sets, 200 predicted aggregators and 97 predicted non-aggregators were purchased.

Refinement of Predictive Models:

Based on the experimental results from the 30 μM detergent-dependent enzyme screen, 732 aggregators and non-aggregators from the predicted set were added to the original training-set of 113 molecules. As noted above, the Random set was withheld and used only as a test set.

Refinement of the RP model:

In refining the RP model, we chose to change to a Random Forest (RF) model[17] because of our ready access to thousands of potentially relevant physicochemical descriptors capturing size, shape, electrostatics, and hydrophobicity, and because of our successful experience building predictive models with this technique. Prior to building the full model using all 732 compounds, we performed ten iterations of 70:30 train:test splits (i.e., build the RF model with 70% of the compounds, then predict on the 30% left out), each time generating 1000 unpruned trees built from subsets of 5,323 descriptors, and found a mean correct prediction rate of 83.3% (low: 79.8%; high: 87.1%). We feel that the full RF model built using all 822 compounds has similar or greater prediction

accuracy, as suggested by results for the 298 randomly-selected compounds.

Refinement of naïve Bayesian model (rNB):

Chemical fingerprint descriptors were calculated as before, except now using Scitegic's FCFP_6 fingerprint. Physico-chemical descriptors were calculated using molconnZ (EduSoft LC, version 4.09). Initially, 765 descriptors were present in the training set. Using the R statistics package, correlated descriptors or descriptors with zero variance were removed, yielding 540 descriptors. The initial Bayesian model used bits present in Scitegic's ECFP_6 fingerprint and the first five principal components derived from PCA of MOE descriptors. Reducing the dimensionality of the MOE descriptor space allowed us to effectively capture the variability of our data in fewer variables; however, PCA confounds interpretation of the contribution of individual descriptors. In the refined model, we avoided PCs, instead using raw variables and a modified version of the variable selection method described by Svetnik et al.[86] The variable selection procedure is as follows. A model was built on 80% of all available data with all descriptors, then scored on the remaining 20% using the Z-factor metric.[51]

Each descriptor was individually removed, and the model rebuilt and reassessed. To reduce noise, the process was repeated 8-10 times. At the end of this stage, the descriptors are rank ordered according to their contribution to the Z-factor. The lowest performing one-half of all descriptors was removed, and the process was repeated. The best descriptor set was determined by maximizing the Z-factor as a function of the number of descriptors. Our final model consisted of 43 descriptors. An ensemble of 25 models was generated using the 43 descriptors, and the probability of aggregation was

determined using the mean of all model scores as described previously.

Supplementary Figure 1.

The probability-based classifier for DLS data.

(**a**) Probability of Aggregation vs. Log Intensity based on the behavior of 49 known aggregators and nonaggregators. Molecules with intensities < 10159 (cnts/s) were classified as non-aggregators; molecules with intensities > 63609 (cnts/s) were classified as aggregators; all other molecules were classified as ambiguous. (**b**) Retrained Probability of Scattering vs Log Intensity. Molecules with intensities < 10991 (cnts/s) were classified as non-aggregators; molecules with intensities > 310 934 (cnts/s); all other molecules were classified as ambiguous.

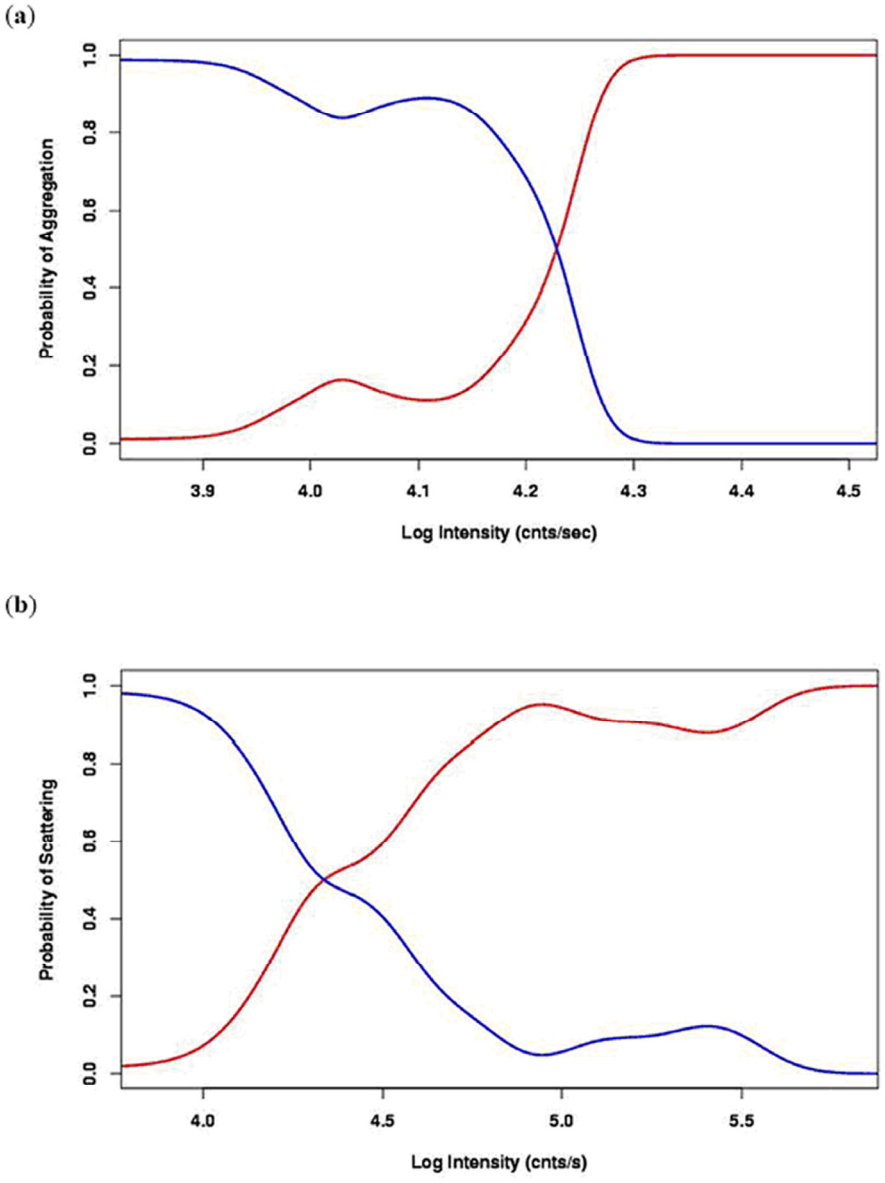

Supplementary Figure 2.

Control Data from High-Throughput Enzyme Assay.

(See Supplementary Methods).

High Throughput Enzyme assay control data. Based on 19 known aggregators and 27 known nonaggregators. (**a**) The assay conducted at 30 uM. Molecules with %activity < 76% were considered aggregators, while molecules with % activity > 88% were considered non-aggregators. Red Bars represent these cutoffs, which were placed at the 95% CI of each population. Molecules with 76% < %activity < 88% were considered ambiguous. (**b**) The assay conducted at 30uM + 0.1% Triton X-100.

(a)

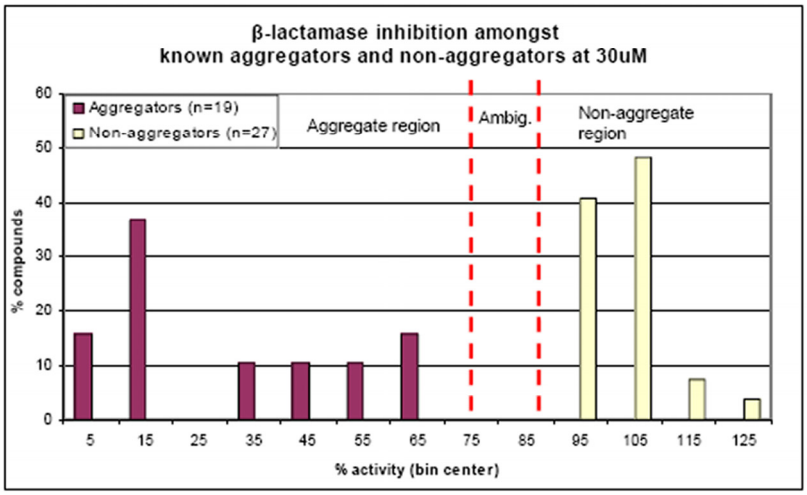

(b)

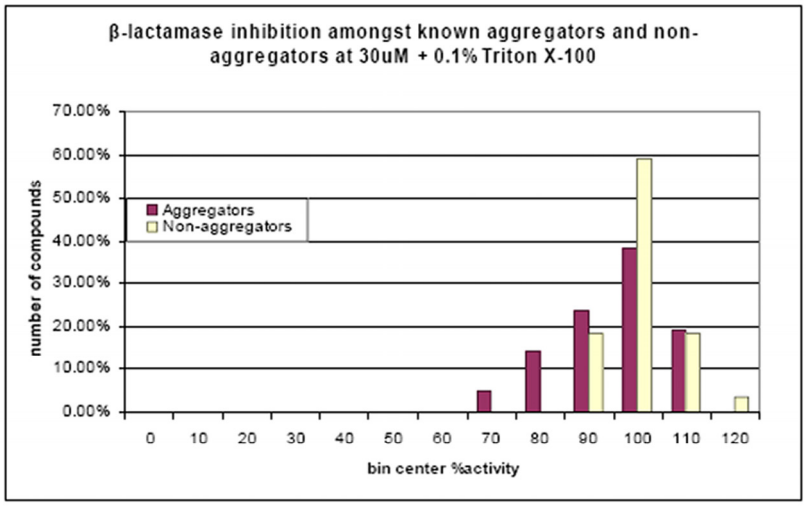

Supplementary Table 1. Interquartile Ranges for common physical properties from the CMC*, and prediction and random sets select from Chemical Diversity, Inc. (See Supplementary Methods).

Property	CMC* (N=7790)	Prediction Sets (N=732)	Random Set (N=298)
AlogP	1.13 - 3.96	2.62 - 4.35	2.12 – 4.02
Molecular Solubility (log ug/ml)	-5.72 – -2.82	-6.22 – -4.39	-5.88 – -3.76
Molecular Weight (Daltons)	261 – 411	303 – 400	309 – 411
Polar Surface Area ($Å^2$)	42 – 105	59 – 100	67 – 102
Total Surface Area ($Å^2$)	255 – 395	282 – 365	289 – 383
# H Donors	1 – 2	1 – 2	1 – 2
# H Acceptors	3 – 6	3 – 5	3 – 5
# N + O Atoms	3 – 7	3 – 6	4 – 6
# Rotable Bonds	3 – 7	4 – 6	4 – 7

Supplementary Table 2.

Results from Low-throughput Enzyme Assays.

Structures (Plate_Well) PubChem#	%inhibition vs. β-lac in HT (30uM)	%inhibition vs. β-lac + TX in HT	%inhibition vs. β-lac in LT (30uM)	%inhibition vs. β-lac + TX in LT	%inhibition vs. β-lac (100uM)	%inhibition vs. Chymotrypsin (100 μM)
Aggregators						
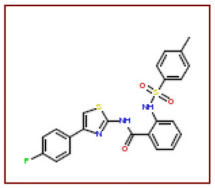	97.5	15.5	97.5	0.0		98.4
A1_D8 (**1**)						
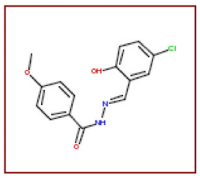	24.6	2.9	79.0	-16.0		50.5
a1_B5 (**2**)						
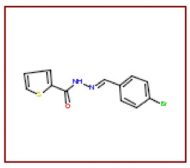	61.6	1.9	97.0	2.4		59.0
A1_C9 (**3**)						
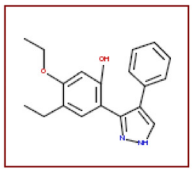	99.8	1.7	100.0	-2.0		66.1
A8_A8 (**4**)						

Structure	%inhibition vs. B-lac in HT (30uM)	%inhibition vs. B-lac + TX in HT	%inhibition vs. B-lac in LT (30uM)	%inhibition vs. B-lac + TX in LT	%inhibition vs. B-lac (100uM)	%inhibition vs. Chymo (100 µM)
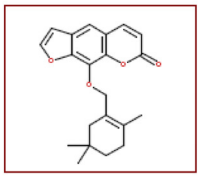	81.4	10.7	79.2	11.0		34.4
A8_D2 (**5**)						
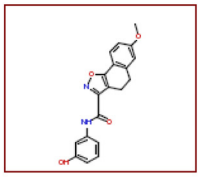	32.6	-9.5	51.3	8.0		92.3
D3_C10 (**6**)						
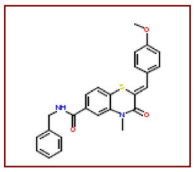	94.0	6.3	99.5	1.0		96.7
D3_E11 (**7**)						
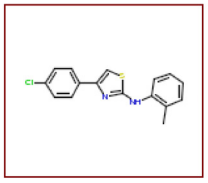	52.0	-1.0	30.0	20.0		41.0
A5_C8 (**8**)						

Structure	%inhibition vs. B-lac in HT (30uM)	%inhibition vs. B-lac + TX in HT	%inhibition vs. B-lac in LT (30uM)	%inhibition vs. B-lac + TX in LT	%inhibition vs. B-lac (100uM)	%inhibition vs. Chymo (100 µM)
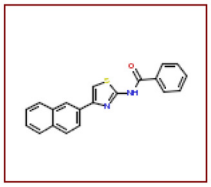	99.0	10.2	9.0	6 (100uM)	79.0	91.5
A6_G3 (**9**)						
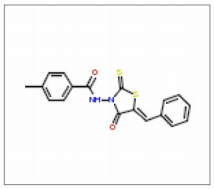	91.3	-2.2	91			
D5_B3 (**10**)						
Non-Aggregators						
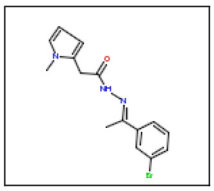	1.5	-6.0	103.7			
A1_H9 (**11**)						
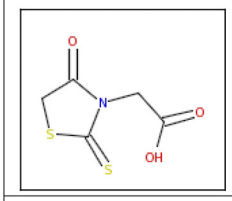	1.0	4.4	104.0			
A1_E4 (**12**)						

Structure	%inhibition vs. B-lac in HT (30uM)	%inhibition vs. B-lac + TX in HT	%inhibition vs. B-lac in LT (30uM)	%inhibition vs. B-lac + TX in LT	%inhibition vs. B-lac (100uM)	%inhibition vs. Chymo (100 µM)
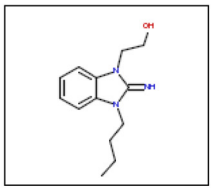	-3.1	-1.5	-2.0			
A1_B10 (**13**)						
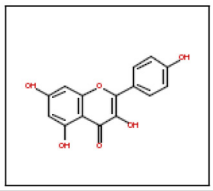	7.3	-5.2	10.0			
A7_H6 (**14**)						
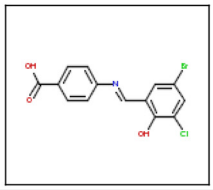	1.6	0.7	19.2			
A7_E2 (**15**)						
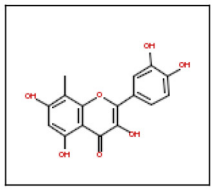	10.1	6.2	7.5	16.2 (100uM)		
A7_G6 (**16**)						

Structure	%inhibition vs. B-lac in HT (30uM)	%inhibition vs. B-lac + TX in HT	%inhibition vs. B-lac in LT (30uM)	%inhibition vs. B-lac + TX in LT	%inhibition vs. B-lac (100uM)	%inhibition vs. Chymo (100 µM)
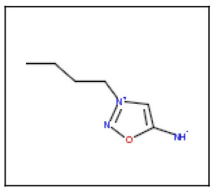	0.2	-2.7	-1.0			
A8_A9 (**17**)						
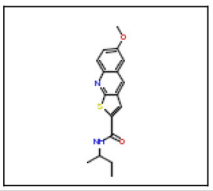	-9.0	5.0	1.0			
D3_D11 (**18**)						
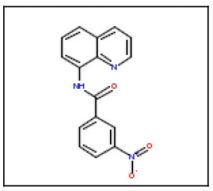	5.1	-2.5	-2.7			
D3_H2 (**19**)						
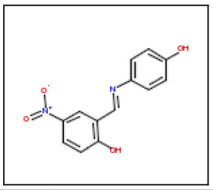	0.1	1.4	-0.6	0.8 (100µM)		
A5_A2 (**20**)						

Structure	%inhibition vs. B-lac in HT (30uM)	%inhibition vs. B-lac + TX in HT	%inhibition vs. B-lac in LT (30uM)	%inhibition vs. B-lac + TX in LT	%inhibition vs. B-lac (100uM)	%inhibition vs. Chymo (100 µM)
Ambiguous						
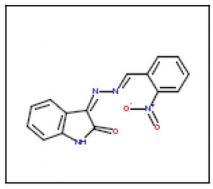	12.3	4.9	18.1	6.3 (100µM)	98.6	75.5 (100 uM)
A7_B3 (**21**)						
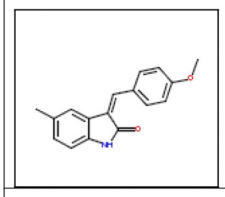	4.6	9.6	16.2	11.3 (100uM)	67.5	33 (100µM)
A7_D6 (**22**)						
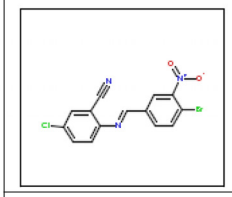	21.3	-1.7	92.4	0.1 (100 µM)		98.8 (100 uM)
A7_H2 (**23**)						
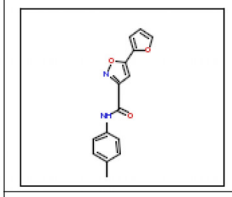	19.7	5.1	52.0	-2 (100µM)	99.0	82.7
D3_B10 (**24**)						

Structure	%inhibition vs. B-lac in HT (30uM)	%inhibition vs. B-lac + TX in HT	%inhibition vs. B-lac in LT (30uM)	%inhibition vs. B-lac + TX in LT	%inhibition vs. B-lac (100uM)	%inhibition vs. Chymo (100 µM)
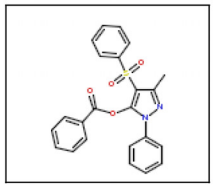	21.0	9.8	22.3	14.2 (100uM)	65.9	98.0
D3_G10 (**25**)						
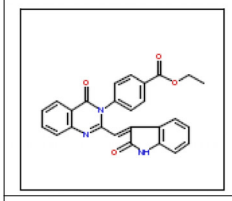	14.0	16.3	22.0	-2 (100µM)	59.0	21.0
A6_A8 (**26**)						
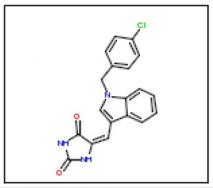	20.8	-3.5	98.0	1.3 (30uM)		68.5% (30uM)
			1.8			
A6_C5 (**27**)						
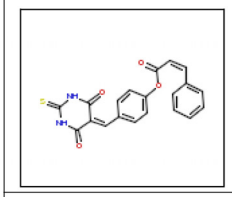	13.4	15.2	23.4	-12 (100uM)	96.5	100.0
A6_H9 (**28**)						

Structure	%inhibition vs. B-lac in HT (30uM)	%inhibition vs. B-lac + TX in HT	%inhibition vs. B-lac in LT (30uM)	%inhibition vs. B-lac + TX in LT	%inhibition vs. B-lac (100uM)	%inhibition vs. Chymo (100 µM)
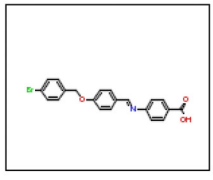	22.0	9.7	8.0	6 (100uM)	99.1	5.2 (100uM)
A6_H10 (**29**)						

Supplementary Table 3.

Results from Low-throughput DLS Assays to confirm HT-DLS.

Scatterers(Plate_Well)	Plate Reader Intensity (cnt/s)	Low-Throughput Intensity (cnt/s) (% laser intensity)	Low-throughput result
A3_A11	2245745	6214800 (20%)	scatterer
A3_F5	1090606	4223930 (20%)	scatterer
A3_C8	408767	3744840 (50%)	scatterer
A7_F2	1784945	4202310 (15%)	scatterer
A7_A3	595528	2227320 (20%)	scatterer
A7_C3	2751395	6714680 (15%)	scatterer
D3_H10	1444535	5719530(20%)	scatterer
D3_H7	846576	4792010(20%)	scatterer
D3_G2	1908206	2458640(50%)	scatterer
D3_B10	981467	2077190(10%)	scatterer
D3_B2	1809250	4284370(10%)	scatterer
A2_D2	638496	2203730 (10%)	scatterer
A3_B9	1033916	2203730 (25%)	scatterer
A1_A6	3128700	1616200(20%)	scatterer
D3_B4	2056390	4.2 mcnt/s (20%)	scatterer
D3_D2	1561510	4.1 mcnt/s (50%)	scatterer
D3_D3	1011644	1.2 mcnt/s	scatterer
Non-scatterers			
D2_D4	5667	18349	non-scatterer
A5_E10	6405	20183	non-scatterer
A5_A8	5876	58464	non-scatterer
A3_F3	5672	39992	non-scatterer
A3_G10	6932	22009	non-scatterer
A3_B5	5976	13781	non-scatterer
A3_B2	4335	28731	non-scatterer
D6_G7	6744	16165	non-scatterer
D6_E9	6653	51411	non-scatterer
D6_B2	6472	30066	non-scatterer
A5_E6	5079	97975	non-scatterer
D3_E6	6848	88345	non-scatterer
Overlap			
D5_H7	7701	17046	non-scatterer
D5_B2	7715	18949	non-scatterer
D3_E3	7267	42096	non-scatterer
D3_D5	7477	125832	non-scatterer
D3_G5	7645	11562	non-scatterer
D3_C4	8298	12327	non-scatterer
D5_G2	8723	16731	non-scatterer
D5_H10	9193	18063	non-scatterer
D3_H2	9202	22087(50%)	non-scatterer
A3_A10	9224	27000	non-scatterer
D5_H2	10477	12867	non-scatterer

Table 3. continued			
	Plate Reader Intensity (cnt/s)	Low-Throughput Intensity (cnt/s) (% laser intensity)	Low-throughput result
A1_H8	12727	71758	non-scatterer
A2_E3	14000	4951030	scatterer
D5_B10	14397	15905	non-scatterer
A3_F6	21923	22019	non-scatterer
A2_A9	22170	4990330 (20%)	scatterer
A3_G8	26015	137034	non-scatterer
A1_F3	26926	100174	non-scatterer
D3_C2	31048	209622	scatterer
D3_H5	42569	1200000	scatterer
D3_G7	139566	31000	non-scatterer
D3_C11	287510	44651	non-scatterer
D3_A11	269113	5900000	scatterer
D3_C7	244458	18943	non-scatterer
D3_D4	236070	3.1 mcnt/s	scatterer
D3_G9	212975	4.2 mcnt/s	scatterer
A5_H8	220434	437029	scatterer
A5_F8	186503	259777	scatterer
A5_A5	204483	2131670	scatterer

Supplementary Table 4. Results from the computational models applied to their respective Predicted sets (RP Set = 88 Aggregators, 290 Non-aggregators; NB Set=118 Aggregators, 144 Nonaggregators), and to the Random Set (57 Aggregators, 219 Non-aggregators). Missclassification rate is defined as: total number of incorrect predictions / total number of prediction.

Model	Performance among Predicted Molecules[1]		Perfomance among Random Molecules (n=276)[2]				
	Recursive Partitioning (n=378)	Initial Bayesian (n=262)	Recursive Partitioning	Random Forest	Initial Bayesian	Refined Bayesian	Bayesian DLS Classifier
Aggregator Precision	32% (79/244)	64% (112/174)	43% (44/103)	83% (34/41)	33% (13/39)	50% (42/84)	40% (37/93)
Aggregator Recall	90% (79/88)	78% (112/144)	77% (44/57)	60% (34/57)	23% (13/57)	74% (42/57)	65% (37/57)
Nonaggregator Precision	93% (125/134)	93% (82/88)	92% (160/173)	90% (212/235)	81% (180/222)	95% (158/167)	97% (33/34)
Nonaggregator Recall	43% (125/290)	57% (82/144)	73% (160/219)	97% (212/219)	82% (180/219)	73% (158/219)	15% (33/219)
Misclassification Rate	46% (174/378)	26% (68/262)	26% (72/276)	11% (30/276)	26% (68/261)	20% (51/251)	45% (103/200)
Not Classified	0%	0%	0%	0%	5% (15/276)	9% (25/276)	54% (149/276)

[1]Computational Model Results for the Prediction Set: The NB has a lower misclassification rate than the RP model. However, performance on the Predicted sets is not an accurate measure of the ability of either model to classify random molecules. An unbiased assessment of our ability to predict promiscuous aggregation would be the performance of the computational model on the Random set.

[2]Computational Model Results for the Random Set: The performance of the initial and refined computational model on the Random set is shown. The RF performs the best, with a remarkably low misclassification rate of 11%. The less complex rNB model, consisting of only 43 descriptors, also performs well. Interestingly, the DLS-based classifier designed to predict particle formation does not perform as well as either computational method. All tests performed on the random subset were conducted prospectively, with no knowledge of the true number of promiscuous molecules in the

set. Refined models were developed by including experimental results from both predicted sets into the training sets for each model.

Supplementary Table 5. Combined assay results for all compounds. NONAGG=non–aggregator by detergent sensitive enzyme assay. AGG=Aggregator by enzyme assay AMBIG=ambiguous molecule by enzyme assay. SCATTER=Light–Scattering molecule by DLS assay with (>90% confidence). SCATTER_80=Light–scattering molecule by DLS assay (>80% confidence). OVERLAP=ambiguous molecule by DLS assay. NON_SCATTER=Non–scattering molecule by DLS assay (>90% confidence). NONSCATTER_80=Non–scattering molecule by DLS assay (>80% confidence). This table is available online at: http://shoichetlab.ucsf.edu.

Appendix B

A Detergent-based Assay for the Detection of Promiscuous Inhibitors

Brian Y. Feng[1] and Brian K. Shoichet[1]

[1]*Department of Pharmaceutical Chemistry & Graduate Group in Chemistry and Chemical Biology, University of California-San Francisco, 1700 4th St., CA 94143-2550. shoichet@cgl.ucsf.edu. Telephone: 415-514-4126. Fax: 415-514-4260. Website: http://shoichetlab.compbio.ucsf.edu.*

Abstract. At micromolar concentrations many small molecules self-associate into colloidal aggregates that nonspecifically inhibit enzymes and other proteins. Here we describe a protocol to identify aggregate-based inhibitors, distinguishing them from small molecules that inhibit *via* specific mechanisms. As a convenient proxy for promiscuous, aggregate-based inhibition, we monitor inhibition of β-lactamase in the absence and presence of detergent. Inhibition that is attenuated in the presence of detergent is characteristic of an aggregate-based mechanism. In the 96-well format assay described here, about 200 molecules can be tested per hour for detergent dependent sensitivity. Furthermore, we also describe simple experiments that can offer additional confirmation of aggregate-based inhibition.

Introduction. Small molecules that specifically inhibit enzymes or modulate protein function are intensely sought. The dominant technique for discovering such

ligands is high throughput screening (HTS). In HTS, large libraries of small molecules are assayed for modulation of a target. Whereas this technique has had important successes, it is plagued by false-positive ligands. These artifactual "hits" can outnumber the true inhibitors in an HTS "hit list." Several mechanisms have been proposed to explain the prevalence of these artifactual hits, including oxidation potential[87], chemical reactivity[10], and spectral properties that interfere with assay read-out[33]. One of the more common mechanisms underlying false positive inhibition is the formation of colloidal aggregates through the self-association of organic molecules in aqueous solutions (Figure 1)[6-9, 35, 46]. These aggregates typically form at micromolar concentrations and are often several hundred nanometers in diameter. Once formed, they sequester proteins and non-specifically inhibit their activity. A wide range of molecules behave this way at screening-relevant concentrations, including Lipinski-compliant members of screening libraries, *bona fide* leads for drug discovery, and even drugs [6, 8, 9]. If the number of different types of molecules that can behave this way is surprising, so too is the actual number of molecules that do so; at 30 μM up to 19% of "drug-like" molecules may form aggregates. At 5 μM, about 1-2% of "drug-like" molecules appear to behave this way, which is still a large percentage considering that many HTS campaigns aim for a hit rate of less than 1%[35]. Here we describe a counter-screen for aggregation that can be deployed on a library-wide level, as well as a checklist of experiments that can be used to confirm if individual inhibitors are acting through an aggregation-based mechanism (see Anticipated Results).

Several alternatives to this assay exist. Among them is direct physical measurement of aggregation by dynamic light scattering (DLS), or apparent solubility by

nephelometry. Though more direct, we found DLS to be both time consuming and harder to interpret, owing to problems with signal-to-noise in the plate-based prototype instrument we were using. The detergent-sensitive enzyme inhibition assay, though admittedly less direct than physical measurement of particle formation, is more robust, faster and more amenable to miniaturization. This protocol was previously described in reference 31, and general discussions of the approach are presented in references 7 and 12. Note that in reference 31, the concentration of detergent used was 0.1% Triton X-100. Here we recommend a lower percentage, 0.01%, which is better tolerated by the enzyme.

Experimental Design:

The counter-screen relies on the detergent-sensitive nature of aggregate-based inhibition: molecules that inhibit an enzyme in the *absence* but not the *presence* of detergent are likely to be inhibiting via the formation of promiscuous aggregates. Thus, the first step of the experiment is to screen molecules for inhibition. AmpC β-lactamase (AmpC) is a convenient choice of enzyme because it has been extensively studied for aggregate-based inhibition and because it is one of the more sensitive enzymes tested for this effect. In principle, however, any soluble enzyme can be used for this protocol– compound aggregation is a physical property of small molecules in aqueous buffers. The only limitation to using other enzymes is how well tolerated Triton X-100 is in different assay systems. For systems that do not tolerate non-ionic detergent, 1 mg/ml bovine serum albumin (BSA) might be considered a replacement. However, BSA is can sequester monomeric small molecules, so this should be used with caution.

The experiments described in the protocol are also amenable to scale-up or scale-down. There are no problems running these experiments in lower, cuvette-based formats. Higher-throughput formats such as 1536-well plates are conceivable. We recommend experiments be conducted at least in duplicate, to ensure statistical significance–aggregating molecules can be capricious and are sensitive to assay conditions and target enzyme concentration, as well as centrifugation or vortexing among other invasive mixing procedures.

Should this protocol be applied to a different enzyme system or significantly different assay conditions, it may be necessary to derive new cutoffs for detecting aggregate-based inhibition. To establish what constituted significant inhibition in the development of our technique, we used a panel of known aggregators and non-aggregators. These molecules are listed on our website (http://shoichetlab.compbio.ucsf.edu), and can be screened as positive controls to identify the window of relevant inhibition (see Anticipated Results and reference 5).

Finally, screening for inhibition in the presence of detergent can be carried out independently from the screening for inhibition in the absence of detergent–each experiment can be done separately, and the procedure for each is the same. However, if adding detergent individually to each well, add it to buffer before any other components.

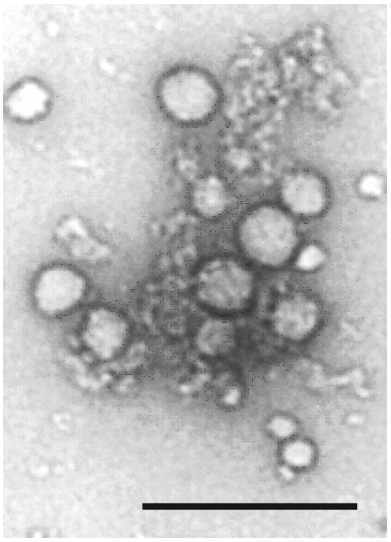

Figure 1. Transmission Electon Micrograph of aggregates of tetraiodophenolphthalein (dark edged circles) associated with β-galactosidase. This association inhibits the enzyme by sequestering it from substrate, though whether these are adsorption or absorption effects is uncertain at this time. Bar = 200nm. Reproduced from Reference 7, Copyright American Chemical Society, 2003.

Materials.

Reagents-

Reaction Buffer: 50 mM Potassium Phosphate (25mM KH_2PO_4 + 25mM K_2HPO_4), pH 7

Detergent Reaction Buffer: 50 mM Potassium Phosphate + 0.01% Triton X-100, pH 7

CRITICAL - Aqueous Triton X-100 solutions become less effective over time and should be made fresh daily.

Protein: 0.00162 mg/ml AmpC β-lactamase, containing 0.0006% Triton X-100 in KPi. 0.00162 mg/ml = **30X.** Store at 4°C. The preparation of AmpC has been previously described;[6, 18] exploratory amounts are available from the Shoichet Lab.

CRITICAL - Prepare working enzyme stocks daily from higher concentration stocks (> 1 mg/ml). Enzyme will gradually adsorb to the surface of the container, thus decreasing the concentration of free enzyme. The very small amount of detergent added to the enzyme stock will attenuate this effect.

Substrate: Nitrocefin. 5mM stock in DMSO. Remel/Oxoid.

Catalog #'s 651063/BR0063A respectively

CRITICAL - Store solid stocks at 4°C and DMSO stocks at -20°C.

Compounds: 10 mM stocks in DMSO.

CRITICAL - DMSO concentration in the reaction should be minimized. AmpC tolerates concentrations < 4% without serious effect.

Equipment-

- A UV-Vis plate reader. Hydrolysis of nitrocefin by AmpC is most sensitively monitored at 482nm, though other wavelengths can also be used.
- A 96-well format liquid handling instrument, such as the Biomek FX.

Consumables-

- 96-well format tips for use with a liquid-handling robot. Example: Molecular Bioproducts part numbers 919-262-05, 918-262-05.
- 96-well plates for reagents and dilutions. Example: Grenier 96-well plates, part number 65020.
- UV transparent 96-well plates for reactions. Example: Corning part number 3679.

Procedure.

A Detergent-based Counter-screen for Aggregation-based Inhibition:

1| Add buffer to each well. For a final reaction volume of 150 µL, you should pipette 142 µL – x µL where x is the amount of compound to be added.

2| Add in 5 µL of the 30x enzyme solution to the wells.

3| Add in x µL of Compound (or DMSO for uninhibited positive control) to the wells.

CRITICAL STEP – Only a few controls are necessary to establish the uninhibited rate of the reaction.

4| Mix by pipetting up and down.

5| Incubate compounds and enzyme for 5 minutes.

CRITICAL STEP – Aggregate-based inhibition is time dependent, therefore the incubation time is key.

6| Add 3 µL 5mM Nitrocefin.

7| Mix by pipetting up and down.

8| Monitor reaction at 482 nm.

TIMELINE

Steps **1-4:** five minutes.

Step **5:** five minutes.

Step **6:** five minutes.

TROUBLESHOOTING

Problem	Possible Reason	Solution
Reaction rate is very low or drops over the course of multiple experiments.	Enzyme adsorption to the reagent container.	Prepare new enzyme stocks throughout the experiments. Reuse the enzyme reagent container.
High variation in control reaction rates.	Poor mixing.	Mix more thoroughly.
Poor reversibility in detergent experiments.	Triton X-100 has gone bad.	Prepare fresh Triton X-100.
Sudden large jumps in absorbance at 482 nm.	Popping bubbles from the presence of Triton X-100.	Mix less vigorously and ensure mixing takes place below the liquid level of the well.

Anticipated Results:

Inhibition:

The initial rate of each reaction is the slope of the best-fit line to the early kinetic data. The percent of inhibited enzyme is defined as:

$$\%Inhibition = 100 * \left(1 - \frac{\nu_i}{\nu_c}\right) \quad \text{(Eq. 1)}$$

Where ν_i and ν_c are the inhibited and uninhibited rates of reaction respectively. We defined statistically significant inhibition as greater than 23.8%, based on the behavior of several known aggregators and non-aggregators at 30 μM [6, 35]. Less than 11% inhibition was considered insignificant. Intervening amounts of inhibition were ambiguous, and may indicate a tendency to aggregate at higher concentrations. These cutoffs were statistically obtained from the behavior of compounds in our hands and on our instruments, and only represent guidelines. These cutoffs may not be extendable to other enzyme systems or significantly different assay conditions or concentrations.

Effect of Detergent:

We consider a broad range of decrease in inhibition upon the application of detergent to be significant. Most aggregators show a greater than two-fold decrease in percent inhibition upon the application of 0.01% Triton X-100, though not all aggregators have the same sensitivity to detergent [7, 35].

If a molecule exhibits significant inhibition of AmpC, and this inhibition is diminished by detergent, it is almost certainly acting as an aggregation-based inhibitor. Marginal detergent sensitivity should not be considered a confirmation of true inhibition–

some aggregators, such as Congo red, require 0.1% Triton X-100 before inhibition is fully reversed. Addressing this widely varying sensitivity definitively may require multiple experiments with different concentrations of detergent or compound. That said, aggregation at one concentration does not rule out a specific mechanism at a lower concentration. If further experimental confirmation of aggregation is required, other hallmarks of this phenomenon can be easily assayed- for example the presence of particles detectable by light scattering, the time dependence of inhibition or the dependence of inhibition on enzyme concentration (See below). However, the detergent-dependent enzyme assay is relatively definitive and is the easiest to incorporate into a large scale screening campaign. It represents a fast and simple way to screen for promiscuous aggregate-based inhibition.

Follow-up experiments for confirmation of aggregate-based inhibition:

When testing only a small number of interesting molecules for aggregation-based inhibition, more detailed, and time-consuming, investigation may be called for. The following experiments, in decreasing order of facility, may be useful:

1. Is inhibition significantly attenuated by small amounts of non-ionic detergent?
    a. If so, the compound is very likely acting through aggregation. We typically use 0.01% Triton-X 100–others favor Tween-20 or CHAPS[15], and we have also used Saponin and Digitonin[9]. Other non-ionic detergents might also work.
    b. In assays that cannot tolerate detergent, e.g. cell-based assays, it may be possible to use high concentrations of serum albumin [6]. This is currently

under investigation—a drawback of this method is that albumin can also sequester well-behaved molecules.

2. Is inhibition significantly attenuated by increasing enzyme concentration?
    a. If so, the compound is very likely an aggregator. Except when the receptor concentration to K_i ratio is high[52], increasing receptor concentration should not affect percent inhibition. Of course, when the receptor is membrane bound or intracellular, this is difficult to probe.
3. Is inhibition competitive? If so, the compound is unlikely to be an aggregator.
4. Does the inhibitor retain activity after spinning for several minutes in a microfuge? If not, particle formation is likely (see point 5, below).
5. Can you directly observe particles in the 50 to 1000 nm size range? We have typically used dynamic light scattering (DLS) for this. Formation of particles does not guarantee promiscuous inhibition, but it is a worrying sign.
6. Is the dose response curve unusually steep? There are classical reasons for steep-dose response curves[52], but it too is a worrying sign.

Few if any of these experiments are completely definitive by themselves, though the detergent test is fairly reliable. When several of these tests are combined, they are strong indicators of aggregation or non-aggregation based mechanisms of action.

Further discussion of characteristic features of aggregation-based inhibition can be found in references [6-9].

Acknowledgements: We thank Andrea McReynolds and Kristin Coan for reading this manuscript, KC for thoughtful discussions and GM71630 for support.

Appendix C.

Low-throughput experiments on small molecule mixtures

Supplementary Table 1. Results of follow-up experiments.

LT RESULTS				HT RESULTS			
	Component % Inhibition	Predicted Mixture % inhibition	Experimental Mixture %inhibition		Component % Inhibition	Predicted Mixture % inhibition	Experimental Mixture %inhibition
Mixture 1		**30**	**83.7**	**Mixture 1**		**60.4**	**98.9**
A2	2.3			A2	4.8		
B2	2.1			B2	7.9		
C2	0.8			C2	0		
D2	1.6			D2	6.1		
E2	9.0			E2	15.7		
F2	11.8			F2	47.8		
G2	0.2			G2	10.4		
H2	3.3			H2	6.5		
A3	3.7			A3	2.5		
B3	4.9			B3	1.4		
Mixture 2		**19.6**	**81.2**	**Mixture 2**		**40.6**	**99**
D3	1.5			D3	8.3		
E3	0			E3	10.3		
F3	3.1			F3	6.7		
G3	5.1			G3	11.3		
H3	3.5			H3	7.1		
A4	1.0			A4	2.7		
B4	3.5			B4	6.5		
C4	3.5			C4	4.4		
D4	0			D4	3.4		
E4	2.3			E4	2.3		
Mixture 3		**33.3**	**94**	**Mixture 3**		**60.7**	**99**
G4	0			G4	4.6		
H4	0			H4	5.2		
A5	1.7			A5	2.0		
B5	23.8			B5	49.2		
C5	0			C5	6.7		
D5	5.6			D5	6.2		
E5	2.8			E5	3.4		
F5	2.0			F5	11.2		
G5	0.7			G5	10.6		
H5	5.3			H5	3.4		
Mixture 4		**53.9**	**2.2**	**Mixture 4**		**96**	**23.2**
B6	1.6			B6	1.2		
C6	5.3			C6	5.0		
D6	11.5			D6	29.9		
E6	10.8			E6	27.9		
F6	4.9			F6	6.5		
G6	0			G6	4.9		
H6	0			H6	4.0		
A7	0.3			A7	12.6		
B7	0			B7	3.6		
C7	44.2			C7	95.8		

Mixture 5		**97.6**	**91.8**	**Mixture 5**		**97.2**	**59.1**
H8	0			H8	1.3		
A9	3.9			A9	8.5		
B9	1.1			B9	97.2		
C9	97.6			C9	5.1		
D9	11.0			D9	5.1		
E9	2.1			E9	0.0		
F9	0			F9	19.6		
G9	12.0			G9	0.6		
H9	0			H9	0.0		
A10	0			A10	3.8		
Mixture 6		**1.9**	**0**	**Mixture 6**		**10.8**	**0**
C10	0			C10	0.0		
D10	0			D10	0.0		
E10	0			E10	0.0		
F10	0			F10	0.0		
G10	0			G10	7.9		
H10	0			H10	0.0		
A11	0			A11	3.4		
B11	1.9			B11	0.0		
C11	0			C11	0.0		
D11	0			D11	0.0		

It is the policy of the University to encourage the distribution of all theses and dissertations. Copies of all UCSF theses and dissertations will be routed to the library via the Graduate Division. The library will make all theses and dissertations accessible to the public and will preserve these to the best of their abilities, in perpetuity.

I hereby grant permission to the Graduate Division of the University of California, San Francisco to release copies of my thesis or dissertation to the Campus Library to provide access and preservation, in whole or in part, in perpetuity.

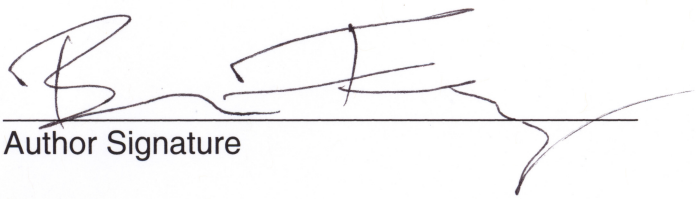

Author Signature

6-11-07

Date